nature portfolio

Peer Review File

Pericytes promote metastasis by regulating tumor local vascular tone and hemodynamics

Corresponding Author: Dr Minfeng Chen

Parts of this Peer Review File have been redacted as indicated to maintain the confidentiality of unpublished data.

This file contains all reviewer reports in order by version, followed by all author rebuttals in order by version.

Version 0:

Reviewer comments:

Reviewer #1

(Remarks to the Author)
In this manuscript, the authors investigated the functions of a novel subpopulation of NKX2-3(high) tumor pericytes in regulating the local tumor vascular tone and hematogenous metastasis. Using radiomics, scRNA-seq, and conditional knockout mice, et al, the authors revealed that the pericyte NKX2-3-induced alterations of tumor vascular structure and hemodynamic changes in primary tumor were associated with tumor hematogenous metastasis. Genetic depletion or pharmacological inhibition of NKX2-3 in tumor pericytes significantly suppressed tumor cell intravasation and tumor metastasis. Mechanistically, NKX2-3 suppressed calcium influx in tumor pericytes via the PDE1C/cAMP/PKA signaling axis, inducing tumor vasodilation and increasing blood flux and vascular leakage. Overall, this study revealed a previously unknown function of pericytes in tumor hematogenous metastasis, and shed a new light in the early diagnosis and therapy for tumor metastasis. The manuscript was well written, and the results were conclusive. This work may be considered for publication after addressing the following issues:
1. Does the compound Z-GP-NB2 had an effect on the body weight of tumor-bearing mice?
2. Whether NB2 exerted an immediate effect on the viability, EMT, migration and invasion of tumor cells?
3. Please determined the effects of NKX2-3-related pericyte contraction and relaxation on the Transendothelial motility of tumor cells using an vessel organoid model.
4. The integrity of the vascular basement membrane as indicated by the laminin/CD31, and the hypoxia condition as indicated by CA9, should be determined in the tumor tissues of allografts or xenografts.
5. Does tumor hypoxia involve in inducing the overexpression of NKX2-3 in tumor pericytes? Please verified and discussed it.
6. The detailed information of patients except for the name should be listed in an Ecxel file.
7. MC-38 xenografts should be “allografts”.
8. In Supplemental Figure 8, H&E staining of other organs such as liver, brain, intestinal tract, et al, should be conducted to determine the safety of conditional knockout of Nkx2-3 in pericytes.

Reviewer #2

(Remarks to the Author)
Li and coworkers report here the link between pericyte activity, hemodynamics and tumor metastasis. Their findings emanate for a multidisciplinary research program which include RNA sequencing, in vivo and in vitro work, molecular biology and different imaging methodologies. The manuscript is coherent in the presentation of the results albeit reading fluency is somehow affected by the numerous abbreviations used.

The following are comments aimed to clarify certain aspects of the methodology and findings:

0) How are capillaries defined in this work? Please provide a rigorous definition and perform analysis accordingly. Some of the vessels segments presented in this work are certainly above the accepted size definition for capillaries (eg Fig 5B, linescan measurements seems to be performed in a vessel of approx 30-40um in diameter). It will be fundamental to

separate vessel response to U46619 (and others) based on their initial diameter.

1) What aspect of "artificial intelligence" was used in the analysis of blood flow? The authors refers to "signal intensity of blood flow was calculated by artificial intelligence" (pp 6, line 120). The method refer to PyRadiomics (pp 26 line 552) albeit details are not clear enough to reproduce analysis. A supplementary figure reproducing the analysis steps can clarify this issue.

2) The authors present ROC curves but no explanation on how those where computed. Was this based on human-labeled datasets? Show examples.

3) Of much concern with respect to the in vitro calcium imaging experiments presented in Fig3 (and supplemental material as well); the authors describe a protocol where the measurements are performed under a calcium free medium: "... Then, TPCs were washed with the calcium-free PBS twice and calcium influx was examined under the Zeiss LSM 800. Under such conditions,..." (supp methods, pp 6). Under such conditions, there is no calcium influx and changes in the indicator intensity can be attributed to internal calcium release, not influx.

4) Further, authors should present "baseline" measurements prior to treatment, computing the relative change and reporting this value. Also make sure to indicate what treatment has been added in each experiment to elicit the reported changes.

5) Of much concern is the statement that a specific treatment/transgenic modification has negligible effects on pericyte density given the significant reduction across all diameter categories is misleading (see for example supp Fig 11B). Deletion of single pericyte has been show to induce changes in vascular physiology.

6) When comparing in vivo between treatments and control for different conditions, please present always relative changes and analysis statistics accordingly (eg correctly done in supp 18D but not in E). The key aspect here is the slope of change; as previously mentioned, plot this changes as a function of the initial vessel diameter.

7) Please provide evidence showing that the AAV vector targeted pericytes by quantifying expression against a pericyte marker (eg. NG2 in proximity to CD31), the data provided in Fig 4I is not sufficient). Data for "baseline" calcium dynamics should be presented in both mouse (control and knockout). Again, data should be presented as relative changes in addition to the nominal expression level.

Reviewer #3

(Remarks to the Author)
Colorectal cancer liver metastasis demonstrates increased blood vessel size and a subset of tumor pericytes (TPCs) were found to be associated with metastasis in patients. In mice, conditional loss of NKX2-3, marking the subset of TPC of interest, reduced blood flow by vasoconstriction, implicating calcium influx signaling, and resulted in decreased metastasis. Vascular leakage, presumed to be driver component of tumor metastasis, was reduced with blockage of NKX2-3 in TPCs. The authors propose NKX2-3 as a marker of TPC may have ‘diagnostic’ (the authors may have meant prognostic?) and therapeutic potential. There are mechanistic regulation studies included, and implication of EVs as possible mediators of TPC regulation with impact on metastasis. Overall, this is a very comprehensive study with an overwhelming amount of data, and yet presented beautifully. This is amongst the most interesting paper this reviewer has had the pleasure to review in recent past. There is nonetheless an important point of confusion with respect to vessel diameter and blood flow detailed further below. This may need additional clarification in the text. The abstract may need to be revised to include more mechanistic information, EVs, and pharmacological design of a new compound with anti-metastatic properties.

1) The introduction places high blood flow in the tumor microenvironment as possibly rate limiting, via shear stress induction for example, for hematogenous metastasis. This appears contradictory to the thesis of the manuscript, wherein high blood flow is presumed to be associated with increased metastasis. Generally, the concept of vessel diameter and blood flow is inversely proportional (Bernoulli’s equation). The larger the diameter of a vessel, the slower the flow, not faster. This would actually make more logically sense with the argument proposed by the authors: altering NKX2-3 pericytes function to relax tumor blood vessels would increase diameter, alter permeability, and reduce sheer stress by reducing local blood flow.

2) Figure 1: how blood flow measurements are made are unclear. What is shown in Figure 1A? What is blood flow signal and how does this translate to velocity (flow) of blood? These measures appear to reflect vascular density (increased angiogenesis) rather than flow. There are no measures of flow in the method, nor data expressed as a velocity of blood (blood volume over time) through vessels. This is a critical point that the authors should carefully review and clarify. The methods may need illustration of the steps taken to arrive at the “signal strength value” in Figure 1A.

3) While vessel diameter and basement membrane continuity data are convincing (Figure 1E-G), it should be noted that this does not equate patency of vessel, and that to make a case for increase vessel diameter is associated with increased flow, the correlation graphs in Figure 1H-J need to be clarified (see point above) as whether this reflects ‘flow’ or merely angiogenesis. Hypoxia increase (Figure 1G) with vessel diameter in LM CRC support that these vessels are likely non patent. This contradicts the thesis that “flow” (as ‘small area emphasis value’??) would be increase in area that have larger

diameter vessels but are also more hypoxic… Taken together, the data is confusing and contradictory: Large diameter vessels in LM CRC have less laminin (likely defective/leaky/non patient) and more hypoxia (logical), but have greater blood 'flow'? (not logical). Please clarify.

4) Figure 1. What is the number of vessels (independent of size or laminin staining) in LM CRC vs NM CRC and is there a positive correlation with 'flow'?

5) scRNASeq data in Figure 2: is NKX2-3 expressed in lymphatic endothelial cells? can the author demonstrate that NKX2-3 is specific to pericytes and not found in endothelial cells or other cells in CRC microenvironment/cancer cells? Supplementary Figure 1 does not address this.

6) The data in Figure 2 related to immunolabeling of tumors is clearly presented and convincing. The authors also validated this finding in breast cancer. Please show uncropped western blots for Figure 2E. Were the authors able to control for possible biases in Figure 2I-J, wherein other features of cancer progression at time of analysis (metastatic burden to other organs, performance status, treatment) to solidify the association between NKX2-3 TPC rich tumors and survival? Where the 93 patients all with LM CRC? Note that the color choice (red and blue) for the curves in I and J is confusing with respect to the panel G above where in red is used for NM CRC and blue is used for LM CRC.

7) Contractility studies in Figure 3 are presented clearly and with appropriate controls. The significance of the quantification for panel L is difficult to appreciate. Consider a bar graph at 48 hours and individual values shown. Is this signaling specific to TPC? Would cancer cells or fibroblasts fail to demonstrate similar response (not worth testing experimentally if not already done, but interesting to include if data exist)? The source for verapamil was not found.

8) Figure 4: generally a well conducted in vivo study. What is the tumor growth kinetics in PClin vs PClin-KO mice? The details of the orthoptic implantation of MC-38 is also not found in the methodology. Please clarify what is measured in D (pericyte coverage, which pericyte marker was used, how was it quantified).

9) Figure 5: the demonstration of blood flow in this experiment is much clearer than the confusions that stemmed from Figure 1. It remains however confusing why the increase in blood vessel diameter is associated with increased blood flow (again, contradictory to Bernoulli's principle). Are the authors observing that vasodilatory properties of NKX2-3+ TPC generates permeability and facilitates extravasation of cancer cells independent of blood flow? The imaging data indicating true flow changes in tumors vs showing more tumor angiogenesis and vascular destabilization? The dynamicity of tumor angiogenesis during tumor growth has been extensively reported, and it is therefore critical that the authors demonstrate tumor volume at time of study, and whether metastases are seen in the liver at that time point.

10) The exosomes study in Figure 6 is interesting and welcome, though the manuscript is already quite dense. The authors may want to mention this axis of regulation in their abstract. The dosing of how much exosomes to use to treat cells and whether this dosing is relevant to human disease is a vexing question in the field. These experimental details must be provided, and dose responses could be included. This may be more convincing than using Rab27a knockdown, given this does not always translate in impaired biogenesis and can impact cargo content. Have exosomes with NEAT1 been captured in the blood of CRC LM (and compared to CRC NM?)?

11) Is NEAT 1 expression in TPC correlating with vessel diameter/'flow'/laminin from Figure 1?

12) Figure 7. the authors used human xenografts, was this because Z-GP-NB2 activity relies on human proteins rather than murine? Ideally, if species cross reactivity is possible, evaluating the anti-metastatic effect of Z-GP-NB2 on the genetically engineered models (GEM) with MC38 orthotopic tumors would be quite interesting. If Z-GP-NB2 fails to show additional benefit (reduced metastasis) in NKX2-3 conditional deletion GEM, it would support target specificity. In vitro, would over expressing NKX2-3 in TPC limit the impact of Z-GP-NB2? Does Z-GP-NB2 limit the impact of tumor derived EVs on TPC?

13) Minor: a typo was found in the abstract: Blood "blow". The author may want to define CRCLM when first used in the text, this reviewer did not see it spelled out.

Reviewer #4

(Remarks to the Author)
In this manuscript submitted by Li X et al the impact of NKX2-3 (in mice Nkx2-3) transcription factor in pericytes in the hematogenic hepatic metastatic expansion of colorectal (and other cancers, including breast cancer and pulmonary metastasis of melanoma) was investigated using an impressive battery of state-of-the-art methodology. The authors have found that in CRC samples with increased blood flow the tumor pericytes (TPCs) contain a specific subset with increased expression of NKX2-3. This increase is associated with reduced contractility via a PDEC1/cAMP/PKA-mediated Ca-dependent mechanism, whereas pericyte-specific deletion of Nkx2-3 (in mice) restores vasoconstriction. One mechanism that may be involved in the upregulation of NKX2-3 in pericytes (hence increased blood flow) is the exosomal transfer of long non-coding RNA NEAT1 interfering with miR-769-5p, thus forming a regulatory loop for NKX2-3 production. As a potential downstream target gene, PDE1C was identified, which upregulation could be prevented by inhibition of NKX2-3 binding to sequence target via FAPa-catalyzed metabolism of a peptide derivative prodrug. The results are consistent and suggest a novel potential approach for reducing hepatic metastasis during the course of CRC. Some issues need

clarification, though.
1. Major concerns:
1.1 What is the expression of pericyte-associated NKX2-3 in the non-malignant segment of colon tissue of the metastatic and non-metastatic samples? On Fig 2G only tumor tissues are presented. This needs to be demonstrated to confirm that the differences are tumor-related without potential individual variations of NKX2-3 variations, irrespectively of the tumor status of the patients. Also, the authors claim that the t-SNE demonstration reveals only the increase of cluster #3 cells – clearly, cluster #1 also shows increase, with NKX2-3 expression spanning both - please clarify.

1.2 Importantly, as the immunohistochemistry uses a polyclonal-polyclonal antibody binding procedure for NKX2-3 staining, control labeling (replacing the specific first Ab with irrelevant Ig) is also needed for both the immunofluorescence and the Western blot analysis (Fig. 2E) to confirm specificity. Also, Supplemental Fig. 2A the pulmonary metastatic breast cancer/NKX2-3 image shows intense red signal in non-vascular/aSMA-negative cells – can the authors define these cells, especially that many of these do not seem to stain with the nuclear marker (specification also missing from the image)?

1.3 The main cellular subsets of the colonic lamina propria with NKX2-3 expression are the CD34-positive endothelial cells and the VAP-1/AOC3-positive pericryptal myofibroblasts (Hsia et al, 2016 PNAS; Gabris et al, 2024, J Histochem Cytochem). In mucosal HEV endothelial cells, NKX2-3 exerts its regulatory function with COUP-TFII (Dinh et al., 2022 Nat Commun), whereas the pericryptal myofibroblasts are involved in the intestinal stem cell niche formation (Hsia et al, 2016 PNAS). Could these pericryptal/non-endothelial cells correspond to the pericytes? And if so, can the modulation of their NKX2-3 activity affect colonic epithelial homeostasis, thus CRC progression?

1.4 The authors claim that the NKX2-3 protein-blocking peptide Z-GP-NB2 has only negligible in vivo effect on normal tissues, demonstrated by H&E staining (supplemental Fig. 16B) of heart, spleen, kidney (NB written as “kiney”) and lung – the authors need to test/demonstrate the expression of mucosal HEV MAdCAM-1 (as one cardinal NKX2-3 target), to exclude non-pericyte target effects.

1.5. CRC also often generates lymph node metastases – have the authors observed any effect of Nkx2-3 deletion in TPCs on the degree of mesenteric lymph node infiltration?

1.6. Regarding TPC isolation and downstream scRNAseq: The Materials and methods is very vague/brief on how TPCs were isolated, and Authors refer to their recent publication (Li X et al, Gut, 2023) where this dataset was generated; but even in this cited previous work the Materials and methods are not too descriptive. How are Authors sure of the cells’ TPC identity? Also, it would be important to show the tSNEs of the 4 individual samples (eg. as Supplementary Figure 1A, or main Figure 2B) to be able to assess patient variation, and also to show how many cells/patients are included in the analysis. Furthermore, while in both this current work and the cited publication a total of 13 clusters of TPC are visible, the tSNE looks different – why? If it’s exactly the same dataset, did authors modify analysis settings? If yes, why?

2. Minor points:
2.1 Some figures have insufficient explanation. In addition to the ones above, Fig. 1E and F microvascular surface area % and CA9 staining intensity % are described - % of what? Fold difference, rather? Furthermore, how reliable is 2D/conventional microscopy in determining these parameters (especially surface area, diameter, length)? Confocal microscopy/3D might be better.

2.2 Supplemental Fig. 7A is confusing – I surmise that in PClin wt NKX2.3 PCR product is detected (450 bp in the upper left inset) whereas the floxed allele is slightly larger (lower left) – but what is being shown in the upper right inset (with no product) and the lower right (perhaps the Cre-complemented Floxed NKX2-3 genotype sample with 386 bp)? NB the images are now presented with slightly truncated size marking throughout the images.

2.3 Formally the human gene is denoted as NKX2-3, while the mouse equivalent is labeled as Nkx2-3 – please use this form, throughout the manuscript.

2.4 Abstract, line 60; and Line 105: I would add where blood flow and diameter were increased (inside the tumor).
2.5 Line 106: please describe CRCLM abbreviation
2.6 Line 163, Fig2G: does NG2 specifically label pericytes, or can it be expected to recognize neuronal elements as well? Why do Authors use a different staining for TPCs in breast cancer (FigS2A, line 172)?
2.7 Line 258, Fig 4D, Fig S11A: how was pericyte coverage determined?
2.8 Line 314, Figure 6A: NEAT expression is clearly not restricted to Cluster 3/MAPs. Maybe include violin plots to emphasize difference (if there is any)
2.9 Line 315: Figure 6B-C instead of Figure S6B-C
2.10 I don’t understand the sentence beginning in Line 363 and ending in Line 365.
2.11 Supplemental Table 11, antibody list: is the listed anti-Nkx2-3 anti-human or anti-mouse (or both)?

Reviewer #5

(Remarks to the Author)
In this manuscript, the authors identify a specific subpopulation of TPCs, characterized by high expression of the transcription factor NKX2-3, as being associated with hematogenous colorectal cancer metastasis to the liver. This novel

NKX2-3-high subpopulation regulates tumor vascular tone by modulating blood flow and vessel diameter, which has direct implications for metastasis. The data demonstrate that conditional deletion of Nkx2-3 in TPCs induces vasoconstriction, reduces blood flow, and subsequently mitigates tumor metastasis.

The paper gives a wealth of mechanistic insights linking NKX2-3 expression to calcium signaling and metastases. The authors are to be commended for the comprehensive efforts to address the role of the specific perivascular cells. However, I have some major concerns regarding the validity of the clinical results that build the basis for the downstream analysis. The amount of experimental data makes it hard to judge the validity of the individual results, and the text would, in my opinion, greatly benefit from guiding the reader through the complex experimental approaches used.

Major points

Abstract:
“Here, we found that patients with colorectal cancer liver metastasis were characterized by increased diameter and blood blow”. The meaning is unclear here. What has an increased diameter compared to what? Do the authors mean “blood flow”? Again, in relation to what?

The abstract is unclear on whether the findings were made in primary CRC or in CRLM.

Consider revisiting all instances where protein/RNA is mentioned to meet HUGO nomenclature criteria, this is currently unclear

Consider substantial revision of the last sentence of the abstract. What is the novel mechanism? Have the authors studied “pericytes in tumor metastasis” or how pericytes facilitate intravasation to induce metastases?

L105 The authors should specify here if the data come from primary tumors of metastases, i.e. “increased in CRLM patients” could be anywhere.

L117/8 “in clinical”? Where was blood flow measured? How is “artificial intelligence” needed to calculate signal intensity? This part has to be more specific, explain details, and motivate the choice of methods.

Data related to Figure 1: How were the patients matched? Were TN stages similar in M1 and M0 patients? Tumor location in the colorectum? This is crucial to compare the results, which could just be derived from different locoregional stages. No details on ultrasound measurements are given.

Data related to Figure 2: Are data in Figure 2 a re-analysis from previously generated scRNA-seq? Are those related to the measurements in Figure 1? This should at least be clarified. How was ensured that there were no significant differences other M0 and M1 in the sc-seq dataset?

Data related to Figure 3 (L179 ff): How were these cell lines/primary cultures derived? This is crucial to be able to judge any of the downstream experiments presented and should be included, at least briefly, in the main text.

L 271: U46619 is not introduced. Why was it used?

L284: An explanation of how “tumor blood velocity” can be assessed by two-photon microscopy would be very helpful here. Was this done by done by ultrafast scanning of erythrocytes?

L297: What are “constructed mouse vessel organoids”? Where are they derived from and
Despite studying the Supplementary Material, the Methods description is generally not specific enough to assess the results in all detail, mainly related to there being such a variety of experimental approaches use. For example, l. 478 “The images and specimens of all patients were confirmed by the pathology department”, what does this mean? What was confirmed and by whom? How is the pathology department involved in “images”?

For patients with liver metastases and an advanced primary tumor, it seems highly unlikely that no preoperative chemotherapy was administered, given current international guidelines (related to the statement in L 479). Can the authors comment on this?

What were the cas9 mice used for that are mentioned in the results? (L484)?

Other points

Title: Consider omitting ”tumor” as this is clear from “metastasis”

Introduction
L 75 “is the main approach”, do the authors mean “main mechanism”=

L 79 The assertion that intravasation is a “rate limiting step” is somewhat speculative, suggest to remove.

L176 “predictive marker”?

L259 “Light-sheet and fluorescent microscopy”: Wasn’t LS microscopy fluorescent?

L493 Were the mouse bred, instead of “hybridized”?

Reviewer #6

(Remarks to the Author)
Strengths of This Study:
This study shows strong evidence that NKX2-3 plays a key role in liver metastasis of colorectal cancer. It demonstrates that NKX2-3 affects blood vessel permeability and blood flow in tumor-associated pericytes, helping cancer spread. The study also explains how NKX2-3 is controlled by the NEAT1/miR-769-5p axis, revealing a new network of molecules involved in metastasis. Moreover, the findings suggest that the PDE1C/cAMP/PKA pathway, which controls blood vessel constriction, may also influence liver metastasis. This suggests NKX2-3 could be a good target for new therapies to prevent cancer from spreading.

Suggested Revisions:
Regarding Figure 3C: Please provide additional details on the criteria for gene selection, including the experimental techniques used and the number of RNA sequencing samples analyzed.

Relationship with Other Genes: Could you elaborate on the relationship between NKX2-3 and other key genes commonly associated with liver metastasis, such as KRAS, TP53, VEGF, and CXCR4?

Lymph node metastasis: The involvement of NKX2-3 in lymph node metastasis is not mentioned in the manuscript. Can you provide further clarification on this point?

Drug resistance: this manuscript does not address whether NKX2-3 is associated with resistance to anticancer drug therapy. Do you have data on this information?

Microsatellite Status: Could you provide more information on the relationship between NKX2-3 expression and microsatellite status?

Reviewer #7

(Remarks to the Author)
This manuscript describes that a subpopulation of NKX2-3-high TPCs are involved with metastasis of cancer, and NKX2-3 suppresses calcium influx in TPCs, induces tumor vasodilation, and increases vascular leakage. Authors also shows that the blocking of NKX2-3 using a FAP alpha-targeted Z-GP-NB2 peptide inhibits the binding of NKX2-3 to PDE1C promoter in TPCs and restores the tumor vasoconstriction and tumor metastasis. The idea is novel, and authors provide robust data related with the role for TPCs in tumor vasculature and metastasis.

However, this manuscript lacks data showing the delivery of Z-GP-NB2 into TPC-NK
X2-3-high cells is mediated by FAP alpha on the surface of the cells.

Why is FAP alpha expression increased in TPC-NKX2-3-high cells (Fig. S15C, D)? Is there a specific reason for choosing FAP alpha as a target of TPC-NKX2-3-high cells?

How is Z-GP-NB2 delivered into TPC-NKX2-3-high cells? In other words, what is the mechanism of Z-GP-NB2 internalization into TPC-NKX2-3-high cells? Is not only Z-GP-NB2 but also NB2 internalized into TPC-NKX2-3-high cells? Is the FAP alpha internalizing receptor?

To demonstrate the FAP alpha-mediated delivery of NB2, it is recommended to include the treatment of TPC-NKX2-3-high cells with NB2 as a control of Z-GP-NB2 and/or include the treatment of the cells with FAP alpha-blocking antibody (Fig. S15G-K and Fig. 7E, F).

Reviewer #8

(Remarks to the Author)
I co-reviewed this manuscript with one of the reviewers who provided the listed reports. This is part of the Nature Communications initiative to facilitate training in peer review and to provide appropriate recognition for Early Career Researchers who co-review manuscripts.

Reviewer #9

(Remarks to the Author)

I co-reviewed this manuscript with one of the reviewers who provided the listed reports. This is part of the Nature Communications initiative to facilitate training in peer review and to provide appropriate recognition for Early Career Researchers who co-review manuscriptsA′″…←

Version 1:

Reviewer comments:

Reviewer #1

(Remarks to the Author)
The authors have added several new experimental data to address the concerns raised in previous cycle, the revised manuscript has been further strengthened. No further comments.

Reviewer #2

(Remarks to the Author)
This are comments to the revised (R1) version which shows a significant effort by the authors to address the previous comments.

The following numbering refers to the original comments from this reviewer.

0) The reviewer agrees with the note that tumor capillaries (and vessels in general) are different from normal capillaries. Definition of a capillary might be more complex that addressed here as a single marker is not sufficient (certainly not α-SMA as done by the here). As previously stated, the responses can depend on original vessel size , the authors have not provided the requested information (i.e. a plot of relative diameter change against vessel diameter). This will help to further disentangle whether responses are indeed in capillaries or arterial-like vessels (in the tumor). More over, still of much concern, is the fact that vessels categories smaller than 50um (Supp Fig 15b) are significantly larger in the knockout.

1) No further comments.

2) No further comments.

3) The original mistake in wording was clarified. No further comments.

4) The experimental data is presented now as required, hopefully making it more clear for all readers.

5) With respect to the PClin-KO, the authors have to make it clear in the main text that the vascular network is different in nature from the WT (again, based on the significant changes presented in Supp Fig 15b). The following updated lines fail to do so, it is not just a matter of mean vessel diameter; changing the proportion of small vessels (higher in the KO) alters baseline hemodynamics, unrelated to any treatment.

261 Light-sheet and confocal fluorescence microscopy were applied to analyze vascular
262 morphology and structure. Conditional deletion of Nkx2-3 had negligible effects on
263 pericyte coverage (Supplementary Fig. 15a) and vessel density (Fig. 4d); however,
264 vessel diameter was significantly decreased in PClin-KO mice compared with that in PClin
265 mice (Fig. 4d; Supplementary Fig. 15b)

6) Same as in previous comments, the data should be presented for the different vessels diameters measured. Currently data is averaged over animals making it more difficult to appreciated the detailed responses in each treatment as this can be dependent on biological or experimental bias (i.e. having sampled more vessel of a specific diameter). The authors can present a scatter plot for all the vessels measured across treatments, here again plotting % change (as now implemented) vs baseline average vessel diameter.

7) No further comments are required here.

Reviewer #4

(Remarks to the Author)
The authors have satisfactorily addressed all my points. No more queries are raised from this Reviewer.

Reviewer #5

(Remarks to the Author)
In their comprehensive rebuttal, the authors provide a wealth of additional data to the already exceptionally rich manuscript.

In their rebuttal, the authors state that “We apologize for the misleading description of artificial intelligence. Blood flow in tumor was measured by doppler ultrasound imaging, and the images of tumors derived from colorectal cancer patients with or without liver-metastasis were collected and analyzed using Open CV, rather than “artificial intelligence”. In ultrasound

Doppler images, red and blue regions conventionally represent blood flow, with red indicating arterial flow and blue indicating venous flow."
- I find it of significant concern that the authors initially provided an incorrect description of the method used to analyze the major hypothesis-driving analyses, and this could raise fundamental concerns as to the validity and methods description of the remaining experiments.
- In Doppler images, red and blue regions do not conventionally represent arterial and venous flow, as stated by the authors. Rather, blood flow is color-coded according to the flow direction to or from the transducer, entirely unrelated to the vessel being a vein or artery. This fundamental principle of the technique is misstated.

The authors now provide some clinical data, as suggested, which allows for a more detailed assessment of the results presented in Figure. However, clinical data are presented stratified by blood flow results in Supplementary Tables 5 and 6, while the groups in Figure 1 are stratified into patients with and without metastases. Hence, the data are not aligned, and a thorough assessment of the effect postulated from Figure 1 is not possible based on the presented tables. However, what becomes evident is that earlier, early-stage tumors (T1/2) have lower flow than later-stage tumors (T3/4). Given this confounder, it is not acceptable to simply state (L 123) "(…) results showed that blood flow was significantly increased in CRC patients with liver metastasis compared with that in non-metastatic patients", and neglect tumor stage as a potential alternative explanation. This statement ignores a confounding variable, and no evidence is presented to show that the results hold even after correcting for tumor size. Please see also a comment below on further systematic differences between early and advanced tumors.

Figure 2a, and and Figure R25: The tSNEs seem to have been generated from the whole dataset and then separated. The effect of cluster 3 being present only in the LM group is exceptionally strong and, given the size of the cohort (n=2 in each), is likely driven by the tumor biology of an individual tumor or by batch effects. Showing separate parts of the dataset without, for example, in grey dots, the entire dataset is somewhat misleading, although not entirely uncommon. To be more convincing, the authors should highlight the individual patients in the Supplementary data to be able to see batch effects.

The authors state: "Concerning the colorectal cancer patients with liver metastasis or locally advanced stage (T4), although preoperative neoadjuvant radiotherapy or chemotherapy is an important treatment option, a large number of cases with complications require palliative surgical resection or fistula treatment, which is also in line with the Chinese Society of Clinical Oncology (CSCO) guidelines for colorectal cancer version 202458. Therefore, to rule out the effects of preoperative neoadjuvant therapy on the metastasis, colorectal cancer patients without radiotherapy or chemotherapy prior to surgery were included in this study as a source of clinical specimens."
- If the authors collected specimens from emergency/palliative operations of advanced tumors, I am afraid this adds another confounder to the data in Figure 1 because T1/2 tumors were operated electively, while T4 tumors, for which the authors showed increased blood flow, were operated due to, e.g., ileus or fistula. This would invariably lead to inflammation and increased blood flow, questioning the results presented in Figure 1.

In their rebuttal, the authors state:
"Anti-angiogenic therapies including bevacizumab and DC101 are frequently used to treat tumor in clinic, however, which often result in local invasion and distant metastasis while blunting tumor growth". This is incorrect, at least for the clinical setting. While there are mouse data to suggest increased metastases on monotherapies with antiangiogenic drugs, this is not commonly observed in the clinical setting, as stated here by the authors. While the combination with chemotherapy might partly explain this phenomenon, Ramucirumab, e.g., is approved as a single therapy (REGARD trial, Lancet 2014).

Minor points:
On page 10, the authors state "the downregulated genes in TPCLMgNKX2-3(637) were defined by Venn diagram (https://bioinfogp.cnb.csic.es/tools/venny/)."
- Venn diagrams are used to visualize overlapping data; the authors have simply identified overlapping genes in two lists.

The authors added data on lymph node metastases in a mouse model (Suppl Figure 14) and state "Mouse metastasis was detected by in vivo imaging system and H&E staining." In vivo imaging (IVIS) cannot reasonably distinguish caecal tumor growth (where tumor cells were injected to) to lymphnode metastases as it lacks anatomical resolution for this, rather, it measures overall tumor growth. On the histological images shown, it is hard to see any tumor cells due to the limited resolution, but I cannot discern a clear primary tumor in the caecum.

Reviewer #7

(Remarks to the Author)
The authors successfully addressed the comments and questions raised by this reviewer. I have no further comments and recommend this manuscript for publication.

Reviewer #8

(Remarks to the Author)
I co-reviewed this manuscript with one of the reviewers who provided the listed reports. This is part of the Nature Communications initiative to facilitate training in peer review and to provide appropriate recognition for Early Career Researchers who co-review manuscripts.

Reviewer #10

(Remarks to the Author)
The majority of Reviewer#3's concerns were satisfactorily addressed.The following minor clarifications are required.

1. For experiments involving PClin mice and PClin-KO mice there seem not to be enough information/evidence on a) whether the efficiency of tamoxifen-mediated PC lineage labelling is comparable between PClin and PClin-KO mice and b) to what extent and when the tamoxifen-mediated depletion of NKX2-3 expression in the PClin-KO mice is achieved and maintained throughout the length of the experiment. It will be helpful to provide some quantitation as e.g. Supplementary Fig. 11 b-d fall short to inform this, hence, to characterise the model.

2. For western blot analysis, particularly those shown in Fig. 2e, the authors must clarify in the Fig. legend how the membrane was processed e.g. are the blots presented belong to the same membrane, which was cut, and each part probed the desired target? Or are the blots presented belong to the same membrane, which was probed first for one target, stripped, and subsequently re-probed for another target? Or are the blots presented belong to different membranes performed with the same samples/protein lysates? This is relevant as for analysis (quantitation) and data interpretation purposes. This comment applies to all the western blots presented in this manuscript.

3. For contractility studies, particularly those shown Fig. 3l, the representative images shown by the authors for TPCNMNKX2-3 + siPDE1C in the presence or absence of Verapamil do not align with what they have shown in the associated quantitation plot. It will be good for the authors to check if those 2 images are mislabelled/misplaced?

4. For microvascular density in primary tumours, particularly that shown in Supplementary Fig. 15, the representative image shown for PClin appears to have more CD31 positive vessels than that shown for PClin-KO. This is relevant as the authors claim that microvascular density is not different between genotypes, further I understand the % of BV with different diameters is calculated considering the total number of BV, hence microvascular density. Please clarify and replace image as needed.

5. For the EVs analysis, particularly that shown in Supplementary Fig. 21, as currently shown Z-GP-NB2 seems to upregulate NKX2-3 expression. It will be good for the authors to crosscheck if the blot image is mislabelled (?) as TPCs should have been incubated with DLD-1NEAT1 EVs and further treated (akas + in the legend) with Z-GP-NB2. Please clarify.

6. In general, throughout the whole manuscript, the n numbers in the figure legends and/or in the methods text seems poorly described. For examples, n=3 in Supplementary Fig. 21 is it for number of TPC samples treated or for number of WB performed with same samples? A more precise description is needed.

Reviewer #11

(Remarks to the Author)
I co-reviewed this manuscript with one of the reviewers who provided the listed reports. This is part of the Nature Communications initiative to facilitate training in peer review and to provide appropriate recognition for Early Career Researchers who co-review manuscripts.

Version 2:

Reviewer comments:

Reviewer #2

(Remarks to the Author)
The authors have done tremendous amount of work to comply with the requested changes and have addressed all concerns. I would like to still point to the fact that vessels diameters (at baseline) are very distinct between experimental groups). It might pay to highlight this and state it clearly.

Reviewer #5

(Remarks to the Author)
The authors have addressed most of my concerns.

Reviewer #10

(Remarks to the Author)
The authors has satisfied all my comments.

Reviewer #11

(Remarks to the Author)
I co-reviewed this manuscript with one of the reviewers who provided the listed reports. This is part of the Nature

Communications initiative to facilitate training in peer review and to provide appropriate recognition for Early Career Researchers who co-review manuscripts.

Point-by-point response letter

Point-by-point responses to the reviewers' comments

The authors thank all the reviewers for their constructive comments and suggestions. The manuscript had been revised accordingly. We responded point-by-point to all comments raised as follows:

Response to Reviewer 1 (expert in exosomes/miRNA)

Comments to the Author:

In this manuscript, the authors investigated the functions of a novel subpopulation of NKX2-3(high) tumor pericytes in regulating the local tumor vascular tone and hematogenous metastasis. Using radiomics, scRNA-seq, and conditional knockout mice, et al, the authors revealed that the pericyte NKX2-3-induced alterations of tumor vascular structure and hemodynamic changes in primary tumor were associated with tumor hematogenous metastasis. Genetic depletion or pharmacological inhibition of NKX2-3 in tumor pericytes significantly suppressed tumor cell intravasation and tumor metastasis. Mechanistically, NKX2-3 suppressed calcium influx in tumor pericytes via the PDE1C/cAMP/PKA signaling axis, inducing tumor vasodilation and increasing blood flux and vascular leakage. Overall, this study revealed a previously unknown function of pericytes in tumor hematogenous metastasis, and shed a new light in the early diagnosis and therapy for tumor metastasis. The manuscript was well written, and the results were conclusive. This work may be considered for publication after addressing the following issues:

1. Does the compound Z-GP-NB2 had an effect on the body weight of tumor-bearing mice?

Response: Thanks for your comments. The body weight of mice bearing HCT116 xenografts have been detected and the results showed that Z-GP-NB2 had negligible effects on the body weight of tumor-bearing mice **(Figure R1) (Please see page 19, line 390-391 in the revised manuscript; Supplementary Figure 22d in the revised Supplementary Information).**

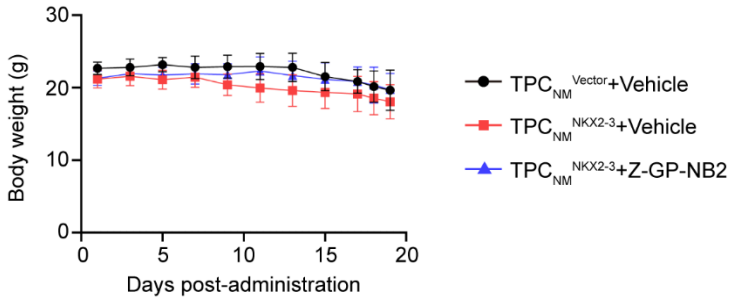

Figure R1. Z-GP-NB2 has negligible effects on the body weight of tumor-bearing mice. Body weight curves of mice bearing HCT116 xenografts (n = 6). Data are presented as mean ± SEM. TPC, tumor pericyte.

2. Whether NB2 exerted an immediate effect on the viability, EMT, migration and invasion of tumor cells?

Response: Thanks for your insightful question. The effects of NB2 on the viability, epithelial-mesenchymal transition (EMT), migration and invasion of tumor cells were examined by the authors. The results revealed that NB2 had negligible effects on the viability of HCT116 cells **(Figure R2a)**. NB2 also exerted negligible effects on the EMT of tumor cells, as indicated by the similar level of epithelial marker (E-cadherin) and mesenchymal markers (Vimentin, N-cadherin) in vehicle and NB2 treatment group **(Figure R2b)**. Transwell assay was used to determine the effects of NB2 on migration and invasion of HCT116 cells, while no significant difference was observed in the vehicle and NB2 group **(Figure R2c)**. Taken together, these data revealed that NB2 had negligible effects on the viability, EMT, migration and invasion of tumor cells **(Please see page 18, line 376-377 in the revised manuscript; Supplementary Figure 21a-c in the revised Supplementary Information).**

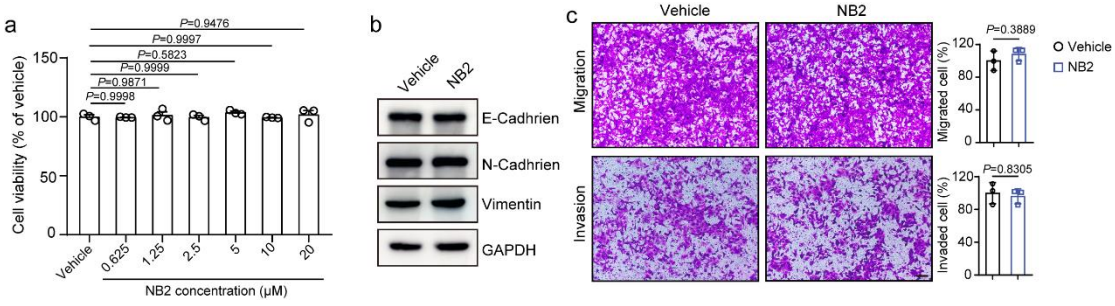

Figure R2. NB2 has negligible effects on the viability, EMT, migration and

invasion of tumor cells. a Cell Counting Kit-8 (CCK-8) assay for HCT116 cell viability treated with NB2 (n = 3). **b** Western blot analysis of epithelial marker (E-cadherin) and mesenchymal marker (N-cadherin, Vimentin) expression in HCT116 cells treated with NB2 (n = 3). **c** Migration and invasion assay for HCT116 cells treated with vehicle or NB2 (n = 3). Scale bar, 100 μm. Data are presented as mean ± SEM. NS, *P* values were determined by one-way ANOVA followed by Tukey's post hoc test (**a**) and two-tailed unpaired *t*-test (**c**). EMT, epithelial-mesenchymal transition.

3. Please determined the effects of NKX2-3-related pericyte contraction and relaxation on the Transendothelial motility of tumor cells using an vessel organoid model.

Response: Thanks for your constructive comments. As suggested, the effects of NKX2-3-related pericyte contraction and relaxation on the trans-endothelial migration of tumor cells were examined with microfluidic vascular chip models **(Figure R3a)**. The lower and upper channels of microfluidic chip (LNP-Bl, FluidicLab) were pre-coated with 50 μg/mL fibronectin (Yeasen) for 1 h to allow the cells adhere to the surface. To mimic tumor vessels, GFP-transfected TPCs (2×10^4, green fluorescence) were added to the bottom channel and cultured for 4 h, and then, endothelial cells (1×10^5) were added to the TPCs-coated channel and further cultured for 4 h to form endothelial layer. Unadhered cells were removed by gentle wash with PBS. The prepared microfluidic chip was placed at 37°C atmosphere containing 5% CO_2 overnight. The next day, PKH26-labeled HCT116 cells (red fluorescence) were added to the upper channel with a directional flow at bottom channel and upper channel, respectively. Tumor cells and mimetic blood vessels were observed, and images were acquired with a confocal microscope (Revvity, Opera Phenix Plus). The results showed that compared to TPC_{NM}^{Vector}, TPC_{NM}^{NKX2-3} significantly facilitated transmigration of HCT116 cells through vascular barrier **(Figure R3b)**, indicating that relaxed TPC_{NM}^{NKX2-3} is a key regulator for the transendothelial motility of tumor cells **(Please see page 15, line 300-303; Figure 5g, h in the in the revised manuscript).**

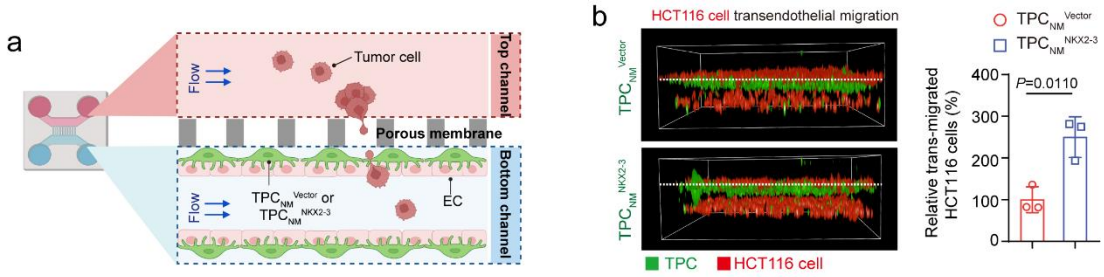

Figure R3. NKX2-3 in TPCs facilitates tumor cell transendothelial migration. a Schematic diagram describing the microfluidic chip. **b** Immunofluorescence assay for the transendothelial migration of HCT116 cells. White dotted lines indicate the porous membrane between the top channel and bottom channel. Data are presented as mean ± SEM. *P* value was determined by two-tailed unpaired *t*-test. TPC, tumor pericyte.

4. The integrity of the vascular basement membrane as indicated by the laminin/CD31, and the hypoxia condition as indicated by CA9, should be determined in the tumor tissues of allografts or xenografts.

Response: We appreciated your kind comments. As suggested, the integrity of vascular basement membrane and tumor hypoxia in mice bearing HCT116 xenografts were examined by immunofluorescence. The results showed that pharmacological inhibition of NKX2-3 with Z-GP-NB2 augmented the integrity of basement membrane, as indicated by the increased laminin area surrounding $CD31^+$ tumor vessels **(Figure R4a)**, meanwhile, Z-GP-NB2 attenuated hypoxia condition mediated by NKX2-3 in TPCs, as shown by the decreased CA9 expression in tumor regions **(Figure R4b) (Please see page 19, line 395-397 in the revised manuscript; Supplementary Figure 24b, d in the revised Supplementary Information).**

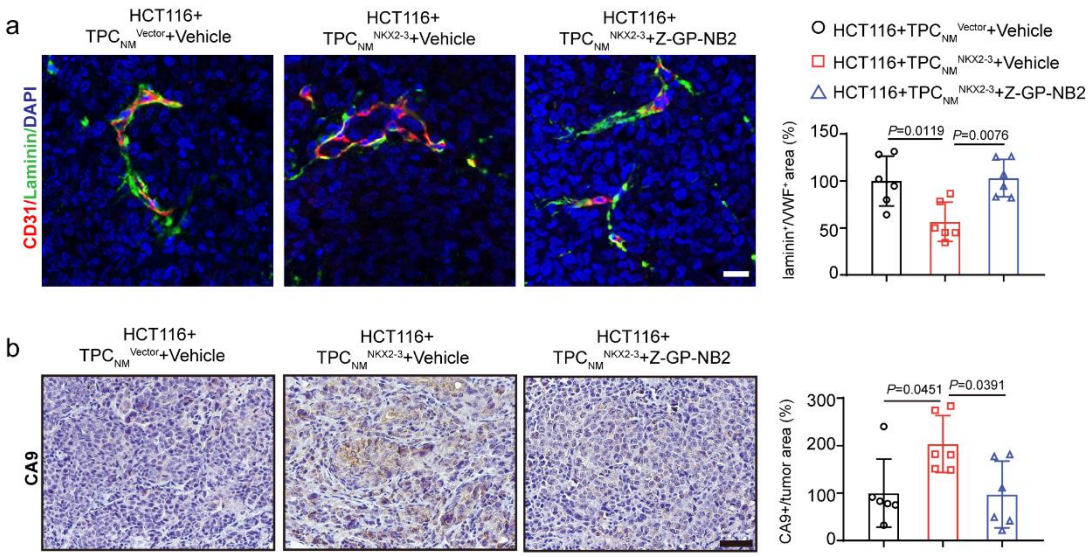

Figure R4. Z-GP-NB2 increases vascular integrity. a Immunofluorescence assay for laminin$^+$/CD31$^+$ area per field in HCT116 xenografts treated with or without Z-GP-NB2 (n = 6). Scale bar, 20 μm. **b** Immunohistochemistry analysis of CA9$^+$/tumor area in the HCT116 xenografts treated with or without Z-GP-NB2 (n = 6). Scale bar, 50 μm. *P* values were determined by one-way ANOVA followed by Tukey's post hoc test. TPC, tumor pericyte.

5. Does tumor hypoxia involve in inducing the overexpression of NKX2-3 in tumor pericytes? Please verified and discussed it.

Response: Thanks for your valuable comments. The effects of hypoxia on the expression of NKX2-3 was investigated *in vitro*. The results indicated that compared to the normoxic condition (5% O_2), hypoxic condition (1% O_2) significantly increased the expression of HIF-1α and NKX2-3 in TPC_{NM} **(Figure R5)**. Hypoxia is a potent regulator for tumor metastatic cascade[1], our result is consistent with a previous study indicating that pericyte relax when oxygen is needed but contract if the oxygen levels are sufficient, which may be associated with NKX2-3 regulation under hypoxia condition [2]. Therefore, in addition to tumor-derived *NEAT1*-enriched extracellular vesicles, hypoxia is also an important factor leading to the upregulation of NKX2-3 in TPCs. These data and description have been added **(Please see page 21, line 437-440 in the revised manuscript; Supplementary Figure 25 in the revised Supplementary**

Information).

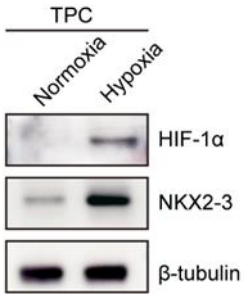

Figure R5. Hypoxia induces NKX2-3 expression in TPCs. Western blot analysis of HIF-1α and NKX2-3 expression in TPCs under normoxia and hypoxia condition (n = 3). TPC, tumor pericyte.

6. The detailed information of patients except for the name should be listed in an Ecxel file.

Response: Thanks for your suggestions. We have added the detailed information of patients and updated the Excel files **(Please see Supplementary Table 5-12 in the revised Supplementary Information).**

7. MC-38 xenografts should be “allografts”.

Response: Thank you very much for pointing out this mistake. We have corrected all these MC-38 xenografts into allografts **(Please see page 23, line 489 in the revised manuscript).**

8. In Supplemental Figure 8, H&E staining of other organs such as liver, brain, intestinal tract, et al, should be conducted to determine the safety of conditional knockout of Nkx2-3 in pericytes.

Response: Thank you for your insightful question. H&E staining was performed to examine the organs of brain, intestinal tract, ovary and testis. The results showed specific deletion of *Nkx2-3* in pericytes had negligible effects on these tissues **(Figure R6)**, indicating that conditional knockout of *Nkx2-3* in pericytes is safe to the normal organs of mouse **(Please see Supplementary Figure 11d in the revised Supplementary Information).**

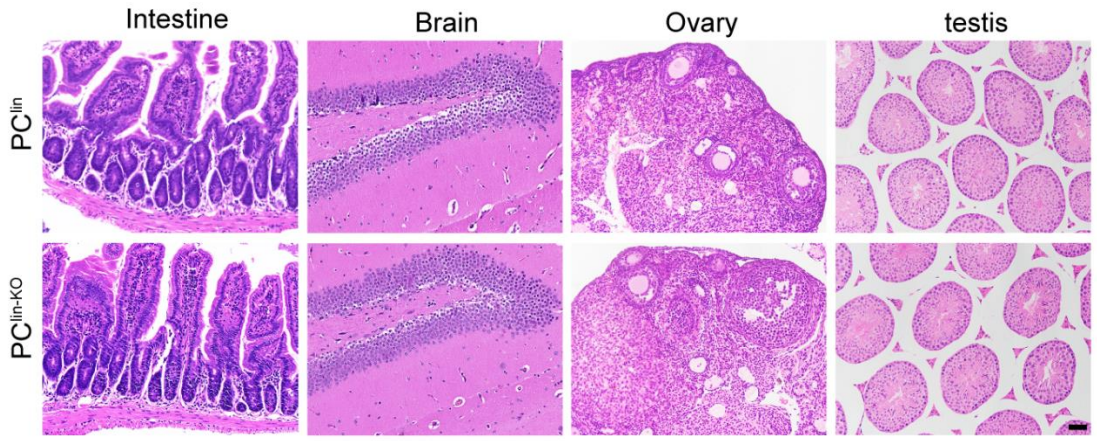

Figure R6. Conditional knockout of *Nkx2-3* in pericytes has negligible effects on normal tissues. Representative images of H&E staining for intestine, brain, ovary and testis derived from PC^{lin} and $PC^{lin\text{-}KO}$ mice (n = 6). Scale bar, 50 μm.

Response to Reviewer 2 (expert in vasculature (hemodynamics, calcium signaling), intravital imaging)

Comments to the Author:

Li and coworkers report here the link between pericyte activity, hemodynamics and tumor metastasis. Their findings emanate for a multidisciplinary research program which include RNA sequencing, in vivo and in vitro work, molecular biology and different imaging methodologies. The manuscript is coherent in the presentation of the results albeit reading fluency is somehow affected by the numerous abbreviations used.

Response: Thanks for your kind comments. We are sorry that the numerous abbreviations used in this study disturbed your reading. We have corrected the description and added full names.

The following are comments aimed to clarify certain aspects of the methodology and findings:

0) How are capillaries defined in this work? Please provide a rigorous definition and perform analysis accordingly. Some of the vessels segments presented in this work are certainly above the accepted size definition for capillaries (eg Fig 5B, linescan

measurements seems to be performed in a vessel of approx 30-40um in diameter). It will be fundamental to separate vessel response to U46619 (and others) based on their initial diameter.

Response: Thanks for your kind comments. The tumor vessels are different from those in healthy tissues, which maintained a tortuous capillary-like structure, including a number of progressively dilated vessels that reached diameters as large as 200 μm in some cases (capillaries normally have diameters less than 12 μm) [3, 4]. Diameters of vessels with capillary wall structure range from 6 μm to 55 μm in the human primary tumors (renal clear cell carcinoma, basalioma), and from 5 μm to 80 μm in xenografted tumors (sarcomas, colon carcinoma)[5]. In our previous study[6], we found that $NG2^+$ and $PDGFR\beta^+$ TPCs were distributed in capillaries with diameters between 10 and 40 μm. Therefore, we selected tumor capillaries with a diameter in the range of 10-40 μm for study **(Please see page 20, line 413-414 in the revised manuscript)**.

As the reviewer suggested, vessel response to U46619 and nitroprusside is heterogenous, and this response is related to the initial diameter of the blood vessel and endothelial cells [7-9]. In our study, U46619 and nitroprusside were used respectively to induce vasoconstriction and vasodilation in tumor vessels with an initial diameter of 10-40 μm, and these vessels generate similar response to the vasoconstrictor U46619 and vasodilator nitroprusside.

1) What aspect of "artificial intelligence" was used in the analysis of blood flow? The authors refers to "signal intensity of blood flow was calculated by artificial intelligence" (pp 6, line 120). The method refer to PyRadiomics (pp 26 line 552) albeit details are not clear enough to reproduce analysis. A supplementary figure reproducing the analysis steps can clarify this issue.

Response: Thanks for your constructive suggestions and pointing out the incorrect description. Doppler ultrasound images of tumors derived from colorectal cancer patients with or without liver-metastasis were processed and the signal intensity of blood was calculated using Open CV, not "artificial intelligence" **(Please see page 6, line 123 in the revised manuscript)**. In ultrasound Doppler images, red and blue

regions conventionally represent blood flow, with red indicating arterial flow and blue indicating venous flow. To quantify these regions, Open Source Computer Vision Library (OpenCV, https://opencv.org) was utilized for image processing. First, the color space was converted from BGR to HSV to facilitate precise segmentation of color-coded areas. Then specific HSV color ranges were defined for both red and blue flow regions, applying these ranges to create binary masks that isolated the areas of interest. These masks were applied to extract the corresponding blood flow regions from the original image. To further improve the segmentation accuracy, OpenCV's edge detection algorithms were employed, refining the boundaries of the extracted regions. Finally, within these segmented regions, the average saturation and brightness values were calculated to evaluate the blood flow signal strength, resulting in an objective quantification of blood flow intensity within the ultrasound Doppler images **(Please see page 26, line 553-566 in the revised manuscript)**.

The detailed steps of CT-based radiomic analysis were shown in **Figure R7** and code for radiomic feature extraction was presented in **Figure R8 (Please see Supplementary Figure 29 in the revised Supplementary Information).**

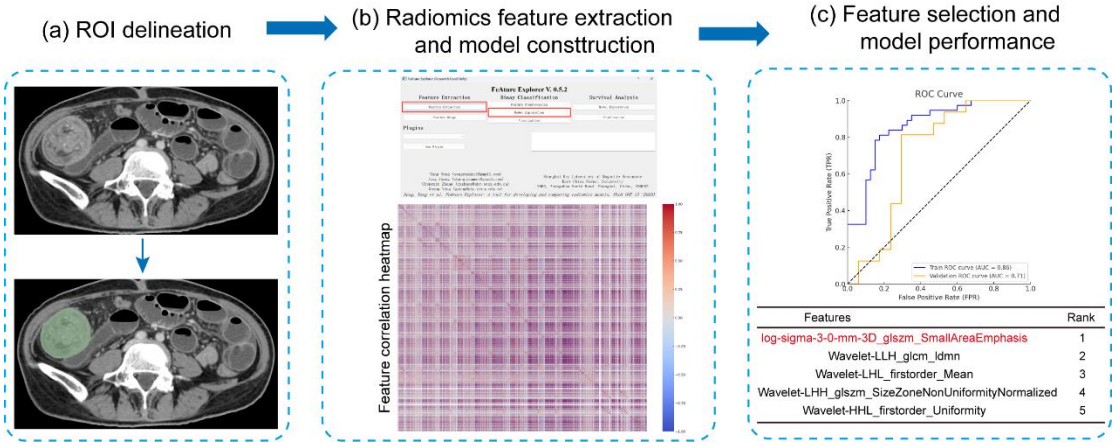

Figure R7. Radiomics workflow. CT-based radiomics begins with region of interest (ROI) delineation to define the area of analysis in the contrast-enhanced CT images. Radiomics features are extracted and the most significant 5 features are identified. Small Area Emphasis (SAE) represents vascular enhancement and ranks first in these 5 features. Finally, SAE value in the CT images of non-metastatic and liver-metastatic colorectal cancer patients are analyzed.

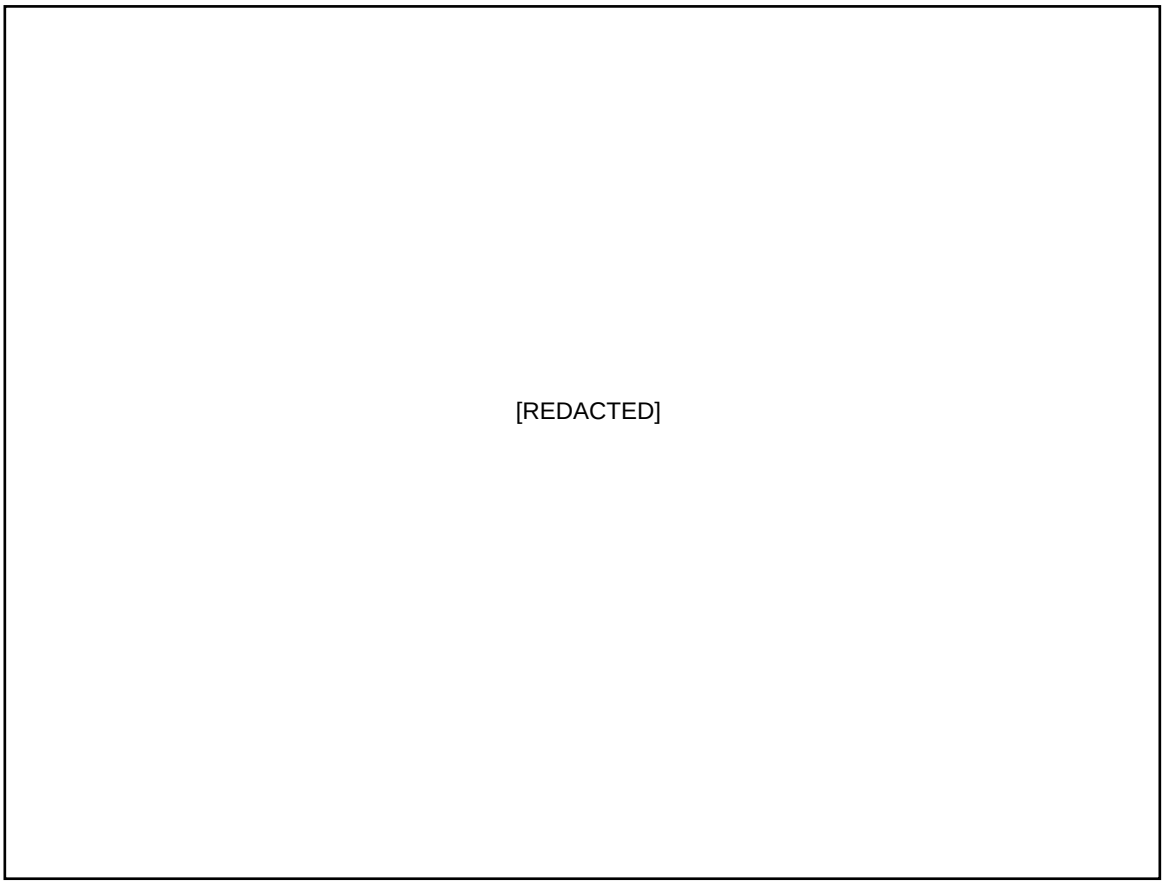

Figure R8. Radiomics feature extraction codes. The codes and parameters used to extract radiomics feature from CT images.

2) The authors present ROC curves but no explanation on how those where computed. Was this based on human-labeled datasets? Show examples.

Response: Thanks for your question. ROC curve analysis was based on the data collected from the first affiliated hospital of Jinan University and analyzed by ourselves. For colorectal cancer (CRC), a total of 93 patient specimens were involved, among them, 44 CRC patients developed liver metastasis and 49 patients without metastasis. The ratio of NKX2-3$^+$ TPCs in the primary tumor of 93 CRC patients was analyzed by immunofluorescence and quantified (**Figure 2g**). Then ROC curve was created in Graphpad Prism software (https://www.graphpad.com/guides/prism/latest/statistics/stat_howto_roc.htm), and the raw data has been uploaded in the Source Data file. The optimal cutoff value of NKX2-3$^+$ TPC ratio to predict CRC liver metastasis was determined according to the ROC

curve. For lung cancer, a total of 90 patient specimens were involved, among which, 49 patients developed hematogenous metastasis and 41 patients without metastasis. The ratio of NKX2-3^{+} TPCs in each specimen was analyzed (**Supplementary Figure 5c**) and ROC curve was created in the same way. We have added the corresponding description in the supplementary methods **(Please see page 6 in the revised Supplementary Information).**

3) Of much concern with respect to the in vitro calcium imaging experiments presented in Fig3 (and supplemental material as well); the authors describe a protocol where the measurements are performed under a calcium free medium: "... Then, TPCs were washed with the calcium-free PBS twice and calcium influx was examined under the Zeiss LSM 800. Under such conditions,..." (supp methods, pp 6). Under such conditions, there is no calcium influx and changes in the indicator intensity can be attributed to internal calcium release, not influx.

Response: Thank you for pointing out this mistake, we are sorry for the misleading description. For calcium imaging, TPCs were washed with the calcium-free PBS (KCl 2.7 mM, KH_2PO_4 2.0 mM, NaCl 137 mM, Na_2HPO_4 10 mM) twice and finally incubated with Kreb's solution (NaCl 119 mM, KCl 4.7 mM, $NaHCO_3$ 25 mM, KH_2PO_4 1.2 mM, $MgCl_2 \cdot 2H_2O$ 1.0mM, $CaCl_2 \cdot 2H_2O$ 2.5 mM, D glucose 11.1 mM) supplemented with (S)-(-)-Bay K8644 (10 μM). (S)-(-)-Bay K8644 was used to activate the L-type calcium channel and intracellular influx of calcium derived from the Kreb's solution. The calcium influx before and after (S)-(-)-Bay K8644 (10 μM) treatment was examined under the Zeiss LSM 800 confocal microscope and analyzed by GraphPad Prism. Therefore, (S)-(-)-Bay K8644-induced calcium influx was derived from extracellular calcium. The corresponding description has been added in the methods **(Please see page 8-9 in the revised Supplementary Information).**

4) Further, authors should present "baseline" measurements prior to treatment, computing the relative change and reporting this value. Also make sure to indicate what treatment has been added in each experiment to elicit the reported changes.

Response: Thanks for your valuable suggestion. We have presented the baseline measurement prior to (S)-(-)-Bay K8644 (BayK) treatment and the relative changes of Fluo-4AM fluorescence intensity in each experiment **(Figure R9)**. The treatment for each calcium imaging assay was clearly indicated **(Please see Figure 3b, f, i, j in the revised manuscript; Supplementary Figure 7a, g, k, l, Supplementary Figure 8a and Supplementary Figure 21e in the Supplementary Information).**

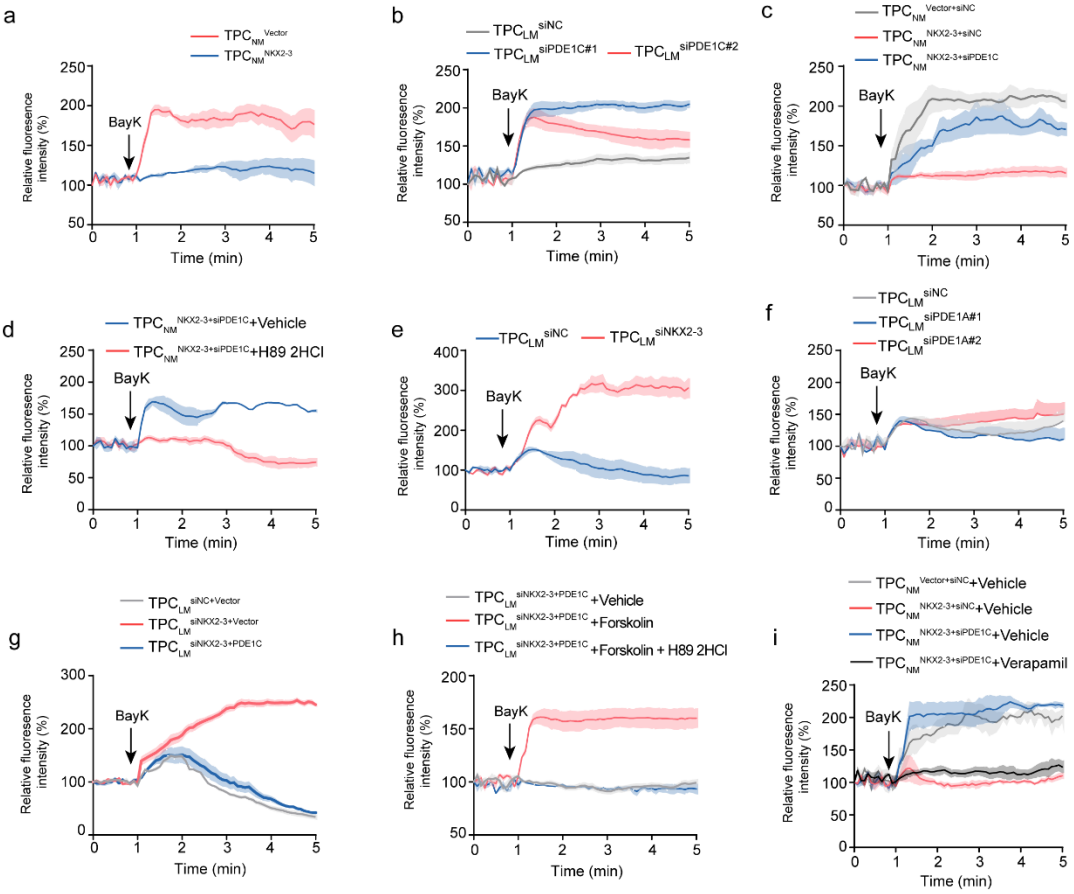

Figure R9. Fluo-4AM assay for calcium detection. a Fluo-4AM fluorescence intensities in TPC_{NM}^{Vector} and TPC_{NM}^{NKX2-3} (n = 3). **b** Differential changes of Fluo-4AM intensity in PDE1C-knockdown TPC_{LM} (n = 3). **c** Fluo-4AM fluorescence analysis of intracellular calcium in NKX2-3-overexpressing TPCs with PDE1C-knockdown (n = 3). **d** Fluo-4AM fluorescence assay for the intracellular calcium in $TPC_{NM}^{NKX2-3+siPDE1C}$ pre-treated with or without H89 2HCl (10 μM) (n = 3). **e** Fluo–4AM fluorescence intensities of TPC_{LM}^{siNC} and $TPC_{LM}^{siNKX2-3}$ (n = 3). **f** Differential changes of Fluo-4AM intensity in response to PDE1A-knockdown in TPC_{LM} (n = 3). **g** Fluo-4AM fluorescence analysis of intracellular calcium in TPC_{LM}^{siNC} and $TPC_{LM}^{siNKX2-3}$ with

indicated transfection (n = 3). **h** Fluo-4AM fluorescence analysis of intracellular calcium in $TPC_{LM}^{siNKX2-3+PDE1C}$ pre-treated with forskolin (10 μM) or H89 2HCl (10 μM) (n = 3). **i** Fluo-4AM fluorescence analysis of intracellular calcium in TPCs with indicated transfection and verapamil (5 μM) (n = 3). Data are presented as mean ± SEM. BayK, (S)-(-)-Bay K8644. TPC, tumor pericyte.

5) Of much concern is the statement that a specific treatment/transgenic modification has negligible effects on pericyte density given the significant reduction across all diameter categories is misleading (see for example supp Fig 11B). Deletion of single pericyte has been show to induce changes in vascular physiology.

Response: Thanks for your comments. The Supplementary Figure 11B (revised **Supplementary Figure 15b)** showed that specific deletion of *Nkx2-3* in TPCs reduced vascular diameter, compared to PC^{lin} mice, the proportion of small vessels with a diameter of 0-50 μm was significantly higher in PC^{lin-KO} mice, while the proportion of large vessels with a diameter over 50 μm was decreased in PC^{lin-KO} mice. Therefore, the average of vessel diameter was significantly decreased in PC^{lin-KO} mice compared with that in PC^{lin} mice.

Pericyte is indeed a critical regulator for vascular physiology, including vascular permeability, perfusion, pericyte-endothelial interaction, vascular tone and blood flow[10-13]. However, pericyte density is not the only cause leading to the change of vessel diameter, various factors including optogenetic stimulation, chemical stimulus and calcium transition could induce vasodilation or vasoconstriction without altering pericyte coverage[14-16]. Our results showed that genetic or pharmacological manipulation of NKX2-3 in pericytes had negligible effects on pericyte coverage, whereas NKX2-3 suppressed TPC contraction and induced vasodilation through inhibiting calcium influx**.**

6) When comparing in vivo between treatments and control for different conditions, please present always relative changes and analysis statistics accordingly (eg correctly done in supp 18D but not in E). The key aspect here is the slope of change; as previously

mentioned, plot this changes as a function of the initial vessel diameter.

Response: Thanks for your insightful comments, the data in **Supplementary Figure 23e** was re-analyzed and presented as RBC velocity change (%) **(Figure R10)**. The function is (v2-v1)/v1×100% **(Please see Supplementary Figure 23e in the revised Supplementary Information).**

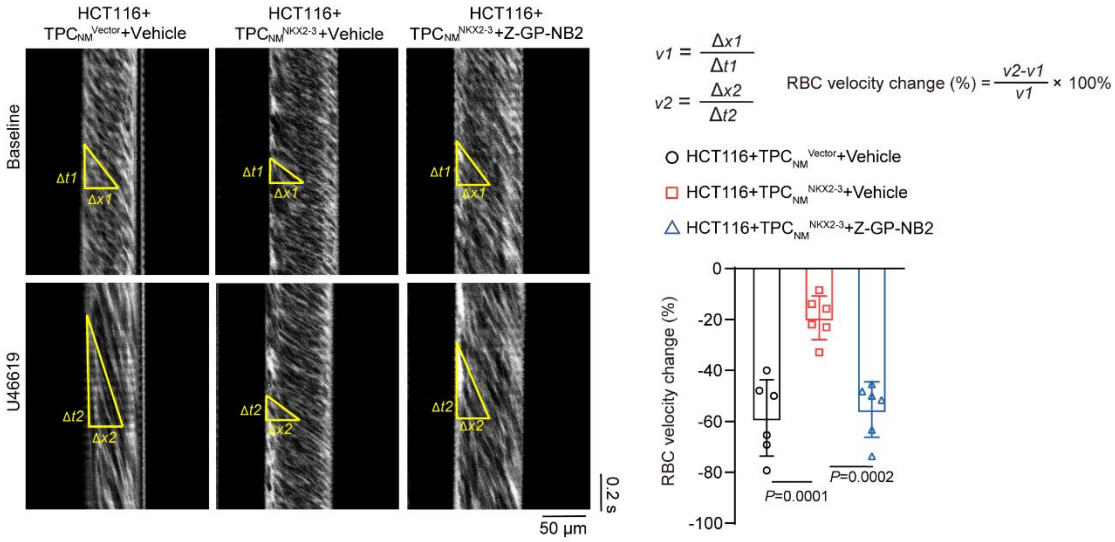

Figure R10. Z-GP-NB2 decreases RBC velocity in HCT116 xenografts. Two-photon microscopy analysis for relative RBC velocity changes in HCT116 xenografts-bearing mice before and post-treatment with U46619. Data are presented as mean ± SEM, *P* values were determined by one-way ANOVA followed by Tukey's post hoc test. RBC, red blood cell.

7) Please provide evidence showing that the AAV vector targeted pericytes by quantifying expression against a pericyte marker (eg. NG2 in proximity to CD31), the data provided in Fig 4I is not sufficient). Data for "baseline" calcium dynamics should be presented in both mouse (control and knockout). Again, data should be presented as relative changes in addition to the nominal expression level.

Response: Thanks for your valuable suggestions, to investigate the specific localization and expression of GCamp6 in TPCs, AAV-CMV bGlobin-FLEX-Gcamp6-WPRE-hGH polyA virus induced by *Cspg4*-Cre recombinase were intravenously (i.v.) administered into PC^{lin} and PC$^{lin\text{-}KO}$ mice. Therefore, GCaMP6 was only expressed in NG2^{+} TPCs surrounding tumor vessels. The calcium dynamics in PC$^{lin\text{--}GCaMP6}$ and PC$^{lin\text{-}KO\text{--}GCaMP6}$

mice was quantified and presented as relative changes **(Figure R11) (Please see page Figure 4g in the revised manuscript).**

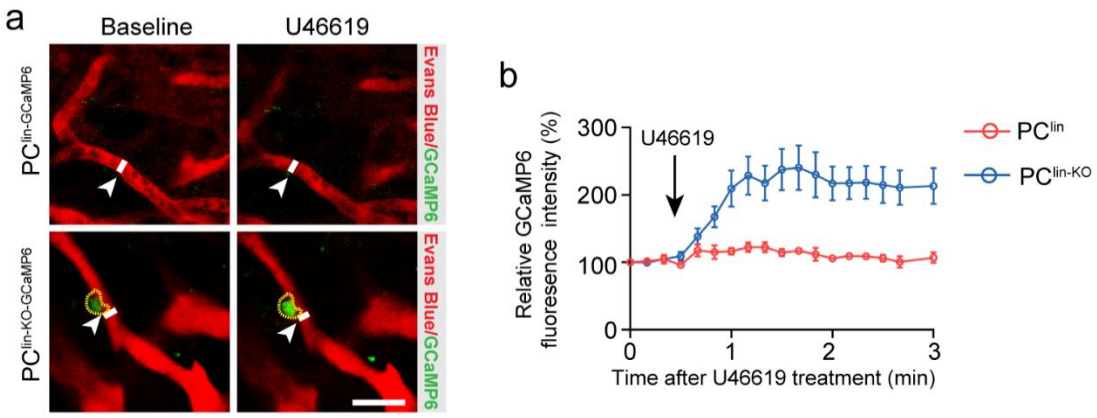

Figure R11. Pericyte-specific deletion of *Nkx2-3* increases TPC calcium level. a Representative images of GCaMP6 expression in TPCs from $PC^{lin\text{-}GCaMP6}$ and $PC^{lin\text{-}KO\text{-}GCaMP6}$ mice treated with U46619. Scale bar, 20 μm. Yellow circles indicate GCaMP6 expression in TPCs, white arrows and lines indicate vascular diameter in mouse tumor. **b** Quantification of calcium dynamics in TPCs. Data are presented as mean ± SEM (n = 6). TPC, tumor pericyte.

Response to Reviewer 3 (expert in pericytes, metastasis)

Comments to the Author:

Colorectal cancer liver metastasis demonstrates increased blood vessel size and a subset of tumor pericytes (TPCs) were found to be associated with metastasis in patients. In mice, conditional loss of NKX2-3, marking the subset of TPC of interest, reduced blood flow by vasoconstriction, implicating calcium influx signaling, and resulted in decreased metastasis. Vascular leakage, presumed to be driver component of tumor metastasis, was reduced with blockage of NKX2-3 in TPCs. The authors propose NKX2-3 as a marker of TPC may have 'diagnostic' (the authors may have meant prognostic?) and therapeutic potential. There are mechanistic regulation studies included, and implication of EVs as possible mediators of TPC regulation with impact on metastasis. Overall, this is a very comprehensive study with an overwhelming amount of data, and yet presented beautifully. This is amongst the most interesting

paper this reviewer has had the pleasure to review in recent past. There is nonetheless an important point of confusion with respect to vessel diameter and blood flow detailed further below. This may need additional clarification in the text. The abstract may need to be revised to include more mechanistic information, EVs, and pharmacological design of a new compound with anti-metastatic properties.

Response: We feel great thanks for your professional review work on our study. As you are concerned, there are several problems need to be addressed. According to your kind suggestion, we have discussed the association between vessel diameter and blood flow, and made extensive corrections to our previous abstract **(Please see page 3, line 65-67 in the revised manuscript).** As the reviewer suggested, the "diagnostic" has been corrected into "prognostic" **(Please see page 4, line 73; page 21, line 453 in the revised manuscript)**.

1) The introduction places high blood flow in the tumor microenvironment as possibly rate limiting, via shear stress induction for example, for hematogenous metastasis. This appears contradictory to the thesis of the manuscript, wherein high blood flow is presumed to be associated with increased metastasis. Generally, the concept of vessel diameter and blood flow is inversely proportional (Bernoulli's equation). The larger the diameter of a vessel, the slower the flow, not faster. This would actually make more logically sense with the argument proposed by the authors: altering NKX2-3 pericytes function to relax tumor blood vessels would increase diameter, alter permeability, and reduce sheer stress by reducing local blood flow.

Response: We appreciated your valuable comments. There are several things that keep Bernoulli's principle from being straightforwardly applied in blood flow. Bernoulli considered, for simplicity, fluids that are nonviscous or frictionless under steady streamline flow, so-called "ideal" fluids. Blood flow in a vascular network is positively associated with pressure difference between the arterial and venous and negatively associated with viscous and geometric resistances[17]. The main shortcomings of the Bernoulli equation are that it overlooks blood cells and viscosity of blood flow, which creates viscous resistance. Additionally, blood circulation is a closed system with

laminar flow and turbulent flow, and blood vessels, especially capillaries have multiple parallel branches and various diameters, which generates geometric resistance and makes it unsuitable to apply Bernoulli's equation[18, 19]. Quantities of studies support that vascular mural cells including smooth muscle cells and pericytes exert vasodilation effects and leading to increased blood flow [14-16, 20, 21]. Indeed, the increase of blood flow generates high shear stress, which can dissociate circulating tumor cell (CTC) clusters and favor CTC fragmentation. However, reduced flow promoted early arrest of CTCs in the blood flow and impaired tumor metastasis [22, 23]. Thus, pro-metastatic vascular regions are characterized by intermediate flow profiles that are sufficiently low to favor the survival and adhesion of CTCs, and sufficiently high to stimulate endothelial remodeling and CTC extravasation. In this study, we found NKX2-3 in TPCs induced vasodilation and increased blood flow, thus facilitating tumor metastasis. We will further investigate the effects of pericyte-NKX2-3 on the shear stress of tumor blood flow, and explored the combined effects of blood flow and shear stress on tumor cell metastasis**.**

2) Figure 1: how blood flow measurements are made are unclear. What is shown in Figure 1A? What is blood flow signal and how does this translate to velocity (flow) of blood? These measures appear to reflect vascular density (increased angiogenesis) rather than flow. There are no measures of flow in the method, nor data expressed as a velocity of blood (blood volume over time) through vessels. This is a critical point that the authors should carefully review and clarify. The methods may need illustration of the steps taken to arrive at the "signal strength value" in Figure 1A.

Response: Thanks for your valuable questions. Blood flow in tumor was measured by Doppler ultrasound imaging and the images of tumors derived from colorectal cancer patients with or without liver-metastasis were collected and analyzed by us. **Figure 1a** presented the blood flow signal strength in the primary tumor of non-metastatic colorectal cancer (NM CRC) and liver-metastatic colorectal cancer patients (LM CRC), and the quantification was shown in the right. In ultrasound Doppler images, red and blue regions conventionally represent blood flow rather than vascular density, with red

indicating arterial flow and blue indicating venous flow. To quantify these regions, Open Source Computer Vision Library (OpenCV, https://opencv.org) was utilized for image processing. First, the color space was converted from BGR to HSV to facilitate precise segmentation of color-coded areas. Then specific HSV color ranges were defined for both red and blue flow regions, applying these ranges to create binary masks that isolated the areas of interest. These masks were applied to extract the corresponding blood flow regions from the original image. To further improve the segmentation accuracy, OpenCV's edge detection algorithms were employed, refining the boundaries of the extracted regions. Finally, within these segmented regions, the average saturation and brightness values were calculated to evaluate the blood flow signal strength, resulting in an objective quantification of blood flow intensity within the ultrasound Doppler images. The detailed description about the analytic methods has been added in the methods **(Please see page 26, line 553-566 in the revised manuscript)**.

3) While vessel diameter and basement membrane continuity data are convincing (Figure 1E-G), it should be noted that this does not equate patency of vessel, and that to make a case for increase vessel diameter is associated with increased flow, the correlation graphs in Figure 1H-J need to be clarified (see point above) as whether this reflects 'flow' or merely angiogenesis. Hypoxia increase (Figure 1G) with vessel diameter in LM CRC support that these vessels are likely non patent. This contradicts the thesis that "flow" (as 'small area emphasis value'??) would be increase in area that have larger diameter vessels but are also more hypoxic… Taken together, the data is confusing and contradictory: Large diameter vessels in LM CRC have less laminin (likely defective/leaky/non patient) and more hypoxia (logical), but have greater blood 'flow'? (not logical). Please clarify.

Response: We thank the reviewer for the highly valuable comments. In **Figure 1i-k**, small area emphasis value indicates the blood flow in the tumor region, rather than angiogenesis. We have added description about Figure 1a, b **(Please see page 35, line 742-745 in the revised manuscript).**

We supposed that tumor hypoxia condition is not only affected by the local blood

flow, but also the flow patterns (e.g., laminar or turbulent), and the geometry of the vessel (e.g., straight or curved/branched), tumor vessels turned to be irregular and leaky in metastatic cancer patients, thus impaired oxygen supply and leading to hypoxia condition [24]. Concerning vascular leakiness and greater blood flow[25, 26], we suggested it was caused by pericyte relaxation, NKX2-3 overexpression suppressed TPC calcium influx and induced TPC relaxation, leading to vasodilation and increased blood flow, meanwhile, TPC relaxation loosened the tight junctions between endothelial cells and increased vascular permeability, thus the tumor vessels in metastatic patients have greater leakiness and blood flow **(Please see page 20, line 413-424 in the revised manuscript).**

4) Figure 1. What is the number of vessels (independent of size or laminin staining) in LM CRC vs NM CRC and is there a positive correlation with 'flow'?

Response: Thanks for your comments. The number of vessels was calculated as microvessel density. As shown in **Figure 1e**, no significant difference was observed in microvessel density between LM CRC and NM CRC. The correlation between microvessel density and blood flow was analyzed, and the results showed that there was no positive correlation **(Figure R12) (Please see page 7, line 139-141; Figure 1h in the revised manuscript).**

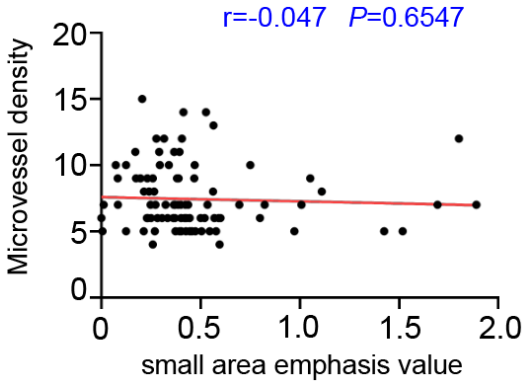

Figure R12. Microvessel density is not correlated with blood flow. Pearson correlation analysis of microvessel density with the signal of blood flow (small area emphasis value) in the primary tumor of colorectal cancer patients (n = 93).

5) scRNASeq data in Figure 2: is NKX2-3 expressed in lymphatic endothelial cells? can the author demonstrate that NKX2-3 is specific to pericytes and not found in endothelial cells or other cells in CRC microenvironment/cancer cells? Supplementary Figure 1 does not address this.

Response: Thanks for your constructive questions. ScRNA-seq was performed on the TPCs derived from the primary tumor of non-metastatic and liver-metastatic colorectal cancer patients, which only contains data of TPCs. The expression of NKX2-3 in TPCs, smooth muscle cells (SMCs), endothelial cells (ECs), lymphatic endothelial cells (LECs), cancer-associated fibroblasts (CAFs) and HCT116 cells were examined by western blot. The results showed that NKX2-3 was specifically highly expressed in TPCs derived from CRC patients with liver metastasis compared with other cells **(Figure R13) (Please see page 8, line 165-167 in the revised manuscript; Supplementary Figure 3c in the revised Supplementary Information).**

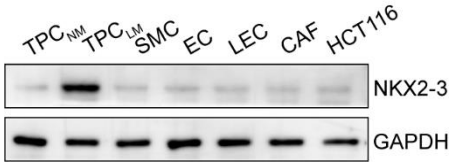

Figure R13. NKX2-3 is specifically expressed in TPC$_{LM}$. Western blot assay for NKX2-3 expression in TPC$_{NM}$, TPC$_{LM}$, SMC, EC, LEC, CAF and HC116 cells. CAF, cancer-associated fibroblast; EC, endothelial cell; LEC, lymphatic endothelial cell; SMC, smooth muscle cell; TPC, tumor pericyte.

6) The data in Figure 2 related to immunolabeling of tumors is clearly presented and convincing. The authors also validated this finding in breast cancer. Please show uncropped western blots for Figure 2E. Were the authors able to control for possible biases in Figure 2I-J, wherein other features of cancer progression at time of analysis (metastatic burden to other organs, performance status, treatment) to solidify the association between NKX2-3 TPC rich tumors and survival? Where the 93 patients all with LM CRC? Note that the color choice (red and blue) for the curves in I and J is confusing with respect to the panel G above where in red is used for NM CRC and blue is used for LM CRC.

Response: Thank you very much for pointing out these problems. The uncropped bots for Figure 2e were shown below **(Figure R14).** All the uncropped bands were presented in the Source Data.

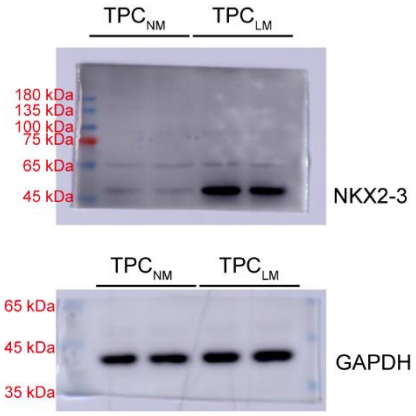

Figure R14. Uncropped bot bands for NKX2-3 and GAPDH.

For survival analysis, a total of 93 colorectal cancer (CRC) patients were involved (patient information was listed in the **revised Supplementary Table 6**), among which, 44 CRC patients experienced liver metastasis (LM CRC), while the remaining 49 CRC patients did not develop metastasis (NM CRC). Those 93 CRC patients did not undergo radiotherapy or chemotherapy before the operation. Univariate analysis was performed to examine the prognostic factors in colorectal cancer patients, M0/M1 stage, tumor stage and NKX2-3^{+} TPC ratio were identified as factors significantly correlated with prognosis (**Table R1**) (**Please see page 9, line 176-178 in the revised manuscript; Supplementary Table 4 in the revised Supplementary Information).**

Table R1. Univariate analysis of the prognostic factors in colorectal cancer patients.

[REDACTED]

Additionally, the colors used in Figure 2j have been changed, the red color indicated survival of patients with NKX2-3^{+} TPC ratio (≤ 43%), while the blue color indicated the survival of patients with NKX2-3^{+} TPC ratio (> 43%) **(Figure R15). (Please see Figure 2i and 2j in the revised manuscript).**

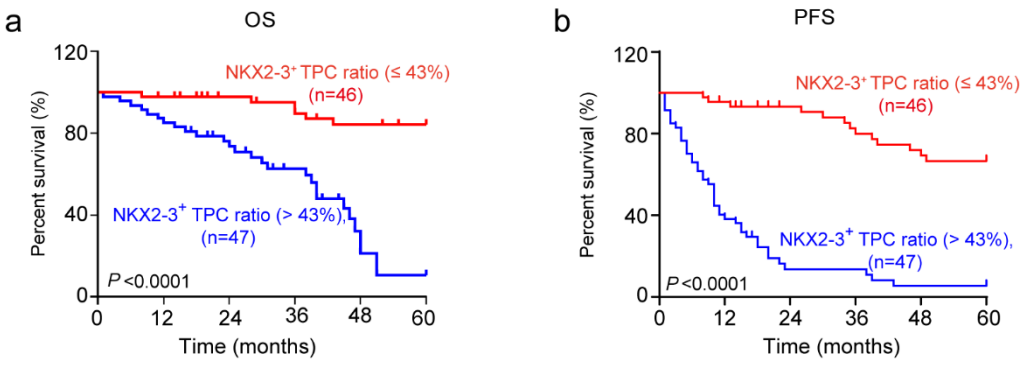

Figure R15. NKX2-3 in TPCs is associated with poor prognosis of colorectal cancer patients. a, b Kaplan-Meier analysis of OS **(a)** and PFS (**b**) in CRC patients with a high (n=47) or low (n=46) NKX2-3$^+$ TPC ratio (optimal cutoff value of 43%). *P* values were determined by log-rank (Mantel-Cox) test. CRC, colorectal cancer; OS, overall survival; PFS, progression-free survival; TPC, tumor pericyte.

7) Contractility studies in Figure 3 are presented clearly and with appropriate controls. The significance of the quantification for panel L is difficult to appreciate. Consider a bar graph at 48 hours and individual values shown. Is this signaling specific to TPC? Would cancer cells or fibroblasts fail to demonstrate similar response (not worth testing experimentally if not already done, but interesting to include if data exist)? The source for verapamil was not found.

Response: Thanks for your remainder, the bar graph at 48 h has been added **(Figure R16) (Please see Figure 3l in the revised manuscript).** As indicated above, NKX2-3 was specifically highly expressed in TPCs, rather than tumor cells and cancer associated fibroblasts (CAFs), therefore, we supposed that NKX2-3-induced cell contraction was specific to TPCs. We are very sorry that we do not have experimental data to support this conclusion currently. The source for verapamil was indicated in the supplementary file **(Please see page 8 in the revised Supplementary Information).**

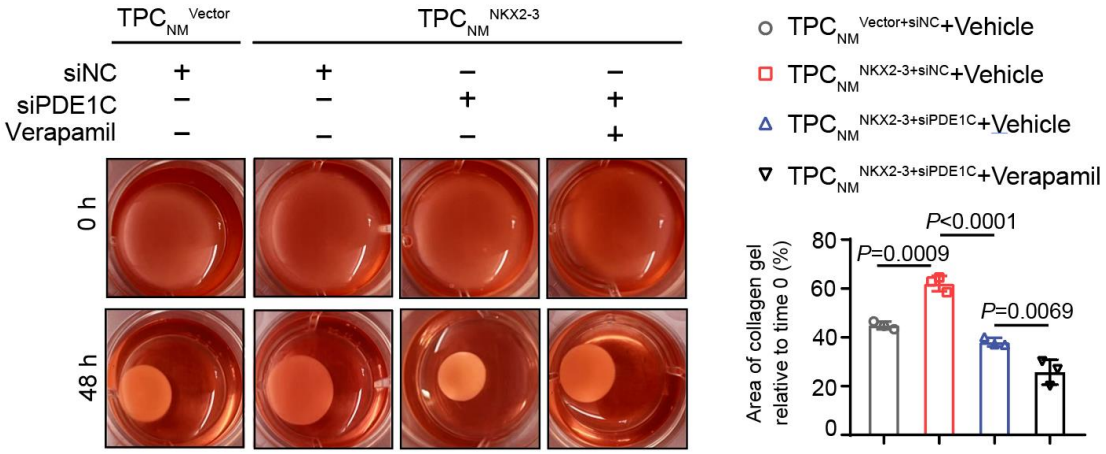

Figure R16. NKX2-3 in TPCs inhibits cell contraction through suppressing the Ca^{2+} axis. Representative images and quantification of collagen contraction induced by the indicated TPC_{NM}^{Vector} and TPC_{NM}^{NKX2-3}. TPCs with indicated transfection were pre-treated with verapamil (5 μM). Data are presented as mean ± SEM (n = 3). *P* values were determined by one-way ANOVA followed by Tukey's post hoc. TPC, tumor pericyte.

8) Figure 4: generally a well conducted in vivo study. What is the tumor growth kinetics in PClin vs PClin-KO mice? The details of the orthoptic implantation of MC-38 is also not found in the methodology. Please clarify what is measured in D (pericyte coverage, which pericyte marker was used, how was it quantified).

Response: We really appreciate the reviewer pointing out these problems. The tumor growth kinetics in PC^{lin} and $PC^{lin\text{-}KO}$ mice bearing MC-38 allografts were detected by *in vivo* bioluminescence assay. Deletion of *Nkx2-3* in pericytes had negligible effects on tumor growth **(Figure R17) (Please see page 12, line 251; Figure 4a in the revised manuscript, Supplementary Figure 12a in the revised Supplementary Information).**

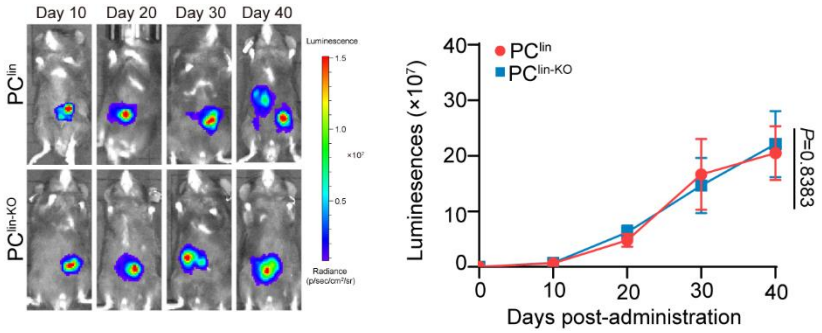

Figure R17. Conditional deletion of *Nkx2-3* in TPCs has negligible effects on tumor growth. bioluminescence assay for the orthotopic tumor growth kinetics in PC^{lin} and $PC^{lin\text{-}KO}$ mice. The luminescence of primary tumor was quantified. *P* value was determined by two-tailed unpaired *t*-test.

For orthotopic implantation of MC-38 allografts, MC-38-luc-LM3 cells or MC-38-GFP-LM3 cells (1×10^5) were suspended in 100 μL of Matrigel and injected into the cecum wall of PC^{lin} and $PC^{lin\text{-}KO}$ mice, which were previously anesthetized with isoflurane inhalation. Mouse tumor growth and metastasis were detected by *in vivo* imaging system **(Please see page 6 in the revised Supplementary Information)**.

Figure 4d is a statistical diagram for pericyte coverage in the primary tumor of PC^{lin} and $PC^{lin\text{-}KO}$ mice, and the representative images were shown in the Supplementary Figure 15a, α-SMA was used to label TPCs and CD31 was used to label tumor vessel endothelial cells. Pericyte coverage was evaluated according to previous study[27], the α-SMA positive area and CD31 positive area were quantified using Image J, and then the ratio of α-SMA positive area to CD31-positive area was calculated as pericyte coverage **(Please see page 11; Supplementary Figure 15a in the revised Supplementary Information).**

9) Figure 5: the demonstration of blood flow in this experiment is much clearer than the confusions that stemmed from Figure 1. It remains however confusing why the increase in blood vessel diameter is associated with increased blood flow (again, contradictory to Bernoulli's principle). Are the authors observing that vasodilatory properties of NKX2-3+ TPC generates permeability and facilitates extravasation of cancer cells independent of blood flow? The imaging data indicating true flow changes

in tumors vs showing more tumor angiogenesis and vascular destabilization? The dynamicity of tumor angiogenesis during tumor growth has been extensively reported, and it is therefore critical that the authors demonstrate tumor volume at time of study, and whether metastases are seen in the liver at that time point.

Response: Thanks for your question. As we discussed above, blood flow is viscosis and unsteady, which could not be explained by Bernoulli's equation. The effects of NKX2-3 in TPCs on tumor cell extravasation was further determined. In contrast to primary tumor, our results showed that NKX2-3 was undetected in TPCs in the liver metastatic tumor derived from CRC patients (**Figure R18**). Therefore, NKX2-3 in TPCs facilitates tumor intravasation and metastasis through regulating vessel permeability and hemodynamics, which has negligible effects on tumor cell extravasation **(Please see page 9, line 170-171 in the revised manuscript; Supplementary Figure 4 in the revised Supplementary Information)**.

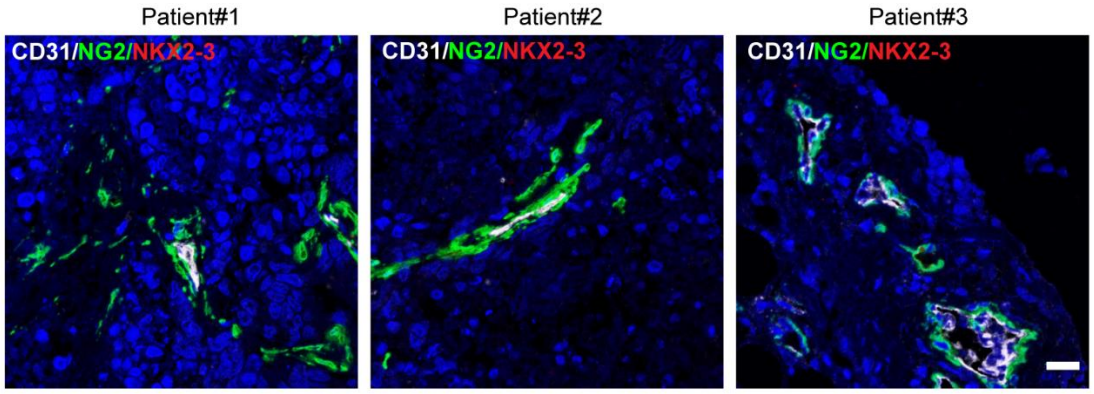

Figure R18. NKX2-3 is undetected in TPCs from the hepatic metastases. Representative images of NKX2-3 staining (red) in TPCs ($NG2^+$, green) in hepatic metastases derived from CRC patients (n = 20). Scale bar, 20 μm. TPC, tumor pericyte.

NKX2-3 overexpression in TPCs indeed induced vascular destabilization as indicated by loosen junctions between endothelial cells and vascular leakiness, however, no significant difference was observed in microvessel density (**Figure 4d**) and pericyte coverage (**Supplementary Figure 15a**) between PC^{lin} and $PC^{lin\text{-}KO}$ group, suggesting that specific deletion of *Nkx2-3* in TPCs had negligible effects on angiogenesis. The tumor growth kinetics in PC^{lin} and $PC^{lin\text{-}KO}$ mice bearing MC-38 allografts were shown in **Figure R19**. At the end of experiments, no significant difference was observed in the

primary tumors of PC^{lin} and $PC^{lin\text{-}KO}$ mice, however, liver metastasis was developed in the PC^{lin} mice (**Figure R19**). These data indicate that deletion of *Nkx2-3* in pericyte had negligible effects on tumor angiogenesis and growth **(Please see page 12, line 251-252; Figure 4a in the revised manuscript, Supplementary Figure 12a in the revised Supplementary Information).**

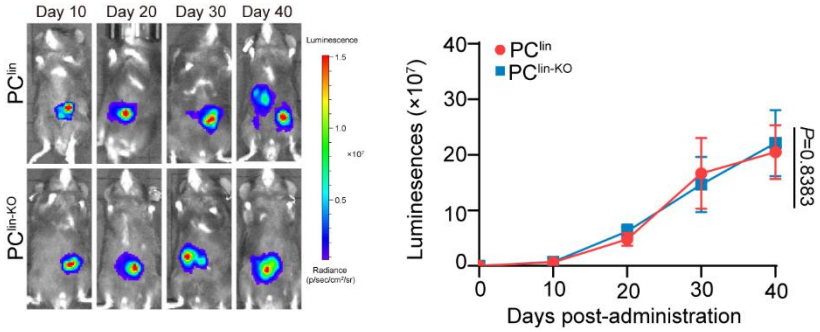

Figure R19. Conditional deletion of *Nkx2-3* in TPCs has negligible effects on tumor growth. bioluminescence assay for the orthotopic tumor growth kinetics in PC^{lin} and $PC^{lin\text{-}KO}$ mice. The luminescence of primary tumor was quantified. *P* value was determined by two-tailed unpaired *t*-test.

10) The exosomes study in Figure 6 is interesting and welcome, though the manuscript is already quite dense. The authors may want to mention this axis of regulation in their abstract. The dosing of how much exosomes to use to treat cells and whether this dosing is relevant to human disease is a vexing question in the field. These experimental details must be provided, and dose responses could be included. This may be more convincing than using Rab27a knockdown, given this does not always translate in impaired biogenesis and can impact cargo content. Have exosomes with NEAT1 been captured in the blood of CRC LM (and compared to CRC NM?)?

Response: Thanks for your insightful comments. As suggested, we have mentioned the extracellular vehicles (EVs)-mediated signaling axis in the abstract (**Please see page 3, line 65-67 in the revised manuscript**). The dose of EVs used in this study was 1 μg, and a dose-dependent experiment was performed, the results showed DLD-1^{NEAT1} EVs induced NKX2-3 upregulation in a dose-dependent manner **(Figure R20a)**.

EVs were isolated from colorectal cancer patients using Exosupur columns (Cat.

ES9P11e, Echobiotech, Beijing, China), and RNA of EVs were extracted with Exosomal RNA Purification Kit (Cat. 5202050, SIMEN, Hangzhou, China) according to the instruction description. the level of EVs-enriched lncRNA *NEAT1* in the blood of LM CRC patients was significantly higher than that in NM CRC patients **(Figure R20b) (Please see page 16, line 337-338, line 343-345; Figure 6m, q in the revised manuscript).**

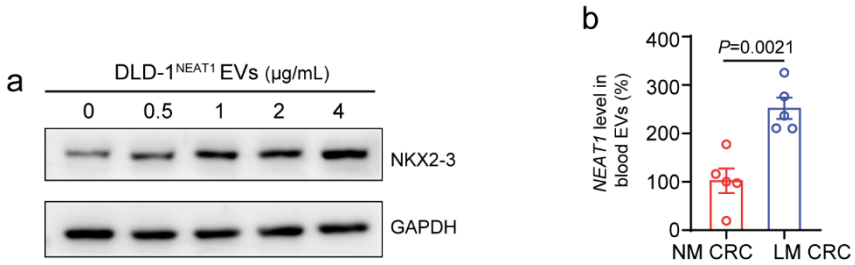

Figure R20. LncRNA *NEAT1* is highly enriched in extracellular vesicles derived from colorectal cancer patients with liver metastasis. a Western blot assay for NKX2-3 expression in TPCs treated with EVs in a does dependent manner. EVs were derived from *NEAT1*-overexpressing DLD-1 cells (n = 3). **b** LncRNA *NEAT1* level in the blood of colorectal cancer patients with (n = 5) or without (n = 5) liver metastasis. Data are presented as mean ± SEM. *P* value was determined by two-tailed unpaired *t*-test. EVs, extracellular vesicles; LM CRC, liver-metastatic colorectal cancer; NM CRC, non-metastatic colorectal cancer.

11) Is NEAT 1 expression in TPC correlating with vessel diameter/'flow'/laminin from Figure 1?

Response: Thanks for your comments. The correlation between *NEAT1* expression in TPCs and vascular diameter, blood flow and laminin were analyzed. The results showed that *NEAT1* expression in TPCs was positively associated with microvessel diameter **(Figure R21a)** and blood flow **(Figure R21b)**, however, *NEAT1* expression was negatively associated % of laminin$^+$/VWF$^+$ area **(Figure R21c) (Please see page 17, line 345-349 the revised manuscript; Supplementary Figure 18o-q in the Supplementary Information).**

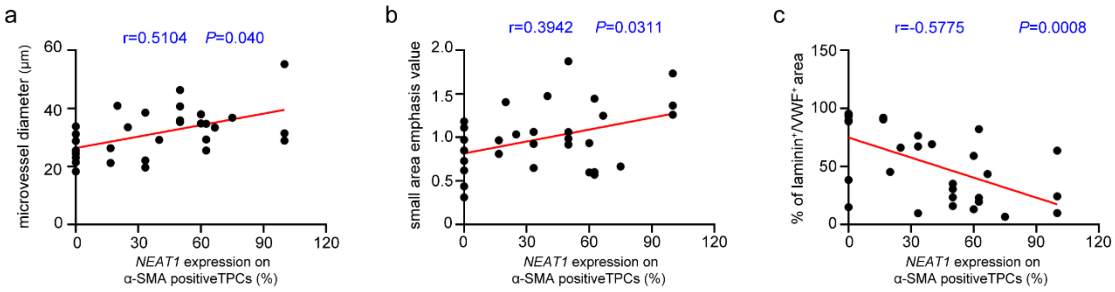

Figure R21. *NEAT1* expression in TPCs is correlated with microvascular diameter, blood flow and laminin. a-c Pearson correlation analysis of microvessel diameter. (**a**), the signal of blood flow (small area emphasis value) (**b**) and % of laminin^{+}/VWF^{+} area (**c**) with *NEAT1* expression in TPCs (n = 30). TPC, tumor pericyte.

12) Figure 7. the authors used human xenografts, was this because Z-GP-NB2 activity relies on human proteins rather than murine? Ideally, if species cross reactivity is possible, evaluating the anti-metastatic effect of Z-GP-NB2 on the genetically engineered models (GEM) with MC38 orthotopic tumors would be quite interesting. If Z-GP-NB2 fails to show additional benefit (reduced metastasis) in NKX2-3 conditional deletion GEM, it would support target specificity. In vitro, would over expressing NKX2-3 in TPC limit the impact of Z-GP-NB2? Does Z-GP-NB2 limit the impact of tumor derived EVs on TPC?

Response: Thanks for your comments. Since NB2 is a peptide designed and synthesized based on human NKX2-3 protein (https://alphafold.ebi.ac.uk/entry/Q8TAU0), which is different from mouse NKX2-3 protein (https://alphafold.ebi.ac.uk/entry/P97334). Therefore, human xenografts and co-injection model were used to investigate the anti-metastatic effects of prodrug Z-GP-NB2. The anti-metastatic effects of Z-GP-NB2 on MC-38 allografts were also evaluated, however, Z-GP-NB2 did not further reduce the liver metastasis of PC$^{lin\text{-}KO}$ mice bearing MC-38 allografts **(Figure R22)**, indicating that Z-GP-NB2 activity relies on human NKX2-3.

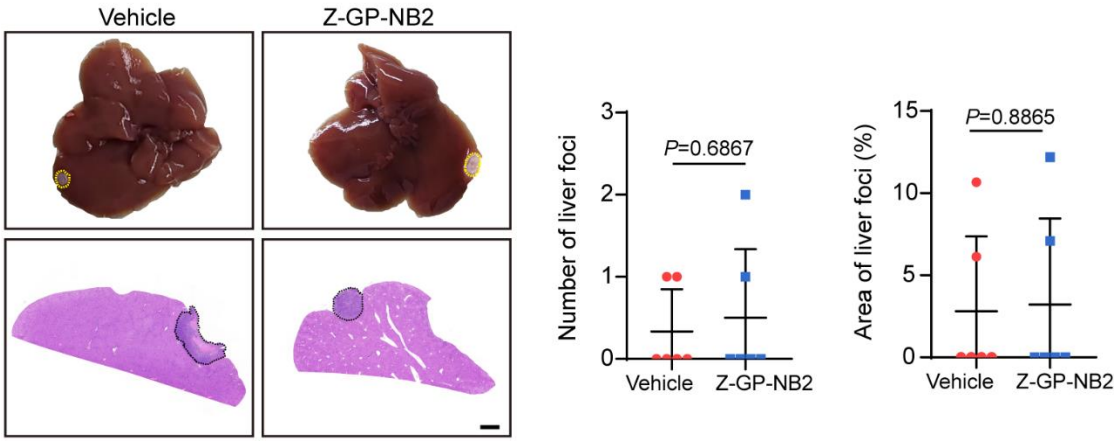

Figure R22. Z-GP-NB2 has negligible effects on MC-38 allografts. Representative images of whole livers and H&E analysis of liver metastatic foci derived from $PC^{lin\text{-}KO}$ mice bearing MC-38-allografts (n = 6). The yellow and black dotted lines indicate the metastatic foci. Scale bar, 500 μm. *P* values was determined by two-tailed unpaired *t*-test.

To investigate whether NKX2-3 in TPCs limit the impact of Z-GP-NB2, TPC_{NM}^{Vector} and $TPC_{NM}^{NKX2\text{-}3}$ were treated with Z-GP-NB2 and TPC contraction was determined by examining the expression of p-$MLC2^{Ser15}$, the results showed that Z-GP-NB2 significantly induced p-$MLC2^{Ser15}$ upregulation $TPC_{NM}^{NKX2\text{-}3}$, while it had negligible effects on TPC_{NM}^{Vector} **(Figure R23a)**. This is because the expression of NKX2-3 is low in TPC_{NM}^{Vector}, and the basal level of p-$MLC2^{Ser15}$ in TPC_{NM}^{Vector} is high. Z-GP-NB2 targeted NKX2-3^{high} TPCs, therefore, overexpression of NKX2-3 in TPCs could not limit the effects of Z-GP-NB2.

Moreover, TPCs incubated with DLD-1^{NEAT1} EVs were further treated with Z-GP-NB2, and then the expression of NKX2-3 in TPCs was detected, the results revealed that Z-GP-NB2 had negligible effects on the expression of NKX2-3 in these two groups **(Figure R23b)**. Z-GP-NB2 is a FAPα-activated prodrug that target NKX2-3^{high} TPCs, which was specifically hydrolyzed into NB2 and penetrated into TPC nucleus, NB2 exerted anti-metastatic effects through suppressing the transcriptional activity of NKX2-3 and hindering the downstream signaling, while tumor derived EVs are the key factors inducing NKX2-3 overexpression in TPCs. Therefore, Z-GP-NB2 could not

limit the effects of tumor derived EVs on TPCs **(Please see page 18, line 380-383 in the revised manuscript; Supplementary Figure 21i-j in the revised Supplementary Information).**

Figure R23. Z-GP-NB2 targets NKX2-3^{high} TPCs. a Western blot assay for p-MLC2^{Ser15} and MLC2 expression in TPC$_{NM}^{Vector}$ and TPC$_{NM}^{NKX2-3}$ treated with Z-GP-NB2 (n = 3). **b** Western blot assay for NKX2-3 expression in TPCs treated with DLD-1 cells-derived EVs and Z-GP-NB2 (n = 3). EVs, extracellular vesicles.

13) Minor: a typo was found in the abstract: Blood “blow”. The author may want to define CRCLM when first used in the text, this reviewer did not see it spelled out.

Response: Thank you for pointing out these mistakes. We have examined the spelling and abbreviations in this manuscript, and corrected these mistakes **(Please see page 3, line 63; page 6, line 107 in the revised manuscript).**

Response to Reviewer 4 (expert in Nkx2.3 biology)

Comments to the Author:

In this manuscript submitted by Li X et al the impact of NKX2-3 (in mice Nkx2-3) transcription factor in pericytes in the hematogenic hepatic metastatic expansion of colorectal (and other cancers, including breast cancer and pulmonary metastasis of melanoma) was investigated using an impressive battery of state-of-the-art methodology. The authors have found that in CRC samples with increased blood flow the tumor pericytes (TPCs) contain a specific subset with increased expression of NKX2-3. This increase is associated with reduced contractility via a PDEC1/cAMP/PKA-mediated Ca-dependent mechanism, whereas pericyte-specific

deletion of Nkx2-3 (in mice) restores vasoconstriction. One mechanism that may be involved in the upregulation of NKX2-3 in pericytes (hence increased blood flow) is the exosomal transfer of long non-coding RNA NEAT1 interfering with miR-769-5p, thus forming a regulatory loop for NKX2-3 production. As a potential downstream target gene, PDE1C was identified, which upregulation could be prevented by inhibition of NKX2-3 binding to sequence target via FAPa-catalyzed metabolism of a peptide derivative prodrug. The results are consistent and suggest a novel potential approach for reducing hepatic metastasis during the course of CRC. Some issues need clarification, though.

1. Major concerns:

1.1 What is the expression of pericyte-associated NKX2-3 in the non-malignant segment of colon tissue of the metastatic and non-metastatic samples? On Fig 2G only tumor tissues are presented. This needs to be demonstrated to confirm that the differences are tumor-related without potential individual variations of NKX2-3 variations, irrespectively of the tumor status of the patients. Also, the authors claim that the t-SNE demonstration reveals only the increase of cluster #3 cells – clearly, cluster #1 also shows increase, with NKX2-3 expression spanning both - please clarify.

Response: We thank the reviewer for these interesting questions. We collected para-carcinoma tissues from colorectal cancer (CRC) patients with or without liver metastasis (**patient information was listed in Supplementary Table 8**), and immunofluorescence staining showed that NKX2-3 was non-detected in the para-carcinoma tissues derived from non-metastatic and liver-metastatic CRC patients **(Figure R24) (Please see page 9, line 169-170 in the revised manuscript; Supplementary Figure 3d in the Supplementary Information).**

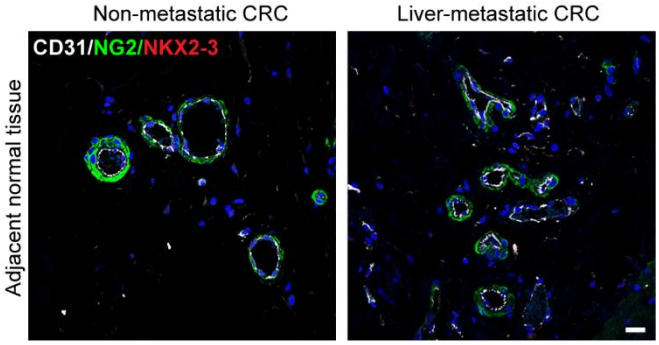

Figure R24. NKX2-3 is non-detected in para-carcinoma tissues of colorectal cancer patients. Representative images of NKX2-3 expression in TPCs derived from the para-carcinoma tissues of colorectal cancer patients (n = 10). Scale bar, 20 μm.

In Figure 2a, the cell counts of cluster 1 in non-metastatic and liver-metastatic samples was 1,997 and 2,607, respectively **(Figure R25a)**. However, the proportion of cluster 1 over all analyzed cells decreased from non-metastatic to liver-metastatic samples (16.0% vs. 10.8%) **(Figure R25b)**. This is because the total number of cells from the non-metastatic samples were much less than the liver-metastatic samples (12,448 vs. 24,237). Therefore, we solely focused on cluster 3. **(Please see Figure 2a in the revised manuscript; Supplementary Figure 2b in the Supplementary Information).**

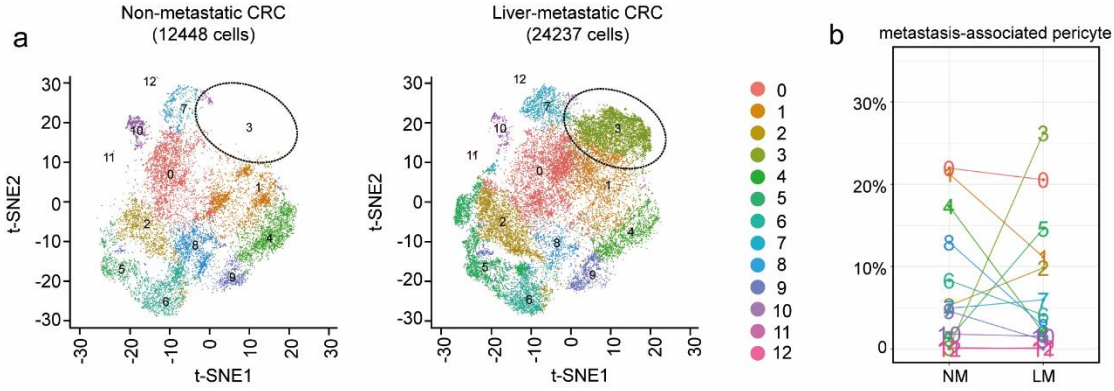

Figure R25. MAP was increased in liver-metastatic CRC. a t-SNE visualization of TPC subsets derived from primary tumor tissues of CRC patients with (n = 2) or without (n = 2) liver metastasis. **b** The ratio of each TPC cluster in non-metastatic CRC and liver-metastatic CRC samples. CRC, colorectal cancer; MAP, metastasi-associated pericyte; t-SNE, t-distributed stochastic neighbor embedding.

1.2 Importantly, as the immunohistochemistry uses a polyclonal-polyclonal antibody binding procedure for NKX2-3 staining, control labeling (replacing the specific first Ab with irrelevant Ig) is also needed for both the immunofluorescence and the Western blot analysis (Fig. 2E) to confirm specificity. Also, Supplemental Fig. 2A the pulmonary metastatic breast cancer/NKX2-3 image shows intense red signal in non-

vascular/aSMA-negative cells – can the authors define these cells, especially that many of these do not seem to stain with the nuclear marker (specification also missing from the image)?

Response: Thanks for your questions. To confirm the specificity of NKX2-3 antibody, in the immunofluorescence and western blot assay, NKX2-3 antibody (RRID: AB_2680088, Sigma) was replaced with Rabbit IgG (Cat. GB111738-100, Servicebio), and other procedures remain the same. No signal or bands of IgG were observed in the western blot **(Figure R26a)** and immunofluorescence analysis **(Figure R26b) (Please see page 8, line 164-165 in the revised manuscript; Supplementary Figure 3a, b in the Supplementary Information).**

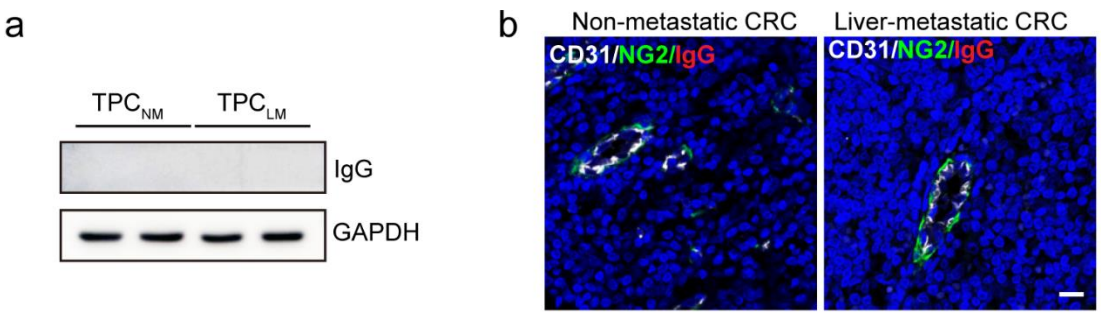

Figure R26. Validation of NKX2-3 antibody. a Western blot assay for IgG expression in TPCs derived from the primary tumor of NM and LM colorectal cancer patients (n = 3). **b** Representative images of IgG expression in TPCs derived from non-metastatic (n = 10) and liver-metastatic (n = 10) colorectal cancer patients. Scale bar, 20 μm. CRC, colorectal cancer; LM, liver-metastatic; NM, non-metastatic.

We apologize for the poor quality of images in Supplementary Fig. 2a, which is misleading and unreadable. We have repeated the immunofluorescence assay and improved the quality of these images **(Figure R27) (Please see Supplementary Figure 5a in the revised Supplementary Information).**

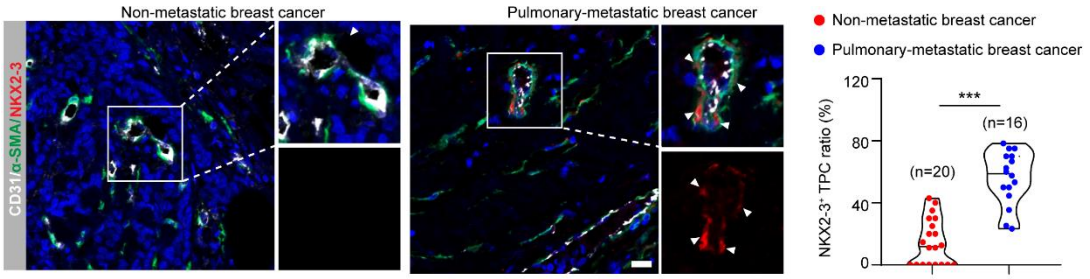

Figure R27. NKX2-3 is highly expressed in pulmonary-metastatic breast cancer patients. Immunofluorescence staining and quantification of the NKX2-3$^+$ TPC ratio in tumor sections from breast cancer patients. The white arrows indicate NKX2-3 staining in TPCs. Scale bar, 20 μm. Each sample in the violin plots represents data from an individual patient. *P* value was determined by two-tailed unpaired *t*-test.

1.3 The main cellular subsets of the colonic lamina propria with NKX2-3 expression are the CD34-positive endothelial cells and the VAP-1/AOC3-positive pericryptal myofibroblasts (Hsia et al, 2016 PNAS; Gabris et al, 2024, J Histochem Cytochem). In mucosal HEV endothelial cells, NKX2-3 exerts its regulatory function with COUP-TFII (Dinh et al., 2022 Nat Commun), whereas the pericryptal myofibroblasts are involved in the intestinal stem cell niche formation (Hsia et al, 2016 PNAS). Could these pericryptal/non-endothelial cells correspond to the pericytes? And if so, can the modulation of their NKX2-3 activity affect colonic epithelial homeostasis, thus CRC progression?

Response: Thanks for your questions. Pericytes are mural cells embedded within the basement membrane of tumor vessels. As the reviewer suggested, NKX2-3 is highly expressed in myofibroblast, endothelial cells and high venous (HEV) endothelial cell[28-31], all these cells are not pericytes. Here, we demonstrated that NKX2-3 in tumor pericytes facilitated tumor metastasis through regulating vasodilation and hemodynamics, however, the effects of myofibroblasts and endothelial cells-derived NKX2-3 on the epithelial homeostasis and tumor progression remain to be further studied.

1.4 The authors claim that the NKX2-3 protein-blocking peptide Z-GP-NB2 has only

negligible in vivo effect on normal tissues, demonstrated by H&E staining (supplemental Fig. 16B) of heart, spleen, kidney (NB written as "kiney") and lung – the authors need to test/demonstrate the expression of mucosal HEV MAdCAM-1 (as one cardinal NKX2-3 target), to exclude non-pericyte target effects.

Response: Thanks for your comments and pointing out the spelling mistake. We have corrected the Kiney into kidney. As the reviewer suggested, NKX2-3 is also expressed in mucosal high endothelial venule (HEV) and regulates the expression of MAdCAM-1in HEV[31, 32], therefore, the expression of MAdCAM-1 in the mouse mucosal HEV after Z-GP-NB2 treatment was examined by immunofluorescence, the results revealed that Z-GP-NB2 had negligible effects on the development of mucosal HEV and MAdCAM-1 expression on HEV cells **(Figure R28) (Please see Please see page 18, line 385-386 in the revised manuscript; Supplementary Figure 22b in the revised Supplementary Information).**

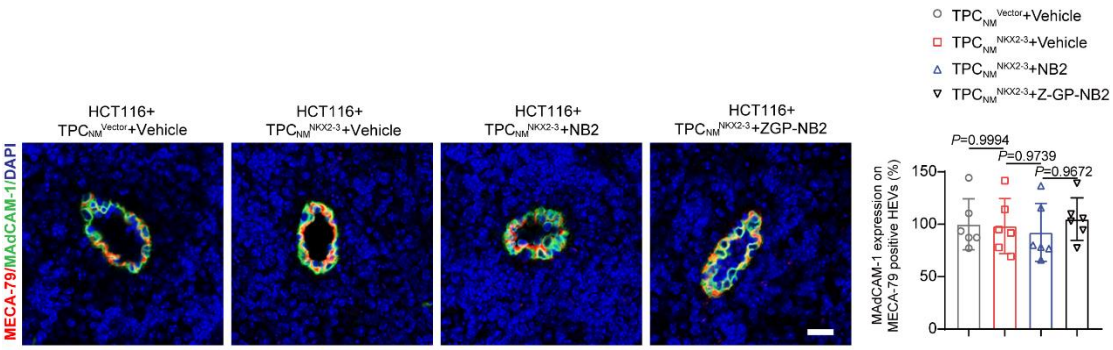

Figure R28. Z-GP-NB2 has negligible effects on the MAdCAM-1 expression in mucosal HEV. Immunofluorescence analysis of MAdCAM-1 expression in mucosal HEVs of HCT116 xenografts-bearing mice (n = 6). Scale bar, 20 μm. Data are presented as mean ± SEM. *P* values were determined by one-way ANOVA followed by Tukey's post hoc test.

1.5. CRC also often generates lymph node metastases – have the authors observed any effect of Nkx2-3 deletion in TPCs on the degree of mesenteric lymph node infiltration?

Response: We appreciate the reviewer's valuable question. To investigate the effects of pericyte NKX2-3 on tumor lymph node metastasis, lymph node-metastatic MC-38 cells were established (MC-38-LNM cells) according to previous study[33]. Metastatic

lymph node (LN) tissues were harvested from MC-38 allografts-bearing mice that developed LN metastasis. Metastatic LN tissues were cut into small pieces (~1 mm^3), and digested with the tumor tissue dissociation kit as described above. Single-cell suspension of digested tissues was filtered through a 100 μm filter and selected with anti-CD326 microbeads (Cat. 130-061-101, Miltenyi Biotec.). The sorted cells were termed as MC-38-LNM cells. MC-38- LNM cells (1×10^5) were suspended in 100 μL of Matrigel and injected into the cecum wall of PC^{lin} and $PC^{lin\text{-}KO}$ mice, which were previously anesthetized with isoflurane inhalation. Mouse metastasis was detected by *in vivo* imaging system and H&E staining. The results showed that specific deletion of *Nkx2-3* in TPCs had negligible effects on lymph node metastasis of CRC **(Figure R29a)**. Both PC^{lin} and $PC^{lin\text{-}KO}$ mice bearing MC-38-LNM allografts developed lymph node infiltration **(Figure R29b)**. Mesenteric lymph node infiltration of tumor cells is mainly through lymphatic vessels[33]. However, lymphatic capillaries are composed of endothelial cells and a thin basement membrane without pericyte coverage, whereas collecting lymphatic vessels contain lymphatic smooth muscle cells[34, 35]. Therefore, conditional deletion of *Nkx2-3* in TPCs had negligible effects on lymphatic vessels and lymph node metastasis **(Please see page 12-13, line 255-257 in the revised manuscript; Supplementary Figure 14 in the revised Supplementary Information).**

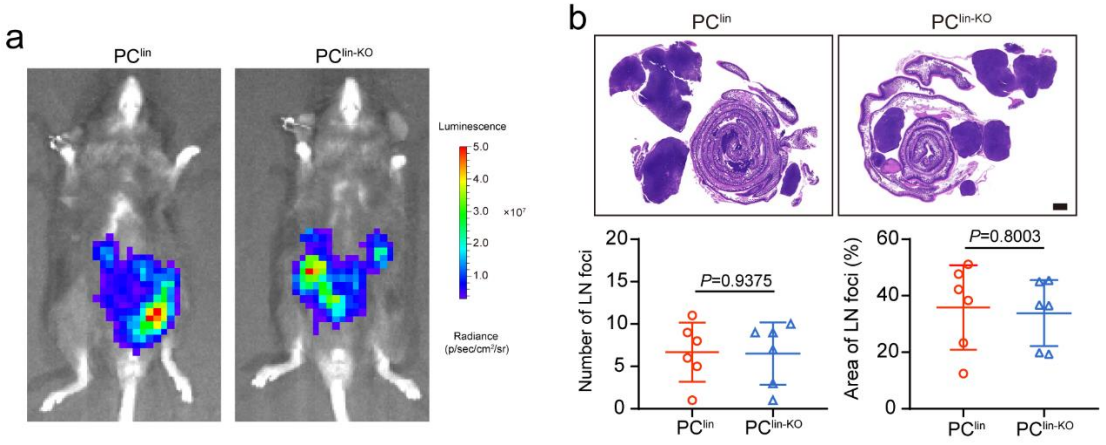

Figure R29. Pericyte specific deletion of *Nkx2-3* has negligible effects on lymph node metastasis. a Representative images of bioluminescence signals in mice orthotopically injected with MC-38-LNM cells. **b** H&E staining and quantification for the number and area of lymph node metastasis in tumor-bearing PC^{lin} and $PC^{lin\text{-}KO}$ mice.

Scale bar, 1 mm. *P* values were determined by two-tailed unpaired *t*-test. LN, lymph node; LNM, lymph node metastasis; PC, pericyte.

1.6. Regarding TPC isolation and downstream scRNAseq: The Materials and methods is very vague/brief on how TPCs were isolated, and Authors refer to their recent publication (Li X et al, Gut, 2023) where this dataset was generated; but even in this cited previous work the Materials and methods are not too descriptive. How are Authors sure of the cells' TPC identity? Also, it would be important to show the tSNEs of the 4 individual samples (eg. as Supplementary Figure 1A, or main Figure 2B) to be able to assess patient variation, and also to show how many cells/patients are included in the analysis. Furthermore, while in both this current work and the cited publication a total of 13 clusters of TPC are visible, the tSNE looks different – why? If it's exactly the same dataset, did authors modify analysis settings? If yes, why?

Response: Thank you for pointing out these problems. TPCs were isolated by microdissection combined with pericyte medium-based approach (MPMA) according to our previous study [6]. As shown in **Figure R30C**[6], freshly resected human CRC tissues were placed in ice-cold DMEM containing PS and transported to the laboratory within 1 h. Following washing with pre-cooled PBS supplemented with 0.1% gentamicin, 0.1% ciprofloxacin, and 0.1% kanamycin in a sterile dissection hood, fibrous, and adipose tissues around the muscular layers of tumor tissues were carefully removed. The remaining tissues were cut into small pieces along the colon mucosa into the muscular layer, followed by fastening in a sylgard-coated petri dish using ice-cold PBS and a surgical needle. For TPC collection, ascending capillaries (diameter ≈ 20 μm) derived from arterioles were gently separated along the mucosa into the submucosa from perivascular adipose tissues using eye scissors (Geuder, G-19745) under a stereomicroscope (SZX7; Olympus) (**Figure R30D, E**). The attached adipose tissues were then removed, and the dissected capillaries were transferred to fresh dishes containing PM. The TPCs migrated from the vascular samples to the culture plate within 14 days (**Figure R30F**). When the cells reached 80% confluence, they were dissociated using trypsin, collected, and transferred to a 60 mm-diameter culture dish.

The culture medium was gently replaced every two days. TPCs were authenticated using STR Multi-amplification Kit, and tested negative for mycoplasma using the Mycoplasma Detection Set[6]. The purity of the isolated TPCs was confirmed using FACSort (**Figure R30G**), and the isolated TPCs were identified by transmission electron microscopy (**Figure R30H**), immunofluorescence (**Figure R30I, J**) and flow cytometry (**Figure R30K, L**) as previously described, which are characterized by high nuclear/cytoplasmic ratio and pericyte markers including NG2, PDGFRβ, and CD146, as well as mesenchymal stromal cell antigens CD44 and CD105. The detailed methods for TPC isolation and identification were added in the Supplementary methods (**Please see page 1 in the revised Supplementary Information**)

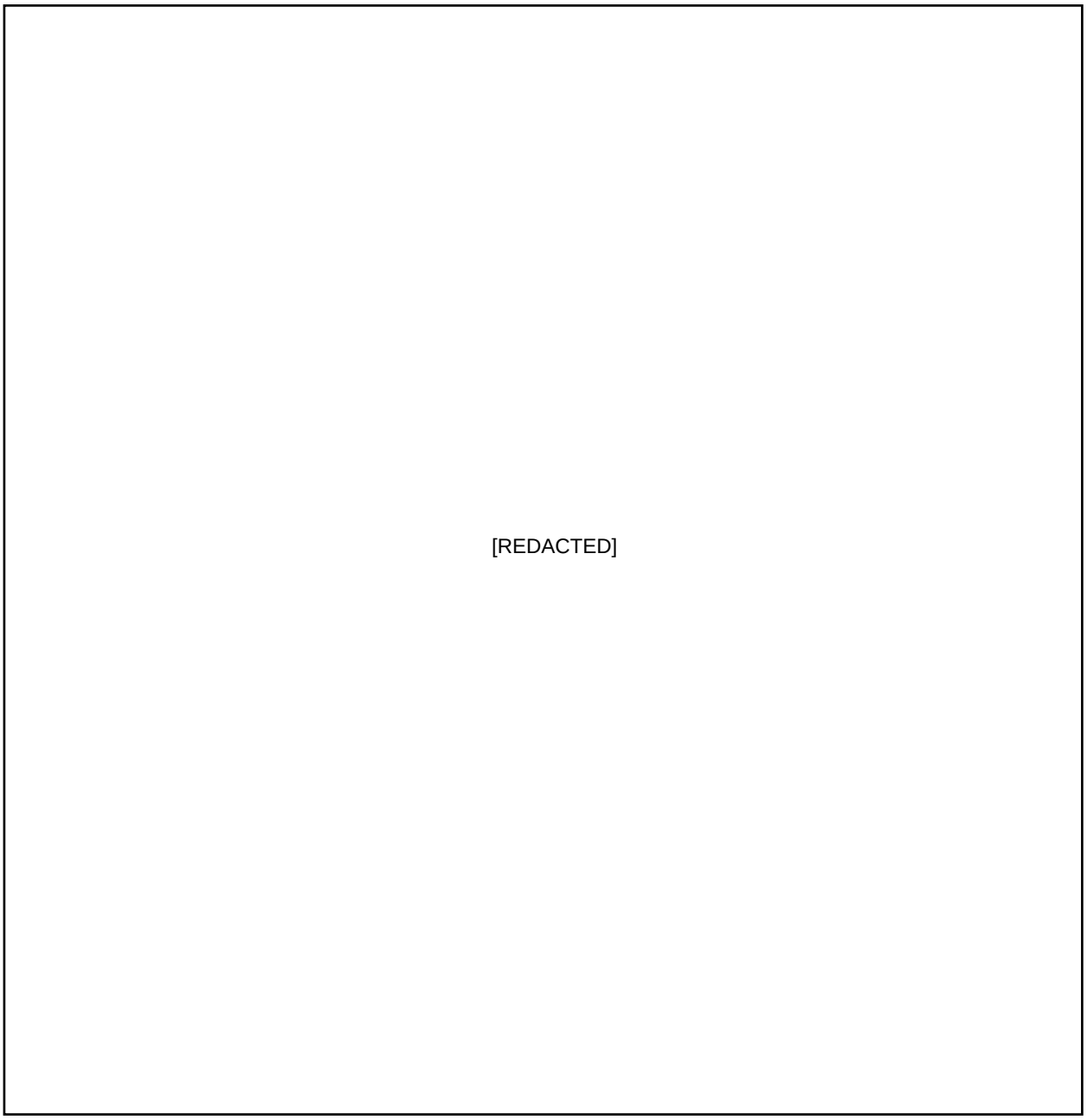

Figure R30. Isolation and validation of TPCs[6]. (A) Immunofluorescence staining for PC markers including NG2 or PDGFRβ (green) in tumor blood vessels (CD31, red) with various diameters (n = 40). The white arrowhead indicates the PCs-containing capillaries. Scale bar, 50 μm. (B) Plot diagram of the diameters in PCs-containing capillaries (n = 40). Data are presented as mean ± SEM. (C) Diagram depicting the isolation of tumor blood vessels from CRC patients. (D) Representative images of blood

vessels dissected from tumor tissues under the stereomicroscope (n = 6). Scale bar, 50 μm. (E) Representative images for the capillary chips (n = 6). Scale bar, 50 μm. (F) Representative images for TPC migration and expansion from the cultured capillary chips (n = 6). Scale bar, 50 μm. (G) Flow cytometry analysis of NG2 expression in TPCs at passage 2 (n = 6). (H) Representative TEM images of the tumor vessels and TPCs (n = 6). Scale bar, 1 μm (left); 2 μm (right). (I) Immunofluorescence analysis of CD31 expression in HMEC-1 cells. Phalloidin-rhodamine was used to identify F-actin. Scale bar, 20 μm. (J) Immunofluorescence analysis of indicated markers in TPCs (n = 6). Phalloidin-rhodamine was used to identify F-actin. Scale bar, 20 μm. (K) Flow cytometry analysis of CD31 in HMEC-1 cells (n = 6). (L) Flow cytometry analysis for the expression of endothelial cells, epithelial cells, mesenchymal stromal cells, and pericyte markers in cultured TPCs (n = 6).

As suggested, the t-SNE of the 4 individual samples were shown **(Figure R31)**. A total of 4 patient TPCs were involved in the scRNA-seq, 2 of which were non-metastatic CRC patients, and the other 2 were liver-metastatic CRC patients. The number of TPCs in each sample was labeled in the images. The tSNE plots are different from the cited publication [36], as 1) the Seurat R package for analysis was different in this study from the original cited publication (v4.4.0 vs. v3.1.1); 2) stochastic process is involved in tSNE (t-distributed stochastic neighbor embedding), which could result in different plot pattern even the same version of R package was used **(Please see page Supplementary Figure 1 in the Supplementary Information).**

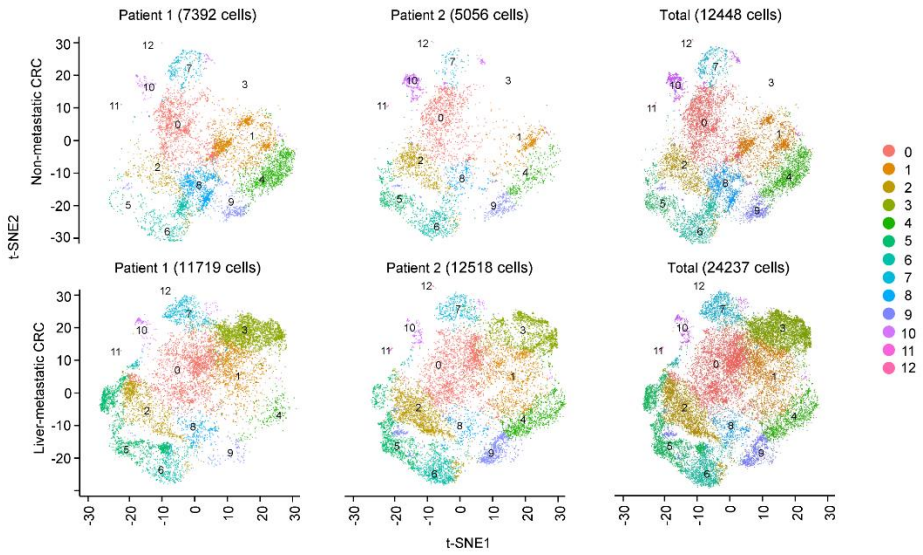

Figure R31. t-SNE of TPC subsets. t-SNE visualization of TPC subsets derived from primary tumor tissues of CRC patients with (n = 2) or without (n = 2) liver metastasis. t-SNE, t-distributed stochastic neighbor embedding

2. Minor points:

2.1 Some figures have insufficient explanation. In addition to the ones above, Fig. 1E and F microvascular surface area % and CA9 staining intensity % are described - % of what? Fold difference, rather? Furthermore, how reliable is 2D/conventional microscopy in determining these parameters (especially surface area, diameter, length)? Confocal microscopy/3D might be better.

Response: Thanks for your questions and pointing out these problems, microvascular surface area, laminin and CA9 were analyzed according to previous study[37, 38], microvascular surface area (%) was calculated as VWF^+ area/tumor area. Laminin expression surrounding endothelial cells was calculated as % of $laminin^+$/ VWF^+ area. CA9 expression was calculated as % of $CA9^+$ /tumor area **(Figure R32) (Please see Figure 1e-g in the revised manuscript).**

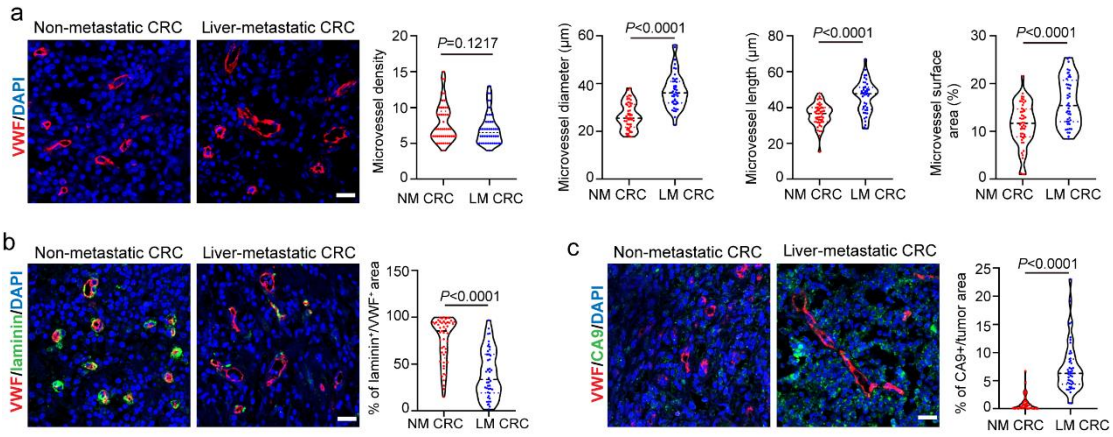

Figure R32. Vessel morphology and integrity in colorectal cancer patents. a Immunofluorescence analysis of microvessel density, microvessel diameter, microvessel length and microvessel surface area in the primary tumor of NM CRC (n = 49) and LM CRC patients (n = 44). Scale bar, 20 μm. **b** Immunofluorescence analysis of laminin^{+}/VWF^{+} area per field in in the primary tumor of NM CRC (n = 49) and LM CRC patients (n = 44). Scale bar, 20 μm. **c** Immunofluorescence analysis of CA9^{+}/tumor area in the primary tumor regions derived from NM CRC (n = 49) and LM CRC patients (n = 44). Scale bar, 20 μm. Each sample in the violin plots represents data from an individual patient. *P* values were determined by two-tailed unpaired *t*-test. LM CRC, liver-metastatic colorectal cancer; NM CRC, non-metastatic colorectal cancer.

The characteristics of microvessels were examined by immunofluorescence and the images were obtained using Zeiss LSM 800 confocal microscopy. Microvessel density, microvessel diameter, length and surface area were quantified by Image J software. The 3D characteristics of mouse tumor vessels was also examined by light-sheet imaging (**Figure 4c**), the results revealed that tumor vessels were more dilated and irregular arranged in PC^{lin} mice compared with that in PC$^{lin\text{-}KO}$ mice **(Please see Figure 4c in the revised manuscript).**

2.2 Supplemental Fig. 7A is confusing – I surmise that in PClin wt NKX2.3 PCR product is detected (450 bp in the upper left inset) whereas the floxed allele is slightly larger (lower left) – but what is being shown in the upper right inset (with no product) and the lower right (perhaps the Cre-complemented Floxed NKX2-3 genotype sample

with 386 bp)? NB the images are now presented with slightly truncated size marking throughout the images.

Response: Thanks for your questions. *Nkx2-3*-flox mice (B6/JGpt-*Nkx2-3*^{em1Cflox}/Gpt; T016620) were acquired from GemPharmatech Co., Ltd. (Nanjing, Jiangsu, China), and the protocol for the validation of mouse *Nkx2-3* genotyping was provided by GemPharmatech Co., Ltd. As shown in the **Figure R33** (https://cn.gempharmatech.com/shop/productDetails/24711), primer 1 and primer 2 were used to identity the 5' arm and 3'arm of *Nkx2-3* flox region. Primer 2 was a pair of common primers, and primer sequences are mutated to increase the specificity to identify *Nkx2-3* flox genotype. Therefore, it was only observed in the PC$^{lin\text{-}KO}$ mouse rather than PC^{lin} mouse.

[REDACTED]

Figure R33. Genotyping report of *Nkx2-3*-flox mice (https://cn.gempharmatech.com/shop/productDetails/24711).

2.3 Formally the human gene is denoted as NKX2-3, while the mouse equivalent is labeled as Nkx2-3 – please use this form, throughout the manuscript.

Response: Thanks for your suggestions, we have corrected the use of human NKX2-3 and mouse Nkx2-3 throughout the manuscript **(Please see page 13, line 262; page 16, line 327; page 45, line 855 in the revised manuscript).**

2.4 Abstract, line 60; and Line 105: I would add where blood flow and diameter were increased (inside the tumor).

Response: We appreciated the reviewer pointing it out. Blood flow and diameter were increased inside the primary tumor. We have added these descriptions **(Please see page 3, line 63, line 64 in the revised manuscript).**

2.5 Line 106: please describe CRCLM abbreviation

Response: Thanks for your reminding, the full name of CRCLM is colorectal cancer liver metastasis, we have described it upon the first use **(Please see page 6, line 107 in the revised manuscript).**

2.6 Line 163, Fig2G: does NG2 specifically label pericytes, or can it be expected to recognize neuronal elements as well? Why do Authors use a different staining for TPCs in breast cancer (FigS2A, line 172)?

Response: Thanks for your questions. NG2 is expressed in pericytes, mesenchymal stem cells, osteoblasts, NG2-glia, and glioblastoma cells[39-41]. In tumor tissues, NG2 is frequently used as a marker for the identification and characterization of tumor pericytes[12, 42, 43]. Cells positive for NG2 and embedded within tumor vessels are considered as tumor pericytes. α-SMA is also a recognized marker for tumor pericyte staining[44-46], therefore, both NG2 and α-SMA were used to label tumor pericytes in this study.

2.7 Line 258, Fig 4D, Fig S11A: how was pericyte coverage determined?

Response: Thanks for your question. Pericyte coverage was examined by

immunofluorescence assay, α-SMA was used to label TPCs and CD31 was used to label tumor vessels. Pericyte coverage was evaluated according to previous study[27], the α-SMA positive area and CD31 positive area were quantified using Image J, and then the ratio of α-SMA positive area to CD31-positive area was calculated as pericyte coverage **(Please see page 11; Supplementary Figure 15a in the revised Supplementary Information).**

2.8 Line 314, Figure 6A: NEAT expression is clearly not restricted to Cluster 3/MAPs. Maybe include violin plots to emphasize difference (if there is any)

Response: Thanks for your comments. As the reviewer suggested, violin plots of *NEAT1* expression in all TPC subsets were shown (**Figure R34**). The result showed that *NEAT1* expression is highly expressed in cluster 3 **(Please see Figure 6a in the revised manuscript).**

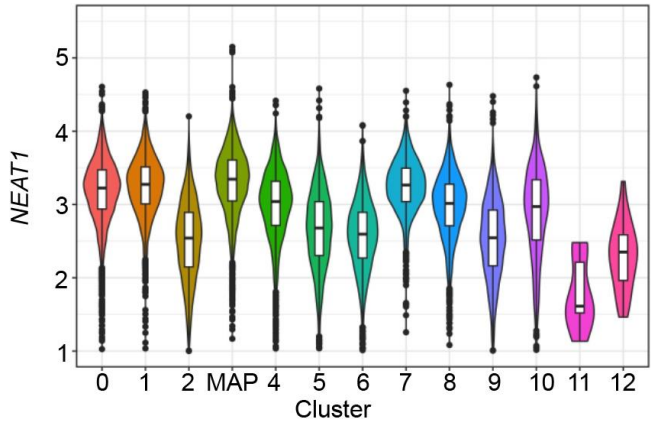

Figure R34. *NEAT1* expression is the highest in MAPs. Violin plot for *NEAT1* expression in all TPC subsets.

2.9 Line 315: Figure 6B-C instead of Figure S6B-C

Response: Thank you very much for pointing out this clerical error, we have corrected it into Figure 6b-c **(Please see page 15, line 319 in the revised manuscript).**

2.10 I don't understand the sentence beginning in Line 363 and ending in Line 365.

Response: Thanks for your comments, Line 363-365 is a brief description about the

FAPα-activated prodrug strategy. FAPα possesses endopeptidase activity that can specifically cleave N-terminal benzyloxy carbonyl–blocked (Z-blocked) Gly-Pro (Z-GP) dipeptide-linked substrates [47], therefore, compounds linked to the Z-GP are substrates of FAPα and serve as FAPα-activated prodrug, which could be hydrolyzed by FAPα-expressing cells and release parent drug[48]. We have added the corresponding description **(Please see page 18, line 368-372 in the revised manuscript).**

2.11 Supplemental Table 11, antibody list: is the listed anti-Nkx2-3 anti-human or anti-mouse (or both)?

Response: Thanks for your comments, NKX2-3 antibody (RRID: AB_2680088, sigma) in Supplementary Table 11 is anti-human. We apologize for missing the information of anti-mouse Nkx2-3 antibody. We have added the information of anti-mouse Nkx2-3 antibody (RRID: AB_10743069, sigma) **(Please see Supplementary Table 19 in the revised Supplementary Information).**

Response to Reviewer 5 (expert in colorectal cancer liver metastasis, scRNA-seq)

Comments to the Author:

In this manuscript, the authors identify a specific subpopulation of TPCs, characterized by high expression of the transcription factor NKX2-3, as being associated with hematogenous colorectal cancer metastasis to the liver. This novel NKX2-3-high subpopulation regulates tumor vascular tone by modulating blood flow and vessel diameter, which has direct implications for metastasis. The data demonstrate that conditional deletion of Nkx2-3 in TPCs induces vasoconstriction, reduces blood flow, and subsequently mitigates tumor metastasis.

The paper gives a wealth of mechanistic insights linking NKX2-3 expression to calcium signaling and metastases. The authors are to be commended for the comprehensive efforts to address the role of the specific perivascular cells. However, I have some major concerns regarding the validity of the clinical results that build the basis for the downstream analysis. The amount of experimental data makes it hard to judge the validity of the individual results, and the text would, in my opinion, greatly benefit from

guiding the reader through the complex experimental approaches used.

Response: We feel great thanks for your professional review work on our manuscript. As you are suggested, there are some problems that need to addressed. According to your nice suggestions, we have made corrections to our manuscript and the detailed information are listed below.

Major points

Abstract:

"Here, we found that patients with colorectal cancer liver metastasis were characterized by increased diameter and blood blow". The meaning is unclear here. What has an increased diameter compared to what? Do the authors mean "blood flow"? Again, in relation to what?

Response: Thanks for your question and pointing out the typo mistake. Here, we found that vascular diameter and blood flow were significantly increased in the primary tumor of colorectal cancer liver-metastatic patients compared with non-metastatic colorectal cancer patients. The detailed description in abstract was corrected **(Please see page 3, line 62-64 in the revised manuscript).**

The abstract is unclear on whether the findings were made in primary CRC or in CRLM.

Response: We apologize for the misleading. Our study is focused on the pericytes-regulated vascular tone and hemodynamics in the primary tumor of colorectal cancer with or without liver metastasis **(Please see page 3, line 63-64 in the revised manuscript).**

Consider revisiting all instances where protein/RNA is mentioned to meet HUGO nomenclature criteria, this is currently unclear

Response: Thanks for your kind suggestions. Human protein/RNA names occurred in this study were checked in Human Genome Organization (HUGO) Gene Nomenclature Committee website, which meet the HUGO nomenclature criteria.

Consider substantial revision of the last sentence of the abstract. What is the novel mechanism? Have the authors studied "pericytes in tumor metastasis" or how pericytes facilitate intravasation to induce metastases?

Response: We really appreciate the reviewer's constructive suggestion. This study first reveals that pericytes drive tumor cell intravasation and metastasis through regulating vasodilation and hemodynamics (**Please see page 4, line 71-72 in the revised manuscript**).

The pro-metastatic effects of pericytes had been widely investigated. Existing studies indicate pericytes facilitate tumor metastasis through pericyte-fibroblast transition (PFT) or interacting with tumor-associated macrophages via IL-33[43, 49]. Additionally, $CD45^{-}$ $VLA\text{-}1^{bri}$ or endosialin-expressing pericytes promote tumor cell intravasation in a cell contact-dependent manner, resulting in elevated numbers of circulating tumor cells[50, 51]. Cell stem cell (CSC)-derived pericyte-like cells display potent capacity of trans-endothelial migration, thus favoring tumor cell intravasation, circulation, extravasation and then de-differentiate into tumorigenic CSCs to form metastases [52]. We had applied multi-omics integration analysis to investigate the role of pericyte in tumor metastasis. We first uncovered the heterogeneity of pericytes in tumor metastasis and found a novel population of $TCF21^{high}$ pericytes associated with tumor metastasis, which increased perivascular extracellular matrix (ECM) stiffness, collagen rearrangement and basement membrane degradation, thus establishing a perivascular metastatic microenvironment to instigate colorectal cancer liver metastasis[36]. Additionally, we found transient receptor potential cation channel, subfamily M, member 8 (TRPM8) and TRPM8 channel associated factor 2 (TCAF2) play important roles in pericyte-mediated tumor metastasis. TCAF2 in pericytes suppressed the expression and ion channel activity of TRPM8, thus promoting tumor cell motility and epithelial-mesenchymal transition (EMT) through activating the Wnt5a/STAT3 signaling axis[6].

L105 The authors should specify here if the data come from primary tumors of metastases, i.e. "increased in CRLM patients" could be anywhere.

Response: Thanks for your important suggestions. Our data come from the primary

tumors of colorectal cancer (CRC) patients with liver-metastasis or non-metastatic CRC patients (**Please see page 6, line 107 in the revised manuscript**).

L117/8 “in clinical”? Where was blood flow measured? How is “artificial intelligence” needed to calculate signal intensity? This part has to be more specific, explain details, and motivate the choice of methods.

Response: Thank you for pointing out the grammar error and incorrect description. “in clinical” has been corrected into “in clinic” (**Please see page 6, line 120 in the revised manuscript**). We apologize for the misleading description of artificial intelligence. Blood flow in tumor was measured by doppler ultrasound imaging, and the images of tumors derived from colorectal cancer patients with or without liver-metastasis were collected and analyzed using Open CV, rather than “artificial intelligence”. In ultrasound Doppler images, red and blue regions conventionally represent blood flow, with red indicating arterial flow and blue indicating venous flow. To quantify these regions, Open Source Computer Vision Library (OpenCV, https://opencv.org)vwas utilized for image processing. First, the color space was converted from BGR to HSV to facilitate precise segmentation of color-coded areas. Then specific HSV color ranges were defined for both red and blue flow regions, applying these ranges to create binary masks that isolated the areas of interest. These masks were applied to extract the corresponding blood flow regions from the original image. To further improve the segmentation accuracy, OpenCV's edge detection algorithms were employed, refining the boundaries of the extracted regions. Finally, within these segmented regions, the average saturation and brightness values were calculated to evaluate the blood flow signal strength, resulting in an objective quantification of blood flow intensity within the ultrasound Doppler images **(page 26, line 553-566 in the revised manuscript)**.

Data related to Figure 1: How were the patients matched? Were TN stages similar in M1 and M0 patients? Tumor location in the colorectum? This is crucial to compare the results, which could just be derived from different locoregional stages. No details on ultrasound measurements are given.

Response: Thanks for your questions. The detailed patient information including age, gender, TNM stage, differentiation stage and tumor location has been listed in the **revised Supplementary Table 5-6**. TN stage, tumor location, tumor size and differentiation stage were different in M1 and M0 patients. The correlation analysis between the signal strength value (**Figure 1a**) and clinicopathologic data was performed, patients in **Figure 1a** were divided into high signal strength value group and low signal strength value group according to the cutoff of 141.4 (**Figure 1b**). However, no statistical association was found between the signal strength value and patient gender, age, tumor location, differentiation and size, but showed a significant correlation with colorectal cancer liver metastasis (CRCLM) (**Table R2**). Similar analysis was performed on the correlation between small area emphasis value (**Figure 1c**) and clinicopathologic parameters, patients in **Figure 1c** were divided into groups with high small area emphasis value and low small area emphasis value according to the cutoff of 0.37 (**Figure 1d**). Our results showed that small area emphasis value in the primary tumor was significantly associated with CRCLM, rather than other parameters (**Table R3**) **(Please see page 7, line 130-133 in the revised manuscript, Supplementary Table 1 and Table 2 in the revised Supplementary Information)**.

Table R2. Correlation analysis between the signal strength value and the clinicopathologic data.

Character	Signal strength value (≤141.4)	Signal strength value (＞141.4)	*P* value
Gender			
Female	8 (40.0%)	12 (60.0%)	0.572
Male	33 (47.1%)	37 (52.9%)	
Age			
≤60	11 (50.0%)	11(50.0%)	0.630
>60	30 (44.1%)	38 (55.9%)	
Location			
Right hemicolon	8 (44.4%)	10 (55.6%)	0.916

Left hemicolon	33 (45.8%)	39 (54.2%)	
Differentiation			
Moderate	27 (45.0%)	33 (55.0%)	0.881
Low	14 (46.7%)	16 (53.5%)	
Size			
≤5cm	34 (43.0%)	45 (57.0%)	0.199
>5cm	7 (63.6%)	4 (36.4%)	
Tumor stage			
I-II	30 (66.7%)	15 (33.3%)	<0.0001
III-IV	11 (24.4%)	34 (75.6%)	
M stage			
M0	30 (66.7%)	15 (33.3%)	<0.0001
M1	11 (24.4%)	34 (75.6%)	
Liver metastasis			
No	30 (66.7%)	15 (33.3%)	<0.0001
Yes	11 (24.4%)	34 (75.6%)	

Table R3. Correlation analysis between the small area emphasis value and the clinicopathologic data.

Character	Small area emphasis value (≤0.37)	Signal strength value (＞0.37)	*P* value
Gender			
Female	9 (30.0%)	21 (70.0%)	0.107
Male	30 (47.6%)	33 (52.4%)	
Age			
≤60	15 (44.1%)	19 (55.9%)	0.746
>60	24 (40.7%)	35 (59.3%)	
Location			
Right hemicolon	11 (52.4%)	10 (47.6%)	0.270
Left hemicolon	28 (38.9%)	44 (61.1%)	
Differentiation			
Moderate	28 (45.9%)	33 (54.1%)	0.285
Low	11 (34.4%)	21 (65.6%)	
Size			
≤5cm	32 (40.0%)	48 (60.0%)	0.348
>5cm	7 (53.8%)	6 (46.2%)	
Tumor stage			
I-II	29 (59.2%)	20 (40.8%)	<0.0001
III-IV	10 (22.7%)	34 (77.3%)	
M stage			
M0	29 (59.2%)	20 (40.8%)	<0.0001
M1	10 (22.7%)	34 (77.3%)	
Liver metastasis			
No	29 (59.2%)	20 (40.8%)	<0.0001
Yes	10 (22.7%)	34 (77.3%)	

For ultrasound measurements, ultrasound images of tumors derived from colorectal cancer patients with or without metastasis were collected from the First Affiliated Hospital of Jinan University. In ultrasound Doppler images, red and blue regions conventionally represent blood flow, with red indicating arterial flow and blue indicating venous flow. To quantify these regions, Open Source Computer Vision Library (OpenCV) was utilized for image processing. First, the color space was converted from BGR to HSV to facilitate precise segmentation of color-coded areas. Then specific HSV color ranges were defined for both red and blue flow regions, applying these ranges to create binary masks that isolated the areas of interest. These masks were applied to extract the corresponding blood flow regions from the original image. To further improve the segmentation accuracy, OpenCV's edge detection algorithms were employed, refining the boundaries of the extracted regions. Finally, within these segmented regions, the average saturation and brightness values were calculated to evaluate the blood flow signal strength, resulting in an objective quantification of blood flow intensity within the ultrasound Doppler images **(Please see page 26, line 553-566 in the revised manuscript)**.

Data related to Figure 2: Are data in Figure 2 a re-analysis from previously generated scRNA-seq? Are those related to the measurements in Figure 1? This should at least be clarified. How was ensured that there were no significant differences other M0 and M1 in the sc-seq dataset?

Response: Thanks for your comments. Raw data in **Figure 2a-d** is derived from our previous study[36]. TPCs analyzed for scRNA-seq (**Figure 2a-d**) and western blot (**Figure 2e**) were derived from another 4 CRC patients, and the patient information were listed in the **revised Supplementary Table 7.** Data in **Figure 1c-k** and **2g-j** was derived from the same 93 CRC patients (patient information was listed in the **revised Supplementary Table 6**). Data in **Figure 1a-b** was from another 90 CRC patients (patient information was listed in the **revised Supplementary Table 5**). Only 4 colorectal cancer patients were involved in the scRNA-seq dataset, tumor location, differentiation stage and TN stages are different in the M0 and M1 patients, therefore,

we could not validate that NKX2-3 expression in TPCs was only associated with M0 and M1 stage in scRNA-seq dataset. However, correlation analysis was performed on 93 colorectal cancer specimens, the results showed that no statistical association was found between NKX2-3^{+} TPC ratio and patient gender, age, tumor location, differentiation, and size, but showed a significant correlation with M0/M1 stage and liver metastasis of tumor (**Table R4**) **(Please see page 9, line 171-172 in the revised manuscript, Supplementary Table 3 in the revised Supplementary Information)**.

Table R4. Correlation analysis between the NKX2-3^{+} TPC ratio and the clinicopathologic data.

Character	NKX2-3+ TPC ratio (≤43%)	NKX2-3+ TPC ratio (＞43%)	*P* value
Gender			
Female	15 (50.0%)	15 (50.0%)	0.943
Male	31 (49.2%)	32 (50.8%)	
Age			
≤60	16 (47.1%)	18 (52.9%)	0.725
>60	30 (50.8%)	29 (49.2%)	
Location			
Right hemicolon	11 (52.4%)	10 (47.6%)	0.761
Left hemicolon	35 (48.6%)	37 (51.4%)	
Differentiation			
Moderate	28 (45.9%)	33 (54.1%)	0.343
Low	18 (56.3%)	14 (43.8%)	
Size			
≤5cm	37 (46.3%)	43 (53.8%)	0.216
>5cm	9 (69.2%)	4 (30.8%)	
Tumor stage			
I-II	45 (91.8%)	4 (8.2%)	<0.0001
III-IV	1 (2.3%)	43 (97.7%)	

M stage			
M0	45 (91.8%)	4 (8.2%)	<0.0001
M1	1 (2.3%)	43 (97.7%)	
Liver metastasis			
No	45 (91.8%)	4 (8.2%)	<0.0001
Yes	1 (2.3%)	43 (97.7%)	

Data related to Figure 3 (L179 ff): How were these cell lines/primary cultures derived? This is crucial to be able to judge any of the downstream experiments presented and should be included, at least briefly, in the main text.

Response: Thanks for your questions. TPCs were isolated by microdissection combined with pericyte medium-based approach (MPMA) according to our previous study[6]. As shown in **Figure R35C**[6], freshly resected human CRC tissues were placed in ice-cold DMEM containing PS and transported to the laboratory within 1 h. Following washing with pre-cooled PBS supplemented with 0.1% gentamicin, 0.1% ciprofloxacin, and 0.1% kanamycin in a sterile dissection hood, fibrous, and adipose tissues around the muscular layers of tumor tissues were carefully removed. The remaining tissues were cut into small pieces along the colon mucosa into the muscular layer, followed by fastening in a sylgard-coated petri dish using ice-cold PBS and a surgical needle. For TPC collection, ascending capillaries (diameter ≈ 20 μm) derived from arterioles were gently separated along the mucosa into the submucosa from perivascular adipose tissues using eye scissors (Geuder, G-19745) under a stereomicroscope (SZX7; Olympus) (**Figure R35D, E**). The attached adipose tissues were then removed, and the dissected capillaries were transferred to fresh dishes containing PM. The TPCs migrated from the vascular samples to the culture plate within 14 days (**Figure R35F**). When the cells reached 80% confluence, they were dissociated using trypsin, collected, and transferred to a 60 mm-diameter culture dish. The culture medium was gently replaced every two days. TPCs were authenticated using STR Multi-amplification Kit, and tested negative for mycoplasma using the

Mycoplasma Detection Set[6]. The purity of the isolated TPCs was confirmed using FACSort (**Figure R35G**), and the isolated TPCs were identified by transmission electron microscopy (**Figure R35H**), immunofluorescence (**Figure R35I, J**) and flow cytometry (**Figure R35K, L**) as previously described, which are characterized by high nuclear/cytoplasmic ratio and pericyte markers including NG2, PDGFRβ, and CD146, as well as mesenchymal stromal cell antigens CD44 and CD105. The detailed methods for TPC isolation and identification were added in the Supplementary methods (**Please see page 1 in the revised Supplementary Information**).

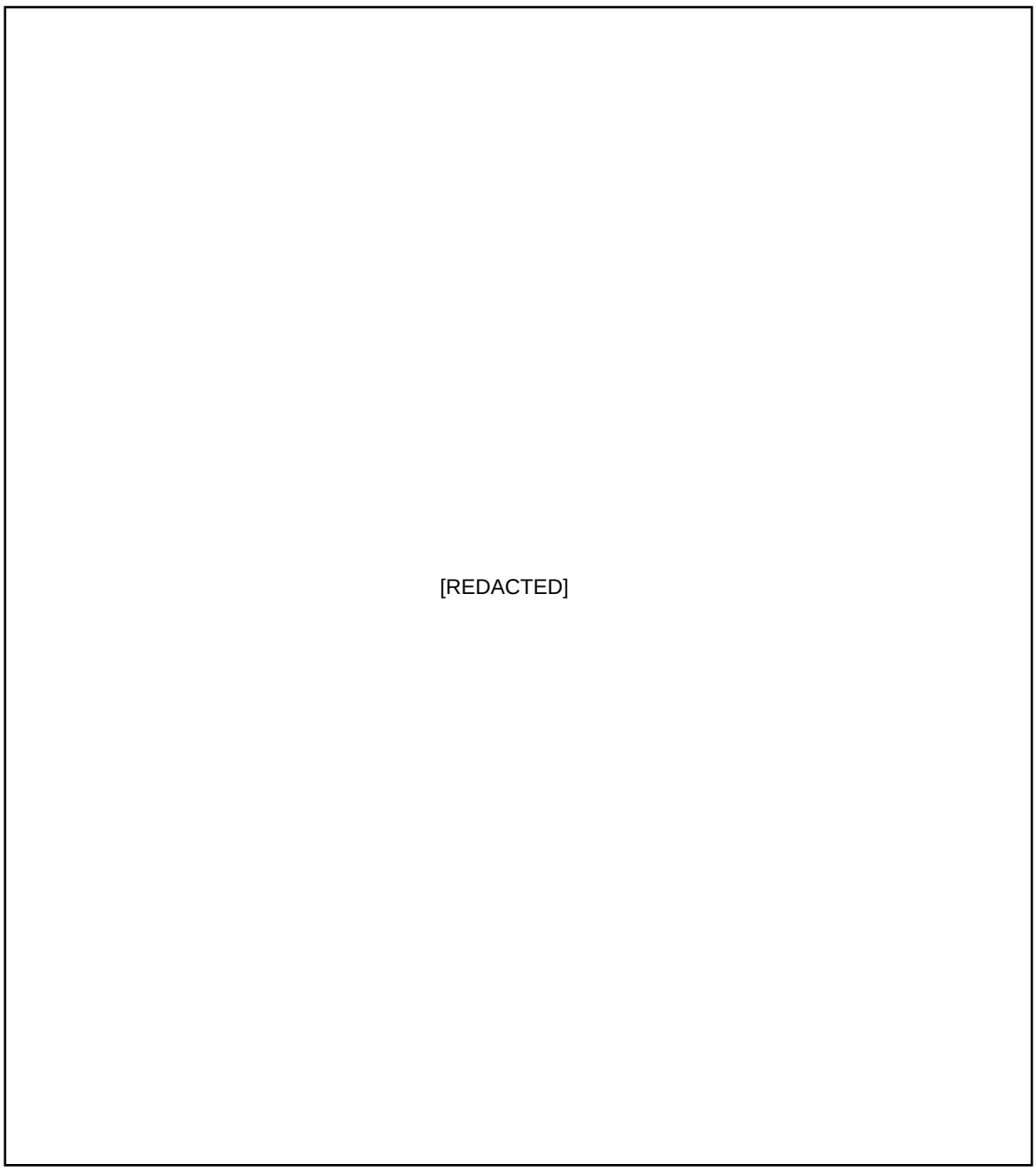

Figure R35. Isolation and validation of TPCs[6]. (A) Immunofluorescence staining for PC markers including NG2 or PDGFRβ (green) in tumor blood vessels (CD31, red) with various diameters (n = 40). The white arrowhead indicates the PCs-containing capillaries. Scale bar, 50 μm. (B) Plot diagram of the diameters in PCs-containing capillaries (n = 40). Data are presented as mean ± SEM. (C) Diagram depicting the isolation of tumor blood vessels from CRC patients. (D) Representative images of blood

vessels dissected from tumor tissues under the stereomicroscope (n = 6). Scale bar, 50 μm. (E) Representative images for the capillary chips (n = 6). Scale bar, 50 μm. (F) Representative images for TPC migration and expansion from the cultured capillary chips (n = 6). Scale bar, 50 μm. (G) Flow cytometry analysis of NG2 expression in TPCs at passage 2 (n = 6). (H) Representative TEM images of the tumor vessels and TPCs (n = 6). Scale bar, 1 μm (left); 2 μm (right). (I) Immunofluorescence analysis of CD31 expression in HMEC-1 cells. Phalloidin-rhodamine was used to identify F-actin. Scale bar, 20 μm. (J) Immunofluorescence analysis of indicated markers in TPCs (n = 6). Phalloidin-rhodamine was used to identify F-actin. Scale bar, 20 μm. (K) Flow cytometry analysis of CD31 in HMEC-1 cells (n = 6). (L) Flow cytometry analysis for the expression of endothelial cells, epithelial cells, mesenchymal stromal cells, and pericyte markers in cultured TPCs (n = 6).

L 271: U46619 is not introduced. Why was it used?

Response: Thanks for your question, we are sorry for missing the introduction about U46619. U44619 is thromboxane A (2) analog, 9,11-dideoxy-9α,11α-methanoepoxy prostaglandin F2α, serving as a vasoconstrictor for capillaries and arteries[7, 53, 54]. U46619 induces cell contraction through facilitating extracellular calcium influx and myosin light chain phosphorylation[55, 56], therefore, it was applied to investigate whether pericyte-specific deletion of *Nkx2-3* induce vasoconstriction through regulating calcium signal, tumor capillaries from PC^{lin} and $PC^{lin\text{-}KO}$ mice were treated with the vasoconstrictor U46619, the results showed that the response of Ca^{2+} to U46619 was significantly increased in $PC^{lin\text{-}KO\text{-}GCaMP6}$ mice compared with $PC^{lin\text{-}GCaMP6}$ mice, indicating that pericyte-specific deletion of *Nkx2-3* activated calcium channel activity, leading to vasoconstriction (**Please see page 13, line 268-269 in the revised manuscript; page 10 in the revised Supplementary Information**).

L284: An explanation of how "tumor blood velocity" can be assessed by two-photon microscopy would be very helpful here. Was this done by done by ultrafast scanning of erythrocytes?

Response: Thanks for your comments. To measure tumor blood velocity, we used line-scan path in two-photon microscopy as previously described[14, 57]. MC-38 allografts-bearing PC^{lin} and $PC^{lin\text{-}KO}$ mice were intravenously injected with FITC-dextran prior to imaging. Intravenous injection of dextran revealed the vascular architecture as well as individual red blood cells (RBCs), which appeared as shadows flowing with the fluorescent plasma. Then, mouse tumor was exposed to 4× objective and rapid line scan (735 lines per second) was used to analyze the blood velocity, the line-scan bisected the central axis of the capillary lumen to track the movement of blood cells, RBC moving through the capillary appeared as oblique shadows from which we determined the tumor blood velocity($\Delta x/\Delta t$) (**Please see page 9-10 in the revised Supplementary Information**).

L297: What are "constructed mouse vessel organoids"? Where are they derived from and despite studying the Supplementary Material, the Methods description is generally not specific enough to assess the results in all detail, mainly related to there being such a variety of experimental approaches use. For example, l. 478 "The images and specimens of all patients were confirmed by the pathology department", what does this mean? What was confirmed and by whom? How is the pathology department involved in "images"?

Response: Thanks for your valuable questions. We apologize for missing the methods for mouse vascular organoids. The primary tumors of PC^{lin} and $PC^{lin\text{-}KO}$ mice were obtained and then tumor capillaries were micro dissected from the tissues. The separated capillaries were embedded in the Matrigel and placed in a transwell chamber to prepare vascular organoid. After maintaining at 37 °C in a humidified atmosphere containing 5% CO_2 for 48 h, MC-38 cells (5×10^3) were added to the vascular organoid and further culturing for 48 h. At the end of experiments, the whole Matrigel was fixed with 4% PFA and subjected to H&E staining (**Please see page 16 in the revised Supplementary Information**).

Patient specimens and information were collected from pathology and Gastrointestinal Surgery department in the First Affiliated Hospital of Jinan University.

All the immunofluorescence images in **Figure 1**, **Figure 2**, **Figure 6** and **Supplementary Figure 3-5** were confirmed by the qualified pathologists in pathology department, they help to confirm the field of view is in the primary tumor, and assist in statistics (**Please see page 22, line 469-471 in the revised manuscript**).

For patients with liver metastases and an advanced primary tumor, it seems highly unlikely that no preoperative chemotherapy was administered, given current international guidelines (related to the statement in L 479). Can the authors comment on this?

Response: Thanks for your question. Concerning the colorectal cancer patients with liver metastasis or locally advanced stage (T4), although preoperative neoadjuvant radiotherapy or chemotherapy is an important treatment option, a large number of cases with complications require palliative surgical resection or fistula treatment, which is also in line with the Chinese Society of Clinical Oncology (CSCO) guidelines for colorectal cancer version 2024[58]. Therefore, to rule out the effects of preoperative neoadjuvant therapy on the metastasis, colorectal cancer patients without radiotherapy or chemotherapy prior to surgery were included in this study as a source of clinical specimens.

What were the cas9 mice used for that are mentioned in the results? (L484)?

Response: Thanks for your question. Concerning the Rosa26-CAG-LSL-Cas9-tdTomato mice, CAG-loxP-STOP-loxP-Cas9-tdTomato was inserted at the mouse Rosa26 locus, and the STOP element prevented CAG from driving the expression of Cas9-tdTomato. After crossing with *Cspg4*-CreERT2 mice, the STOP element was deleted in NG2-expressing cells and the expression of Cas9 and tdTomato was switched on. Therefore, tumor pericytes in PC^{lin} and $PC^{lin\text{-}KO}$ mice were labeled with red fluorescence. To investigate whether *Nkx2-3* was knockdown in TPCs from $PC^{lin\text{-}KO}$ mice, tdTomato was used to localize tumor pericytes because it was expressed in $NG2^{+}$ pericytes surrounding tumor vessels (**Supplementary Figure 11b**). The expression of NKX2-3 was examined in the $tdTomato^{+}$ TPCs, and the results showed that NKX2-3

was significantly decreased in tdTomato^{+}TPCs from PC$^{lin\text{-}KO}$ mice (**Supplementary Figure 11c**) (**Please see page 23, line 483-484 in the revised manuscript**).

Other points

Title: Consider omitting "tumor" as this is clear from "metastasis"

Response: Thanks for your suggestions. The title has been changed into "Pericytes promote metastasis by regulating tumor local vascular tone and hemodynamics" **(Please see title in the revised manuscript).**

Introduction

L 75 "is the main approach", do the authors mean "main mechanism"=

Response: As the reviewer suggested, distant metastasis is the primary cause of cancer death, and hematogenous metastasis is the main mechanism of tumor distant metastasis **(Please see page 5, line 77 in the revised manuscript)**.

L 79 The assertion that intravasation is a "rate limiting step" is somewhat speculative, suggest to remove.

Response: Thanks for your suggestions, we have removed this sentence **(Please see page 5, line 80-81 in the revised manuscript)**.

L176 "predictive marker"?

Response: We really appreciate the reviewer's comments. ROC curve analysis is frequently applied as a predication model in clinical[59, 60]. In this study, ROC curve analysis revealed that NKX2-3^{+} TPC ratio had high diagnostic efficiency for CRCLM at the optimal cutoff value of 43%, as indicated by the area under the ROC curve (AUC) of 0.97 for the NKX2-3^{+} TPC ratio in predicting CRCLM (**Fig. 2h**). Therefore, colorectal cancer patients with higher NKX2-3^{+} TPC ratio (> 43%) have higher risk to develop liver metastasis compared with those with low ratio (≤ 43%). To avoid misunderstanding, we now change the sentence into "These data suggest that NKX2-3 in TPCs could be a risk factor for tumor hematogenous metastasis and associated with

poor prognosis." **(Please see page 9, line 184 in the revised manuscript)**

L259 "Light-sheet and fluorescent microscopy": Wasn't LS microscopy fluorescent?

Response: Thanks for your comments. We are sorry for the misleading description. The vascular morphology was examined by light-sheet (**Figure 4c**) and confocal microscopy (**Figure 4d**), both are fluorescent microscopy **(Please see page 13, line 261 in the revised manuscript)**.

L493 Were the mouse bred, instead of "hybridized"?

Response: Thanks for your comments, we are sorry for the words misused. The words "hybridized" were corrected into "bred" **(Please see page 23, line 485 in the revised manuscript)**.

Response to Reviewer 6 (expert in colorectal cancer liver metastasis, some scRNA-seq/ChIP-seq)

Comments to the Author:

Strengths of This Study:

This study shows strong evidence that NKX2-3 plays a key role in liver metastasis of colorectal cancer. It demonstrates that NKX2-3 affects blood vessel permeability and blood flow in tumor-associated pericytes, helping cancer spread. The study also explains how NKX2-3 is controlled by the NEAT1/miR-769-5p axis, revealing a new network of molecules involved in metastasis. Moreover, the findings suggest that the PDE1C/cAMP/PKA pathway, which controls blood vessel constriction, may also influence liver metastasis. This suggests NKX2-3 could be a good target for new therapies to prevent cancer from spreading.

Suggested Revisions:

Regarding Figure 3C: Please provide additional details on the criteria for gene selection, including the experimental techniques used and the number of RNA sequencing samples analyzed.

Response: Thanks for your kind suggestion. First, chromatin immunoprecipitation

(ChIP)-seq was conducted on TPC_{NM}^{NKX2-3}, and KEGG analysis revealed that the peak genes of NKX2-3 in TPCs were mainly enriched in calcium signaling pathway, the number of peak genes associated with calcium signaling pathway is 110. Then, RNA-seq was performed on $TPC_{LM}^{gNKX2-3}$ (n = 3) vs TPC_{LM}^{gNC} (n = 3), 637 genes were downregulated in $TPC_{LM}^{gNKX2-3}$ compared with TPC_{LM}^{gNC}. To investigate the molecular mechanisms by which NKX2-3 in TPCs regulate calcium signaling, the merge of NKX2-3 peak genes-associated with calcium signaling pathway (110) and the down-regulated genes in $TPC_{LM}^{gNKX2-3}$ (637) were defined by Venn diagram (https://bioinfogp.cnb.csic.es/tools/venny/). Five overlapping genes including *PDE1A*, *PDE1C*, *SLC8A1*, *CAMK2A* and *CAMK2D* were found. We have provided detailed description about the results **(Please see page 10, line 192, line 195-201 in the revised manuscript)**.

Relationship with Other Genes: Could you elaborate on the relationship between NKX2-3 and other key genes commonly associated with liver metastasis, such as KRAS, TP53, VEGF, and CXCR4?

Response: Thanks for your questions. NKX2-3 is closely associated with TP53, VEGF and CXCR4 in tumor progression. According to previous study, NKX2-3 is differentially expressed in wildtype and TP53-mutant cancer, which serves as a prognostic gene in TP53-mutant cancer [61]. The expression of NKX2-3 is positively correlated with VEGFA in human intestinal microvascular endothelial cells (HIMECs), NKX2-3 regulates VEGF-PI3K/AKT-eNOS signaling axis in HIMECs, leading to inflammatory bowel disease[62]. Additionally, NKX2-3 drives the development of marginal-zone lymphomas through activation of CXCR4, which in turn enhance migration, polarization and homing of B cells to splenic and extranodal tissues, eventually driving malignant transformation[63]. The relationship between NKX2-3 and KRAS is unknown, therefore, to investigate the association of these two genes, TPCs were treated with the conditioned medium of KRAS-mutant or -wildtype colorectal cancer cells respectively and the expression of NKX2-3 in TPCs was examined. The results showed that KRAS-mutant tumor cells had negligible effects on the NKX2-3

level in TPCs **(Figure R36)**, indicating NKX2-3 is not related to KRAS. These data have been added in the discussion **(Please see page 21, line 440-442 in the revised manuscript; Supplementary Figure 26 in the revised Supplementary Information)**.

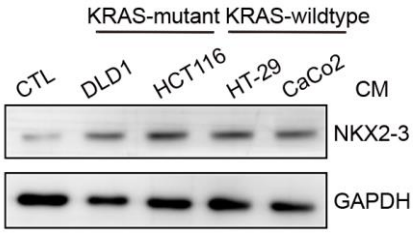

Figure R36. KRAS mutant has negligible effects on the expression of NKX2-3 in TPCs. Western blot assay for NKX2-3 expression in TPCs treated with the conditioned medium of KRAS-mutant or KRAS-wildtype tumor cells.

Lymph node metastasis: The involvement of NKX2-3 in lymph node metastasis is not mentioned in the manuscript. Can you provide further clarification on this point?

Response: Thanks for your question. To investigate the effects of pericyte NKX2-3 on tumor lymph node metastasis, lymph node-metastatic MC-38 cells were established (MC-38-LNM cells) according to previous study[33]. Metastatic lymph node (LN) tissues were harvested from MC-38 allografts-bearing mice that developed LN metastasis. Metastatic LN tissues were cut into small pieces (~1 mm^3), and digested with the tumor tissue dissociation kit as described above. Single-cell suspension of digested tissues was filtered through a 100 μm filter and selected with anti-CD326 microbeads (Cat. 130-061-101, Miltenyi Biotec.). The sorted cells were termed as MC-38-LNM cells. MC-38- LNM cells (1×10^5) were suspended in 100 μL of Matrigel and injected into the cecum wall of PC^{lin} and $PC^{lin\text{-}KO}$ mice, which were previously anesthetized with isoflurane inhalation. Mouse metastasis was detected by *in vivo* imaging system and H&E staining. The results showed that specific deletion of *Nkx2-3* in TPCs had negligible effects on lymph node metastasis of CRC **(Figure R37a)**. Both PC^{lin} and $PC^{lin\text{-}KO}$ mice bearing MC-38-LNM allografts developed lymph node infiltration **(Figure R37b)**. Mesenteric lymph node infiltration of tumor cells is mainly through lymphatic vessels[33]. However, lymphatic capillaries are composed of endothelial cells and a thin basement membrane without pericyte coverage, whereas collecting

lymphatic vessels contain lymphatic smooth muscle cells[34, 35]. Therefore, conditional deletion of *Nkx2-3* in TPCs had negligible effects on lymph node metastasis **(Please see page 12-13, line 255-257 in the revised manuscript; Supplementary Figure 14 in the revised Supplementary Information).**

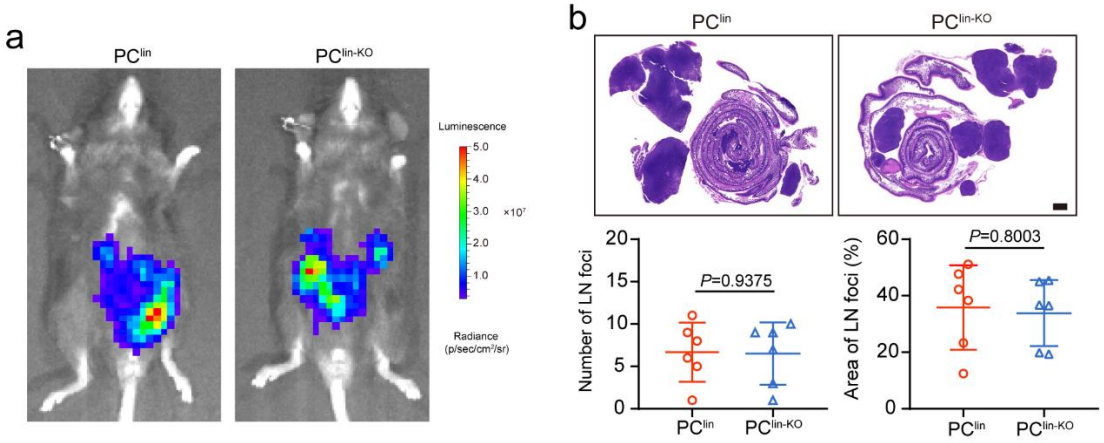

Figure R37. Pericyte specific deletion of *Nkx2-3* has negligible effects on lymph node metastasis. a Representative images of bioluminescence signals in mice orthotopically injected with MC-38-LNM cells. **b** H&E staining and quantification for the number and area of lymph node metastasis in tumor-bearing PC^{lin} and $PC^{lin\text{-}KO}$ mice. Scale bar, 1 mm. *P* values were determined by two-tailed unpaired *t*-test. LN, lymph node; LNM, lymph node metastasis; PC, pericyte.

Drug resistance: this manuscript does not address whether NKX2-3 is associated with resistance to anticancer drug therapy. Do you have data on this information?

Response: Thanks for your constructive question. Anti-angiogenic therapies including bevacizumab and DC101 are frequently used to treat tumor in clinic, however, which often result in local invasion and distant metastasis while blunting tumor growth[64]. TPCs and NKX2-3 might be involved in the pro-metastatic effects of anti-angiogenic therapy. Additionally, to investigate whether NKX2-3 is associated with immune checkpoint blockade (ICB) resistance, we collected scRNA-data of tumors from colorectal cancer patients undergoing PD-1 blockade, which consisted of patients that are resistant (non-responders, n = 3) and sensitive (responders, n = 19) to PD-1 blockade[65]. Then, the raw data was integrated and re-analyzed **(Figure R38a)**, TPCs

(cluster 18 and 20) in these tumors were characterized by *FAP*, *ACTA2*, *PDGFRB*, *RGS5,* and *CSPG4* positive, *CDH5* and *EPCAM* negative **(Figure R38b)**. The expression of *NKX2-3* in TPCs was evaluated in the tumors that are resistant and sensitive to PD-1, the results showed that the level of *NKX2-3* in TPCs was higher in the primary tumor of sensitive patients than that in resistant tumors **(Figure R38c)**, indicating that NKX2-3 may be associated with ICB response, however, further studies are still needed to demonstrate the role of NKX2-3^{high} TPCs in ICB therapy and determine the association of NKX2-3 with other anti-tumor treatment resistance **(Please see page 21, line 443-445 in the revised manuscript; Supplementary Figure 28 in the revised Supplementary Information).**.

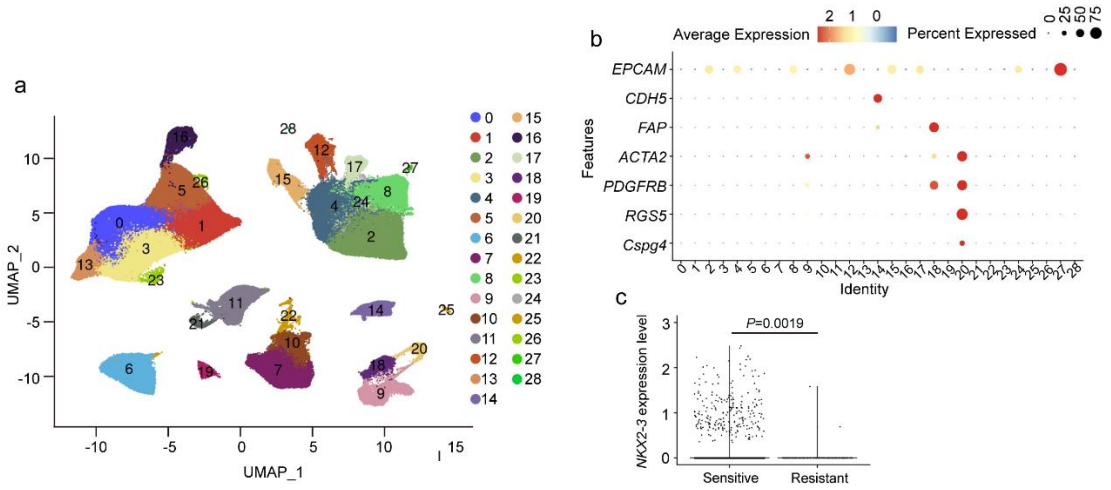

Figure R38. NKX2-3 in TPCs is associated with immunotherapy response of colorectal cancer patients. a UMAP visualization of cells derived from primary tumors of colorectal cancer patients that are resistant (non-responders, n = 3) and sensitive (responders, n = 19) to PD-1 blockade. **b** Identification of TPCs in the primary tumors of anti-PD1-treated colorectal cancer patients. **c** Violin plots for *NKX2-3* gene expression in TPCs derived from anti-PD-1 sensitive or resistant colorectal cancer patients. *P* value was determined by two-tailed Mann-Whitney test. TPC, tumor pericyte; UMAP, uniform manifold approximation and projection.

Microsatellite Status: Could you provide more information on the relationship between NKX2-3 expression and microsatellite status?

Response: We really appreciate the reviewer for the constructive suggestion. To explore the relationship between NKX2-3 expression and microsatellite status, scRNA data of tumors from human colorectal cancer with microsatellite instability-high (MSI-H, n = 28) and microsatellite stability (MSS, n = 34) was collected and further analyzed[66] (**Figure R39a**). As described above, cluster 12 in these tumors were *FAP*, *ACTA2*, *PDGFRB*, *RGS5,* and *CSPG4* positive, *CDH5* and *EPCAM* negative, therefore identified as TPCs (**Figure R39b**). The expression of *NKX2-3* in TPCs was evaluated in colorectal cancer with MSI-high and MSS, and the results showed that the level of *NKX2-3* in TPCs was increased in the primary tumor of MSS patients compared with that in MSI-H patients (**Figure R39c**). These data indicate that NKX2-3 may be associated with microsatellite status in human colorectal cancer **(Please see page 21, line 443-444 in the revised manuscript; Supplementary Figure 27 in the revised Supplementary Information).**

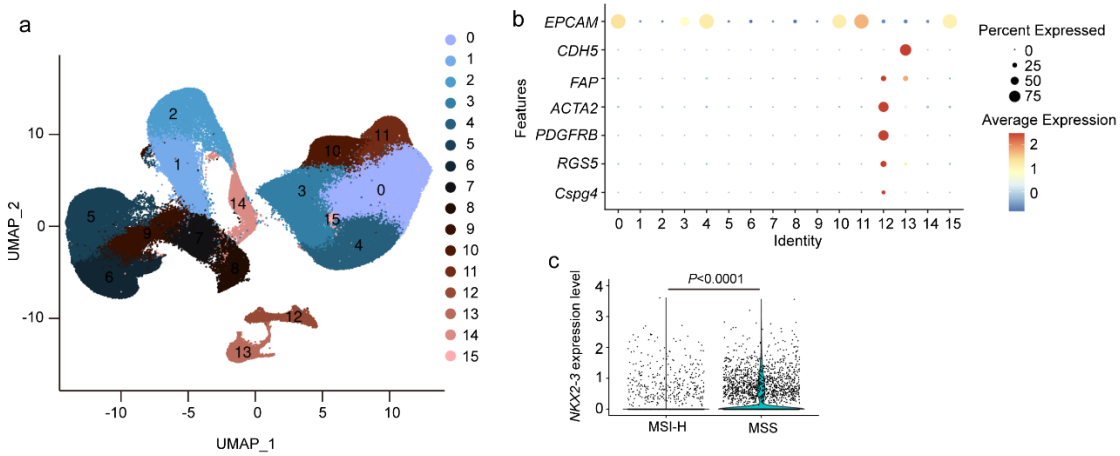

Figure R39. NKX2-3 in TPCs is associated with microsatellite status of colorectal cancer patients. a UMAP visualization of cells derived from primary tumors of MSI-H (n = 34) and MSS patients (n = 28). **b** Identification of TPCs in the primary tumors of MSI-H and MSS patients. **c** Violin plots for the *NKX2-3* gene expression in TPCs derived from MSIH and MSS patients. *P* value was determined by two-tailed Mann-Whitney test. MSI-H, microsatellite instability-high; MSS, microsatellite stability. TPC, tumor pericyte; UMAP, uniform manifold approximation and projection.

Response to Reviewer 7 (expert in peptide drug discovery)

Comments to the Author:

This manuscript describes that a subpopulation of NKX2-3-high TPCs are involved with metastasis of cancer, and NKX2-3 suppresses calcium influx in TPCs, induces tumor vasodilation, and increases vascular leakage. Authors also shows that the blocking of NKX2-3 using a FAP alpha-targeted Z-GP-NB2 peptide inhibits the binding of NKX2-3 to PDE1C promoter in TPCs and restores the tumor vasoconstriction and tumor metastasis. The idea is novel, and authors provide robust data related with the role for TPCs in tumor vasculature and metastasis.

However, this manuscript lacks data showing the delivery of Z-GP-NB2 into TPC-NK X2-3-high cells is mediated by FAP alpha on the surface of the cells.

Response: We thank the reviewer for appreciating the importance of our work and meanwhile making several constructive comments to improve the manuscript. To demonstrate that FAPα mediates the delivery of Z-GP-NB2 into NKX2-3^{high} TPCs, FAPα was knockdown in TPC_{NM}^{NKX2-3} (**Figure R40a**), and then TPC_{NM}^{NKX2-3} was treated with Z-GP-NB2 and the hydrolysis rate was examined by LC/MS. The results showed that compared with negative control group, FAPα knockdown significantly suppressed hydrolysis of Z-GP-NB2 into NB2 (**Figure R40b**), indicating that delivery of Z-GP-NB2 is mediated by the FAPα on the TPC surface. We have added these data **(Please see page 18, line 374-375 in the revised manuscript; Supplementary Figure 20f and g in the revised Supplementary Information).**

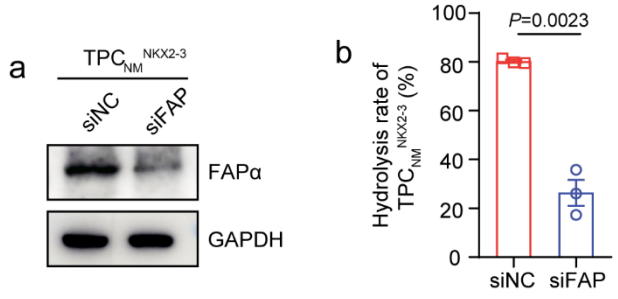

Figure R40. Hydrolysis of Z-GP-NB2 is mediated by FAPα in TPCs. a Western blot analysis of FAPα expression in FAPα-knockdown TPC_{NM}^{NKX2-3} (n = 3). **b** LC-MS detection for the hydrolysis of Z-GP-NB2 in TPC_{NM}^{NKX2-3} transfected with siNC or

siFAP (n = 3). Data are presented as mean ± SEM. *P* value was determined by two-tailed unpaired *t*-test. LC-MS, liquid chromatograph-mass spectrometer; TPC, tumor pericyte

Why is FAP alpha expression increased in TPC-NKX2-3-high cells (Fig. S15C, D)? Is there a specific reason for choosing FAP alpha as a target of TPC-NKX2-3-high cells?

Response: Thanks for your question. It is a key point for FAPα-activated prodrug strategy. FAPα is marker for tumor pericytes in epithelial tumors, which is highly expressed in more than 90% of malignant human epithelial cancers, whereas not detected in benign lesions or normal adult tissues[67, 68]. In addition, FAPα possesses endopeptidase activity that can specifically cleave N-terminal benzyloxy carbonyl–blocked (Z-blocked) Gly-Pro (Z-GP) dipeptide-linked substrates[47]. The specific expression of FAPα in TPCs and dipeptide substrate hydrolytic activity make it an ideal target for TPC-targeting prodrug strategy. Currently, FAPα-targeting strategy has been widely applied for pericytes-associated studies, including FAPα-activated prodrug strategy [48, 69, 70] and FAPα-targeting oncolytic virus [71]. Therefore, to improve the specificity of NB2 to $FAP\alpha^{+}$ pericytes, NB2 was designed as FAPα-activated prodrug Z-GP-NB2 **(Please see page 18, line 368-372 in the revised manuscript)**.

How is Z-GP-NB2 delivered into TPC-NKX2-3-high cells? In other words, what is the mechanism of Z-GP-NB2 internalization into TPC-NKX2-3-high cells? Is not only Z-GP-NB2 but also NB2 internalized into TPC-NKX2-3-high cells? Is the FAP alpha internalizing receptor?

Response: Z-GP-NB2 is designed as FAPα-activated prodrug, which was hydrolyzed into NB2 by FAPα in the TPC surface, and then the parent drug NB2 penetrated into the TPC nucleus after 24-h of treatment. FAPα is a type II transmembrane serine protease, which possesses endopeptidase activity that can specifically cleave N-terminal benzyloxy carbonyl–blocked (Z-blocked) Gly-Pro (Z-GP) dipeptide-linked substrates[47]. Therefore, FAPα exerts hydrolysis effects rather than internalization receptor during Z-GP-NB2 delivery, knockdown of FAPα in TPCs suppressed Z-GP-

NB2 hydrolysis.

To demonstrate the FAP alpha-mediated delivery of NB2, it is recommended to include the treatment of TPC-NKX2-3-high cells with NB2 as a control of Z-GP-NB2 and/or include the treatment of the cells with FAP alpha-blocking antibody (Fig. S15G-K and Fig. 7E, F).

Response: We appreciate the reviewer's valuable comments. As suggested, NB2 treatment group was added in Supplementary Figure 21, the results showed that both Z-GP-NB2 and NB2 restored cAMP production (**Figure R41a**) and L-type calcium transits (**Figure R41b**) hindered by NKX2-3 in TPCs, thereby increasing the contraction ability of $TPC_{NM}^{NKX2\text{-}3}$ (**Figure R41c-e**). In animal experiments, NB2 exerted toxic effects on mouse lung and kidney tissues (**Figure R41f**), therefore, only Z-GP-NB2 was used to examine the anti-metastatic effects. Both NB2 and Z-GP-NB2 could induce TPC contraction through suppressing the transcription activity of NKX2-3, however, the FAPα activated prodrug Z-GP-NB2 could be hydrolyzed by $FAP\alpha^{+}$ TPCs selectively, which improves the selectivity and targeting of NB2 **(Please see page 17, line 377-383; page 18, line 384-387 in the revised manuscript; Supplementary Figure 21d-h, Supplementary Figure 22a in the revised Supplementary Information).**

.

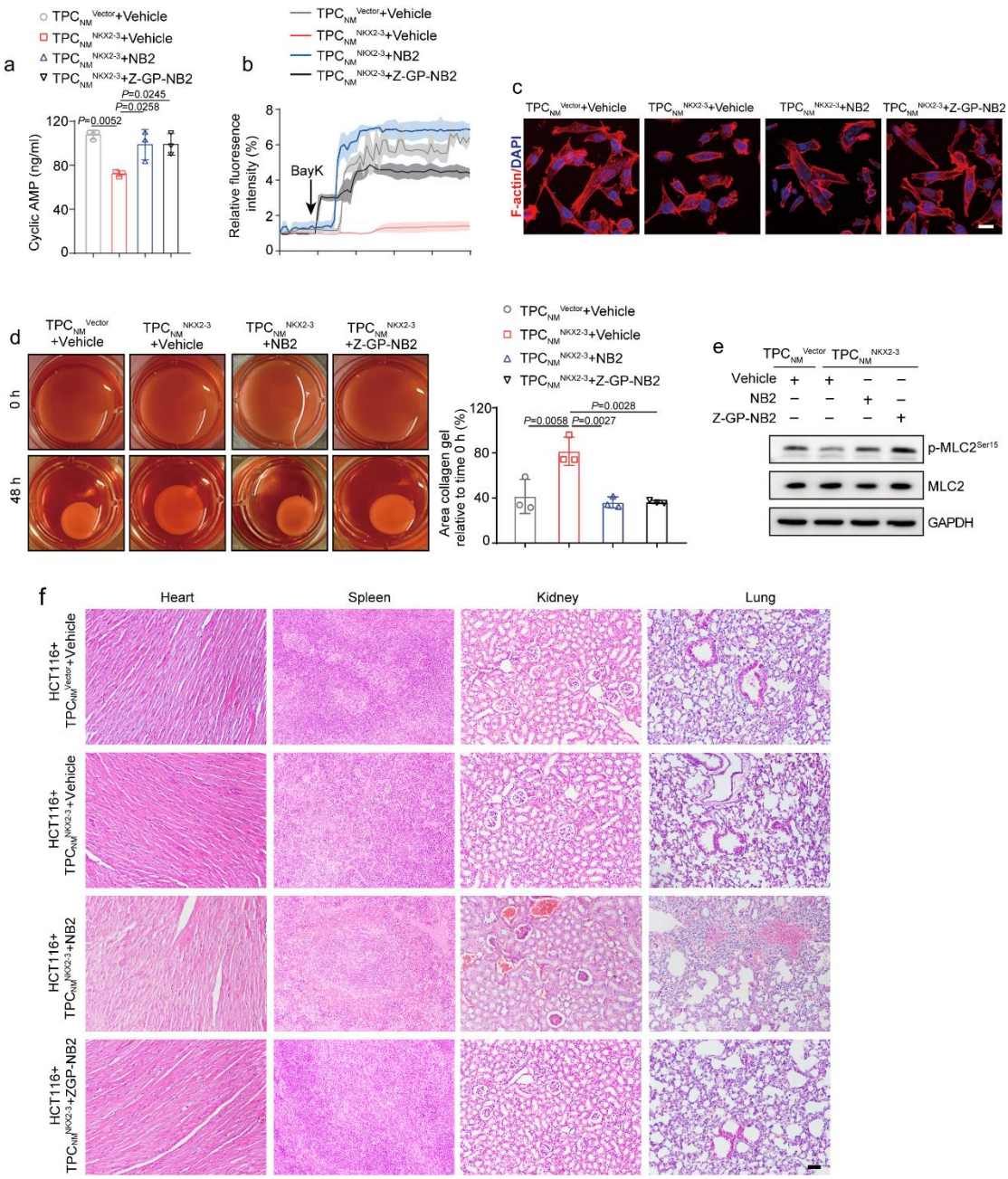

Figure R41. Z-GP-NB2 and NB2 induce TPC contraction and suppress colorectal cancer metastasis. a ELISA analysis for the level of cAMP in TPC_{NM}^{Vector} and $TPC_{NM}^{NKX2\text{-}3}$. $TPC_{NM}^{NKX2\text{-}3}$ was treated with NB2 and Z-GP-NB2 (n = 3). **b** Fluo-4AM fluorescence analysis of intracellular calcium in TPC_{NM}^{Vector} and $TPC_{NM}^{NKX2\text{-}3}$ treated with or without NB2 and Z-GP-NB2 (n = 3). **c** Immunofluorescence analysis of F-actin in TPC_{NM}^{Vector} and $TPC_{NM}^{NKX2\text{-}3}$ with indicated treatment (n = 3). Scale bar, 20 μm. **d** Representative images and quantification of collagen contraction induced by TPC_{NM}^{Vector} and $TPC_{NM}^{NKX2\text{-}3}$. $TPC_{NM}^{NKX2\text{-}3}$ was treated with NB2 or Z-GP-NB2 before

collagen contraction assay (n = 3). **e** Western blot analysis for the expression of MLC2 and p-MLC2^{Ser15} in the indicated TPCs (n = 3). **f** Representative images of H&E staining for lung, spleen, kidney and heart derived from HCT116 xenografts-bearing mice treated with NB2 or Z-GP-NB2 (n = 6). Scale bar, 50 μm. Data are presented as mean ± SEM. *P* values were determined by one-way ANOVA followed by Tukey's post hoc test.

Response to Reviewer 8

I co-reviewed this manuscript with one of the reviewers who provided the listed reports. This is part of the Nature Communications initiative to facilitate training in peer review and to provide appropriate recognition for Early Career Researchers who co-review manuscripts.

Response: Thanks for your insightful and constructive comments. We have now performed a series of new experiments and analyses to address the concerns of the reviewers and carefully revised the manuscript accordingly. The changes are marked red in the manuscript, and point-by-point responses to the reviewers' comments are provided above.

Response to Reviewer 9

I co-reviewed this manuscript with one of the reviewers who provided the listed reports. This is part of the Nature Communications initiative to facilitate training in peer review and to provide appropriate recognition for Early Career Researchers who co-review manuscripts.

Response: We sincerely appreciate your professional review work. We have tried our best to improve the study and made changes to the manuscript. The changes are marked red in the manuscript, and point-by-point responses to the reviewers' comments are provided above.

References

1. Lee K. E. Hypoxia as a regulator of tumor stroma and metastasis. *Am. J. Physiol.*

324, C10-C13 (2023).

2. Hirunpattarasilp C., et al. Hyperoxia evokes pericyte-mediated capillary constriction. *J. Cereb. Blood Flow Metab.* **42**, 2032-2047 (2022).
3. Liotta L. A., Kleinerman J., Saidel G. M. Quantitative relationships of intravascular tumor cells, tumor vessels, and pulmonary metastases following tumor implantation. *Cancer Res.* **34**, 997-1004 (1974).
4. Forster J. C., Harriss-Phillips W. M., Douglass M. J., Bezak E. A review of the development of tumor vasculature and its effects on the tumor microenvironment. *Hypoxia* **5**, 21-32 (2017).
5. Konerding M. A., Miodonski A. J., Lametschwandtner A. Microvascular corrosion casting in the study of tumor vascularity: a review. *Scanning Microsc.* **9**, 1233-1243 (1995).
6. Li X., et al. TCAF2 in Pericytes Promotes Colorectal Cancer Liver Metastasis via Inhibiting Cold-Sensing TRPM8 Channel. *Adv. Sci.* **10**, e2302717 (2023).
7. Heinze C., et al. Disruption of vascular Ca^{2+}-activated chloride currents lowers blood pressure. *J. Clin. Invest.* **124**, 675-686 (2014).
8. Broegger T., Andersson K. E., Aalkjaer C., Forman A., Boedtkjer D. B. Sensitivity to the thromboxane A2 analog U46619 varies with inner diameter in human stem villous arteries. *Placenta* **39**, 111-115 (2016).
9. McKenzie C., MacDonald A., Shaw A. M. Mechanisms of U46619-induced contraction of rat pulmonary arteries in the presence and absence of the endothelium. *Br. J. Pharmacol.* **157**, 581-596 (2009).
10. Hall C. N., et al. Capillary pericytes regulate cerebral blood flow in health and disease. *Nature* **508**, 55-60 (2014).
11. Bergers G., Song S. The role of pericytes in blood-vessel formation and maintenance. *Neuro-Oncology* **7**, 452-464 (2005).
12. Teichert M., et al. Pericyte-expressed Tie2 controls angiogenesis and vessel maturation. *Nat. Commun.* **8**, 16106 (2017).
13. Armulik A., Genové G., Betsholtz C. Pericytes: developmental, physiological, and pathological perspectives, problems, and promises. *Dev. Cell* **21**, 193-215

(2011).

14. Hartmann D. A., et al. Brain capillary pericytes exert a substantial but slow influence on blood flow. *Nat. Neurosci.* **24**, 633-645 (2021).
15. Almaça J., Weitz J., Rodriguez-Diaz R., Pereira E., Caicedo A. The Pericyte of the Pancreatic Islet Regulates Capillary Diameter and Local Blood Flow. *Cell Metab.* **27**, 630-644 (2018).
16. Korte N., et al. The Ca^{2+}-gated channel TMEM16A amplifies capillary pericyte contraction and reduces cerebral blood flow after ischemia. *J Clin Invest* **132**, e154118 (2022).
17. Jain R. K. Determinants of tumor blood flow: a review. *Cancer Res.* **48**, 2641-2658 (1988).
18. Badeer H. S. Hemodynamics for medical students. *Adv Physiol Educ* **25**, 44-52 (2001).
19. Hicks J. W., Badeer H. S. Gravity and the circulation: "open" vs. "closed" systems. *Am J Physiol* **262**, 725-732 (1992).
20. Fuchs C., Ertmer C., Rehberg S. Effects of vasodilators on haemodynamic coherence. *Best Pract. Res., Clin. Anaesthesiol.* **30**, 479-489 (2016).
21. Nasu R., Kimura H., Akagi K., Murata T., Tanaka Y. Blood flow influences vascular growth during tumour angiogenesis. *Br. J. Cancer* **79**, 780-786 (1999).
22. Goetz J. G. Metastases go with the flow. *Science* **362**, 999-1000 (2018).
23. Follain G., et al. Hemodynamic Forces Tune the Arrest, Adhesion, and Extravasation of Circulating Tumor Cells. *Dev. Cell* **45**, 33-52 (2018).
24. Fu B. M. Tumor Metastasis in the Microcirculation. *Adv. Exp. Med. Biol.* **1097**, 201-218 (2018).
25. Oku T., et al. Tumor growth modulation by sense and antisense vascular endothelial growth factor gene expression: effects on angiogenesis, vascular permeability, blood volume, blood flow, fluorodeoxyglucose uptake, and proliferation of human melanoma intracerebral xenografts. *Cancer Res.* **58**, 4185-4192 (1998).
26. Fukumura D., Yuan F., Endo M., Jain R. K. Role of nitric oxide in tumor

microcirculation. Blood flow, vascular permeability, and leukocyte-endothelial interactions. *Am. J. Pathol* **150**, 713-725 (1997).

27. Zhang Y., et al. Platelet-Specific PDGFB Ablation Impairs Tumor Vessel Integrity and Promotes Metastasis. *Cancer Res.* **80**, 3345-3358 (2020).
28. Hsia L. T., et al. Myofibroblasts are distinguished from activated skin fibroblasts by the expression of AOC3 and other associated markers. *Proc. Natl. Acad. Sci. U. S. A.* **113**, 2162-2171 (2016).
29. Gábris F., Kajtár B., Kellermayer Z., Balogh P. Quantitative Analysis of NKX2-3 Expression in Human Colon: An Immunohistochemical Study. *J. Histochem. Cytochem.* **72**, 11-23 (2024).
30. Dinh T. T., et al. An NKX-COUP-TFII morphogenetic code directs mucosal endothelial addressin expression. *Nat. Commun.* **13**, 7448 (2022).
31. Kellermayer Z., et al. Absence of Nkx2-3 homeodomain transcription factor reprograms the endothelial addressin preference for lymphocyte homing in Peyer's patches. *J. Immunol.* **193**, 5284-5293 (2014).
32. Pabst O., Förster R., Lipp M., Engel H., Arnold H. H. NKX2.3 is required for MAdCAM-1 expression and homing of lymphocytes in spleen and mucosa-associated lymphoid tissue. *EMBO J.* **19**, 2015-2023 (2000).
33. Fan S., et al. Targeting FAPα-positive lymph node metastatic tumor cells suppresses colorectal cancer metastasis. *Acta Pharm. Sin. B* **14**, 682-697 (2024).
34. van Splunder H., Villacampa P., Martínez-Romero A., Graupera M. Pericytes in the disease spotlight. *Trends Cell Biol.* **34**, 58-71 (2024).
35. Petrova T. V., Koh G. Y. Biological functions of lymphatic vessels. *Science* **369**, 4063 (2020).
36. Li X., et al. Novel TCF21^{high} pericyte subpopulation promotes colorectal cancer metastasis by remodelling perivascular matrix. *Gut* **72**, 710-721 (2023).
37. Matsumoto K., et al. Inhibition of glycolytic activator PFKFB3 suppresses tumor growth and induces tumor vessel normalization in hepatocellular carcinoma. *Cancer Lett.* **500**, 29-40 (2021).
38. He B., et al. Remodeling of Metastatic Vasculature Reduces Lung Colonization

and Sensitizes Overt Metastases to Immunotherapy. *Cell Rep.* **30**, 714-724 (2020).

39. Nobre A. R., et al. Bone marrow $NG2^{+}$/$Nestin^{+}$ mesenchymal stem cells drive DTC dormancy via TGFβ2. *Nat. Cancer* **2**, 327-339 (2021).
40. Liu Y., et al. NG2 glia protect against prion neurotoxicity by inhibiting microglia-to-neuron prostaglandin E2 signaling. *Nat. Neurosci.* **27**, 1534-1544 (2024).
41. Ampofo E., Schmitt B. M., Menger M. D., Laschke M. W. The regulatory mechanisms of NG2/CSPG4 expression. *Cell. Mol. Biol. Lett.* **22**, 4 (2017).
42. Alex L., et al. Cardiac Pericytes Acquire a Fibrogenic Phenotype and Contribute to Vascular Maturation After Myocardial Infarction. *Circulation* **148**, 882-898 (2023).
43. Hosaka K., et al. Pericyte-fibroblast transition promotes tumor growth and metastasis. *Proc. Natl. Acad. Sci. U. S. A.* **113**, 5618-5627 (2016).
44. Wong P. P., et al. Cancer Burden Is Controlled by Mural Cell-β3-Integrin Regulated Crosstalk with Tumor Cells. *Cell* **181**, 1346-1363 (2020).
45. Meng Y. M., et al. Hexokinase 2-driven glycolysis in pericytes activates their contractility leading to tumor blood vessel abnormalities. *Nat. Commun.* **12**, 6011 (2021).
46. Cortez E., Roswall P., Pietras K. Functional subsets of mesenchymal cell types in the tumor microenvironment. *Semin. Cancer Biol.* **25**, 3-9 (2014).
47. Aertgeerts K., et al. Structural and kinetic analysis of the substrate specificity of human fibroblast activation protein alpha. *J Biol Chem* **280**, 19441-19444 (2005).
48. Chen M., et al. Pericyte-targeting prodrug overcomes tumor resistance to vascular disrupting agents. *J. Clin. Invest.* **127**, 3689-3701 (2017).
49. Yang Y., et al. The PDGF-BB-SOX7 axis-modulated IL-33 in pericytes and stromal cells promotes metastasis through tumour-associated macrophages. *Nat. Commun.* **7**, 11385 (2016).
50. Viski C., et al. Endosialin-Expressing Pericytes Promote Metastatic

Dissemination. *Cancer Res.* **76**, 5313-5325 (2016).

51. Sinha D., et al. Pericytes Promote Malignant Ovarian Cancer Progression in Mice and Predict Poor Prognosis in Serous Ovarian Cancer Patients. *Clin. Cancer Res.* **22**, 1813-1824 (2016).
52. Huang Q., et al. $CD44^+$ lung cancer stem cell-derived pericyte-like cells cause brain metastases through GPR124-enhanced trans-endothelial migration. *Cancer Cell* **41**, 1621-1636 (2023).
53. Fernández-Klett F., Offenhauser N., Dirnagl U., Priller J., Lindauer U. Pericytes in capillaries are contractile in vivo, but arterioles mediate functional hyperemia in the mouse brain. *Proc Natl Acad Sci U S A* **107**, 22290-22295 (2010).
54. Jiang R. S., et al. Signalling pathway of U46619-induced vascular smooth muscle contraction in mouse coronary artery. *Clin. Exp. Pharmacol. Physiol.* **48**, 996-1006 (2021).
55. Hoffmann P., Heinroth-Hoffmann I., Toraason M. Alterations by a thromboxane A2 analog (U46619) of calcium dynamics in isolated rat cardiomyocytes. *J. Pharmacol. Exp. Ther.* **264**, 336-344 (1993).
56. Jiang M. J., Chan C. F., Chang Y. L. Intracellular calcium and myosin light chain phosphorylation during U46619-activated vascular contraction. *Life Sci.* **54**, 2005-2013 (1994).
57. Chaigneau E., Oheim M., Audinat E., Charpak S. Two-photon imaging of capillary blood flow in olfactory bulb glomeruli. *Proc Natl Acad Sci U S A* **100**, 13081-13086 (2003).
58. Chen L., Hu H., Yuan Y., Weng S. CSCO guidelines for colorectal cancer version 2024: Updates and discussions. *Chin. J. Cancer Res.* **36**, 233-239 (2024).
59. Tian F., et al. Prediction of tumor origin in cancers of unknown primary origin with cytology-based deep learning. *Nat. Med.* **30**, 1309-1319 (2024).
60. Niu L., et al. Noninvasive proteomic biomarkers for alcohol-related liver disease. *Nat. Med.* **28**, 1277-1287 (2022).
61. Jin Y., Qin X. Significance of TP53 mutation in treatment and prognosis in head and neck squamous cell carcinoma. *Biomarkers Med.* **15**, 15-28 (2021).

62. Yu W., et al. NKX2-3 transcriptional regulation of endothelin-1 and VEGF signaling in human intestinal microvascular endothelial cells. *PLoS One* **6**, 20454 (2011).

63. Robles E. F., et al. Homeobox NKX2-3 promotes marginal-zone lymphomagenesis by activating B-cell receptor signalling and shaping lymphocyte dynamics. *Nat. Commun.* **7**, 11889 (2016).

64. Paez-Ribes M., Man S., Xu P., Kerbel R. S. Potential Proinvasive or Metastatic Effects of Preclinical Antiangiogenic Therapy Are Prevented by Concurrent Chemotherapy. *Clin. Cancer Res.* **21**, 5488-5498 (2015).

65. Chen Y., et al. Spatiotemporal single-cell analysis decodes cellular dynamics underlying different responses to immunotherapy in colorectal cancer. *Cancer Cell* **42**, 1268-1285 (2024).

66. Pelka K., et al. Spatially organized multicellular immune hubs in human colorectal cancer. *Cell* **184**, 4734-4752 (2021).

67. Santos A. M., Jung J., Aziz N., Kissil J. L., Puré E. Targeting fibroblast activation protein inhibits tumor stromagenesis and growth in mice. *J Clin Invest* **119**, 3613-3625 (2009).

68. Cremasco V., et al. FAP Delineates Heterogeneous and Functionally Divergent Stromal Cells in Immune-Excluded Breast Tumors. *Cancer Immunol. Res.* **6**, 1472-1485 (2018).

69. Qi M., et al. Targeting FAPα-expressing hepatic stellate cells overcomes resistance to antiangiogenics in colorectal cancer liver metastasis models. *J. Clin. Invest.* **132**, 157399 (2022).

70. Brennen W. N., Rosen D. M., Wang H., Isaacs J. T., Denmeade S. R. Targeting carcinoma-associated fibroblasts within the tumor stroma with a fibroblast activation protein-activated prodrug. *J. Natl. Cancer Inst.* **104**, 1320-1334 (2012).

71. Li M., et al. Characterization and oncolytic virus targeting of FAP-expressing tumor-associated pericytes in glioblastoma. *Acta Neuropathol. Commun.* **8**, 221 (2020).

Point-by-point response letter

Point-by-point responses to the reviewers' comments

The authors thank all the reviewers for their constructive comments and suggestions. The manuscript had been revised accordingly. We responded point-by-point to all comments raised as follows:

Reviewer 2 (expert in vasculature (hemodynamics, calcium signaling), intravital imaging)

Comments to the Author:

These are comments to the revised (R1) version which shows a significant effort by the authors to address the previous comments.

The following numbering refers to the original comments from this reviewer.

(0) The reviewer agrees with the note that tumor capillaries (and vessels in general) are different from normal capillaries. Definition of a capillary might be more complex that addressed here as a single marker is not sufficient (certainly not α-SMA as done by the here). As previously stated, the responses can depend on original vessel size, the authors have not provided the requested information (i.e. a plot of relative diameter change against vessel diameter). This will help to further disentangle whether responses are indeed in capillaries or arterial-like vessels (in the tumor). Moreover, still of much concern, is the fact that vessels categories smaller than 50 μm (Supp Fig 15b) are significantly larger in the knockout.

Response: Thank you for your kind review and comments. To accurately define the capillaries and distinguish them from small arterials, tumor pericytes (TPCs) were characterized by NG2 and PDGFRβ, while smooth muscle cells were defined by Myh11 and SM22α (**Figure R1a**). The results revealed that NKX2-3 was highly expressed in $NG2^{+}PDGFR\beta^{+}$ TPCs-wrapped capillaries, rather than Myh11 and SM22α positive smooth muscle cells, which were covered on arterials (**Figure R1b**).

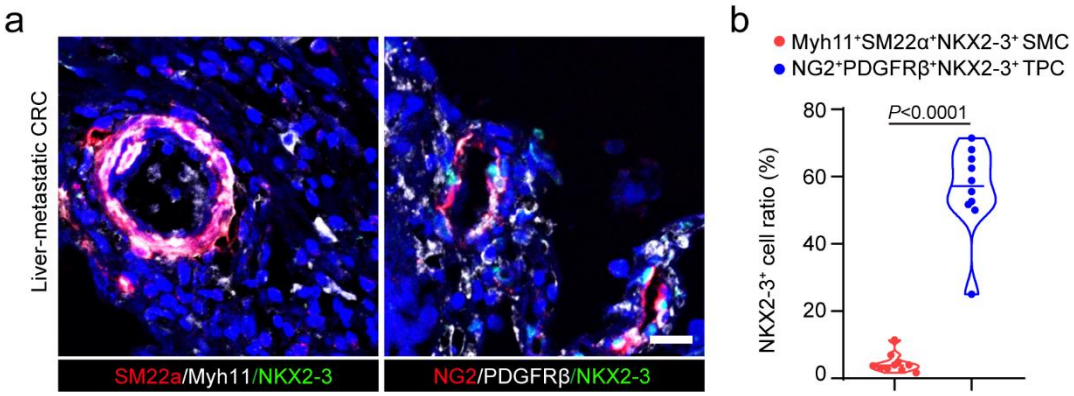

Figure R1. NKX2-3 is expressed in TPCs-wrapped capillaries. a Representative image of NKX2-3 expression in Myh11$^+$SM22α$^+$ SMC and NG2$^+$PDGFRβ$^+$ TPC in the primary tumor of colorectal cancer patients with liver metastasis (n = 10, n denotes the number of patients). Scale bar, 20 μm. **b** Quantification for NKX2-3$^+$Myh11$^+$SM22α$^+$ SMC and NKX2-3$^+$NG2$^+$PDGFRβ$^+$ TPC ratio. *P* value was determined by two-tailed unpaired *t*-test. CRC, colorectal cancer; SMC, smooth muscle cell; TPC, tumor pericyte.

As the reviewer suggested, the scatter diagrams of relative diameter change (%) and relative red blood cell (RBC) velocity change (%) against baseline vessel diameter for Fig. 5b (**Figure R2a, b**) and Supplementary Fig. 25d (**Figure R2c, d**) were given. Moreover, the plot diagram of relative RBC velocity change (%) against baseline vessel diameter for Supplementary Fig. 26a was added (**Figure R2e**). Each plot represented a single vessel, x axis showed the baseline vessel diameter (μm) and y axis showed the relative diameter change (%) or relative RBC velocity change (%). The initial diameters of examined vessels were ranged from10-70 μm.

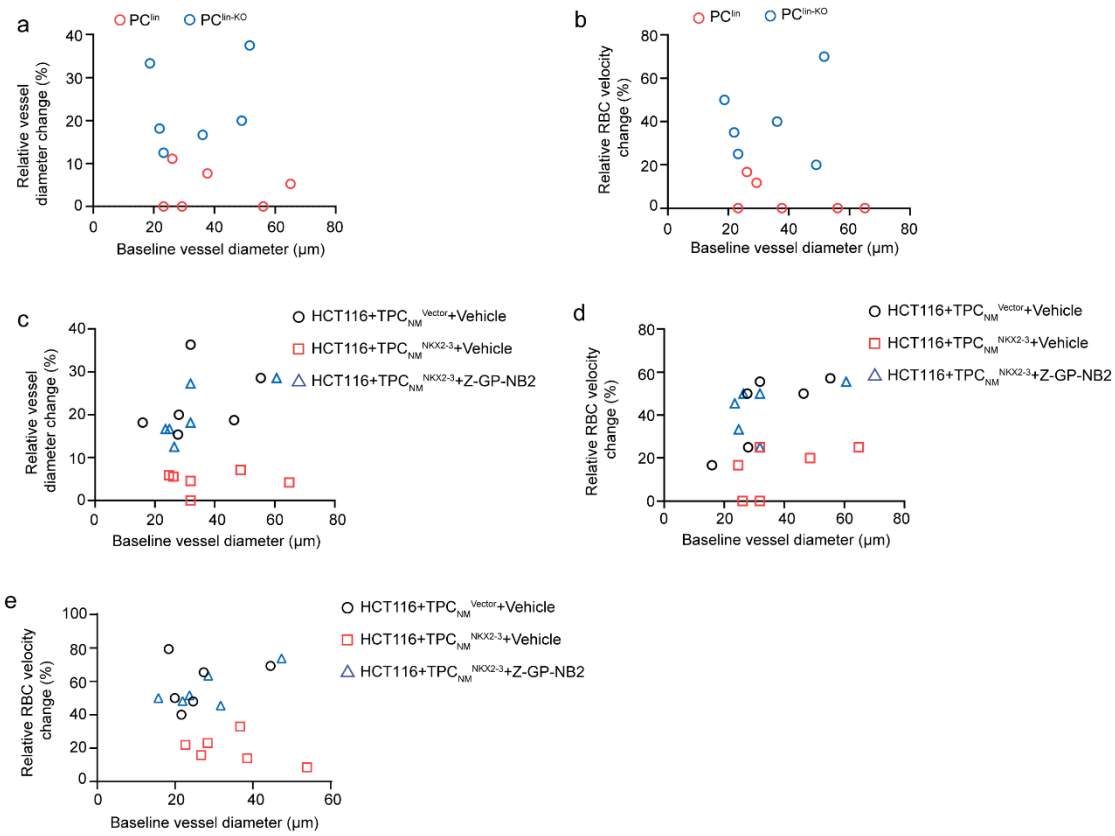

Figure R2. NKX2-3 in TPCs regulates vessel diameter and blood flow velocity. a, b Plot diagram of relative vessel diameter change (%) (**a**) and relative RBC velocity change (%) (**b**) against baseline vessel diameter (μm) in the primary tumor of pericyte-*Nkx2-3* knockdown mice (n = 6). **c, d** Plot diagram of relative vessel diameter change (%) (**c**) and relative RBC velocity change (%) (**d**) against baseline vessel diameter (μm) in the primary tumor of Z-GP-NB2-treated mice (n = 6). **e** Scatter plot of relative RBC velocity change (%) against baseline vessel diameter (μm) in the primary tumor of Z-GP-NB2-treated mice (n = 6); n denotes the number of samples each group. RBC, red blood cell; TPC, tumor pericyte.

Specific deletion of *Nkx2-3* in tumor pericytes induced vasoconstriction and then the diameter of vessels was decreased, therefore the proportion of small vessels below 50 μm was increased, and the proportion of large vessels was relatively decreased **(Please see page 9, line 175-177; page 13, line 269-274 in the revised manuscript; Supplementary Fig. 6, Supplementary Fig. 18b-c, Supplementary Fig. 25e-f, Supplementary Fig. 26b in the revised Supplementary Information).**

(5) With respect to the PC^{lin-KO}, the authors have to make it clear in the main text that the vascular network is different in nature from the WT (again, based on the significant changes presented in Supp Fig 15b). The following updated lines fail to do so, it is not just a matter of mean vessel diameter; changing the proportion of small vessels (higher in the KO) alters baseline hemodynamics, unrelated to any treatment.

261 Light-sheet and confocal fluorescence microscopy were applied to analyze vascular
262 morphology and structure. Conditional deletion of Nkx2-3 had negligible effects on
263 pericyte coverage (Supplementary Fig. 15a) and vessel density (Fig. 4d); however,
264 vessel diameter was significantly decreased in PClin-KO mice compared with that in PClin
265 mice (Fig. 4d; Supplementary Fig. 15b)

Response: We sincerely appreciate the reviewer's insightful comments regarding the vascular changes in PC^{lin-KO} mice. We have corrected the description into "Conditional deletion of *Nkx2-3* had negligible effects on pericyte coverage (Supplementary Fig. 17a) and vessel density (Fig. 4d). However, the architecture of vascular network in the primary tumor of PC^{lin-KO} mice was different from that in PC^{lin} mice, as characterized by a significantly reduced mean vascular diameter compared to that in PC^{lin} mice (Fig. 4d), which might be resulted from the reduced proportion of vascular with large diameter, accompanied by an increased proportion of small-diameter vessels (Supplementary Fig. 17b)." The decrease in the average diameter of tumor vessels might be due to the fact that specific deletion of *Nkx2-3* in TPCs induced vasoconstriction and reduced vascular diameter, therefore the proportion of small vessels was increased, whereas the proportion of large vessels was relatively decreased **(Please see page 13, line 269-274 in the revised manuscript).**

(6) Same as in previous comments, the data should be presented for the different vessels diameters measured. Currently data is averaged over animals making it more difficult to appreciate the detailed responses in each treatment as this can be dependent on biological or experimental bias (i.e. having sampled more vessel of a specific diameter). The authors can present a scatter plot for all the vessels measured across treatments,

here again plotting % change (as now implemented) vs baseline average vessel diameter.

Response: Thanks for your valuable comments. We have re-analyzed the data and now it was presented as relative diameter or RBC velocity change (%) against baseline vessel diameter (μm). The scatter diagrams of relative diameter change (%) and relative red blood cell (RBC) velocity change (%) against baseline vessel diameter for Fig. 5b (**Figure R3a, b**) and Supplementary Fig. 25d (**Figure R3c, d**) were presented below. Moreover, the plot diagram of relative RBC velocity change (%) against baseline vessel diameter for Supplementary Fig. 26a was added (**Figure R3e**). Each plot represented single vessel, x axis showed the baseline vessel diameter (μm) and y axis showed the relative diameter change (%) or relative RBC velocity change (%) **(Please see Supplementary Fig. 18b-c, Supplementary Fig. 25e-f, Supplementary Fig. 26b in the revised Supplementary Information).**

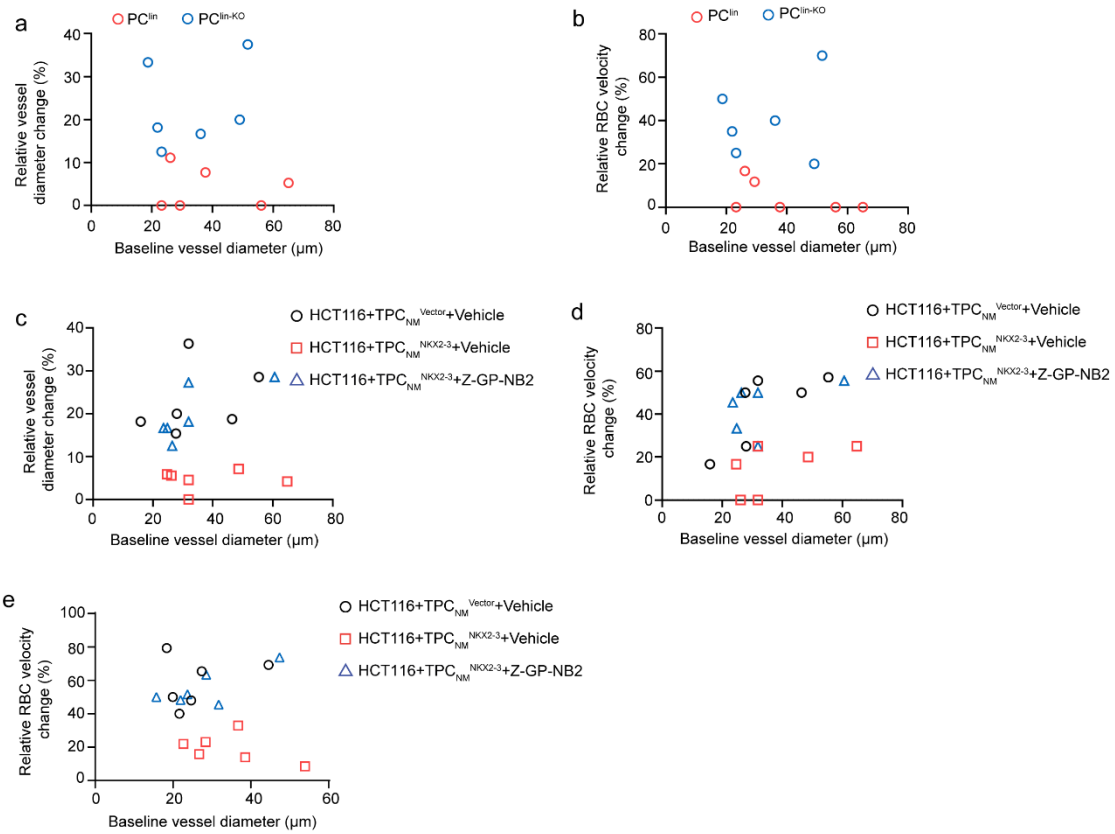

Figure R3. NKX2-3 in TPCs regulates vessel diameter and blood flow velocity. a, b Plot diagram of relative vessel diameter change (%) (**a**) and relative RBC velocity change (%) (**b**) against baseline vessel diameter (μm) in the primary tumor of pericyte-*Nkx2-3* knockdown mice (n = 6). **c, d** Plot diagram of relative vessel diameter change

(%) (**c**) and relative RBC velocity change (%) (**d**) against baseline vessel diameter (μm) in the primary tumor of Z-GP-NB2-treated mice (n = 6). **e** Scatter plot of relative RBC velocity change (%) against baseline vessel diameter (μm) in the primary tumor of Z-GP-NB2-treated mice (n = 6); n denotes the number of samples each group. RBC, red blood cell; TPC, tumor pericyte.

Reviewer #5 (expert in colorectal cancer liver metastasis)

In their comprehensive rebuttal, the authors provide a wealth of additional data to the already exceptionally rich manuscript.

Response: We are extremely grateful to your thorough evaluation and insightful comments, which help us gain a deeper understanding of clinical knowledge. Your expertise and constructive feedback have greatly enhanced the rigor and readability of this study. We have addressed each of your concerns in details, incorporating your suggestions into the revised manuscript and supplementary materials.

In their rebuttal, the authors state that "We apologize for the misleading description of artificial intelligence. Blood flow in tumor was measured by doppler ultrasound imaging, and the images of tumors derived from colorectal cancer patients with or without liver-metastasis were collected and analyzed using Open CV, rather than "artificial intelligence". In ultrasound Doppler images, red and blue regions conventionally represent blood flow, with red indicating arterial flow and blue indicating venous flow."

- I find it of significant concern that the authors initially provided an incorrect description of the method used to analyze the major hypothesis-driving analyses, and this could raise fundamental concerns as to the validity and methods description of the remaining experiments.

Response: The authors really appreciate the reviewer's constructive comments. The method used to measure blood flow in the primary tumor of colorectal cancer patients was Open CV, which was mistakenly described as an algorithm based on AI in the previous manuscript. We appreciated that the reviewer pointing out the mistake and corrected the description in the last round of revision. In this revision, we have further

verified each experimental method and corrected the description about methods and results.

- In Doppler images, red and blue regions do not conventionally represent arterial and venous flow, as stated by the authors. Rather, blood flow is color-coded according to the flow direction to or from the transducer, entirely unrelated to the vessel being a vein or artery. This fundamental principle of the technique is misstated.

Response: We sincerely apologize for the inappropriate description and have thoroughly corrected it in the revised manuscript. After consulting with ultrasound specialists, we realized the previous description was incorrect. Indeed, in Doppler images, red indicates blood flow toward the transducer, while blue indicates blood flow away from the transducer [1, 2]. In this revision, we have corrected the descriptions about experimental methods **(Please see page 26, line 567-568 in the revised manuscript).**

The authors now provide some clinical data, as suggested, which allows for a more detailed assessment of the results presented in Figure. However, clinical data are presented stratified by blood flow results in Supplementary Tables 5 and 6, while the groups in Figure 1 are stratified into patients with and without metastases. Hence, the data are not aligned, and a thorough assessment of the effect postulated from Figure 1 is not possible based on the presented tables. However, what becomes evident is that earlier, early-stage tumors (T1/2) have lower flow than later-stage tumors (T3/4). Given this confounder, it is not acceptable to simply state (L 123) "(…) results showed that blood flow was significantly increased in CRC patients with liver metastasis compared with that in non-metastatic patients", and neglect tumor stage as a potential alternative explanation. This statement ignores a confounding variable, and no evidence is presented to show that the results hold even after correcting for tumor size. Please see also a comment below on further systematic differences between early and advanced tumors.

Response: Thanks for your comments, Supplementary Table 5 and Supplementary Table 6 were patient information, which were stratified into patients without metastasis

and liver metastasis and aligned with the results in Figure 1. Our study aimed to investigate the effects of tumor pericytes on colorectal cancer liver metastasis, therefore we only collected samples from non-metastatic patients (stage I/II) and liver-metastatic patients (stage IV), patient information was listed in Supplementary Table 5 and Supplementary Table 6. We also compared the signal of blood flow in the primary tumors of stage I, II and IV patients, and the results showed the signal of blood was increased in stage IV patients (**Figure R4a, b**). Furthermore, multivariable linear regression analysis was performed to investigate the contribution of gender, age, location, differentiation, maximum diameter, T stage (T1/2 vs T3/4), N stage (N0 vs N1-2) and liver metastasis to the signal of blood flow in Fig. 1a and Fig. 1b, and the result showed only liver metastasis was significantly correlated with the signal strength value (**Table R1**) and small area emphasis value (**Table R2**).

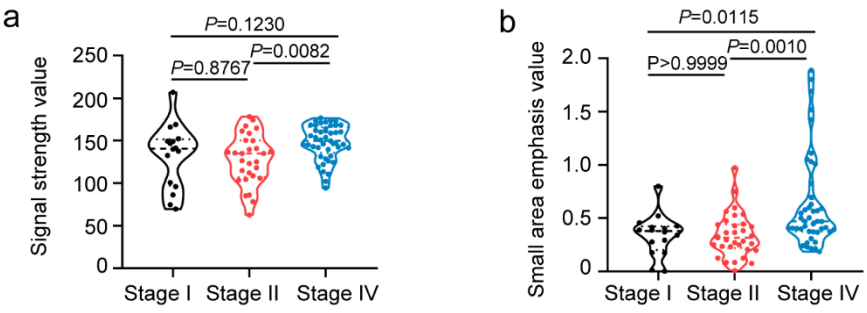

Figure R4. The signal of blood flow in the primary tumor of patients. a Doppler ultrasound analysis for signal strength value in the primary tumor tissues of patients at stage I (n = 16), stage II (n = 29) and stage IV (n = 45). **b** CT analysis for small area emphasis value in the primary tumor tissues of patients at stage I (n = 16), stage II (n = 33) and stage IV (n = 44). *P* values were determined by one-way ANOVA followed by Tukey's post hoc test; n denotes the number of patients.

Table R1. Multivariable linear regression analysis for the correlation between signal strength value and clinicopathologic data.

Variables	Unstandardized coefficients		*P* value	VIF
	β	SEM		

Gender	-7.498	7.141	0.297	1.061
Age	-0.376	0.299	0.212	1.019
Tumor location	-2.531	7.438	0.735	1.021
Differentiation stage	-6.219	6.321	0.328	1.066
maximum diameter	-2.034	2.625	0.441	1.071
T stage (T1/2 vs T3/4)	-0.864	8.692	0.921	1.264
N stage (N0 vs N1-2)	-9.789	11.764	0.408	4.014
Liver metastasis	27.643	11.686	0.020	4.076

Table R2. Multivariable linear regression analysis for the correlation between small area emphasis value and clinicopathologic data.

Variables	Unstandardized coefficients		*P* value	VIF
	β	SEM		
Gender	0.012	0.076	0.874	1.036
Age	0.004	0.003	0.116	1.185
Tumor location	0.077	0.090	0.399	1.082
Differentiation stage	-0.056	0.076	0.459	1.072
maximum diameter	0.012	0.023	0.588	1.047
T stage (T1/2 vs T3/4)	-0.093	0.090	0.300	1.065
N stage (N0 vs N1-2)	-0.098	0.129	0.448	3.203
Liver metastasis	0.402	0.124	0.002	3.127

Therefore, current data only supported that blood flow was increased in CRC patients with liver metastasis (stage IV) compared with that in non-metastatic patients (stage I/II), more data, especially stage III patient data is needed to investigate the blood flow in the early stage and late-stage tumors **(Please see page 7, line 125-127, line 131-132 in the revised manuscript; Supplementary Table 1 and Table 2 in the revised Supplementary Information)**.

Figure 2a, and Figure R25: The tSNEs seem to have been generated from the whole dataset and then separated. The effect of cluster 3 being present only in the LM group is exceptionally strong and, given the size of the cohort (n=2 in each), is likely driven by the tumor biology of an individual tumor or by batch effects. Showing separate parts of the dataset without, for example, in grey dots, the entire dataset is somewhat misleading, although not entirely uncommon. To be more convincing, the authors should highlight the individual patients in the Supplementary data to be able to see batch effects.

Response： Thanks for your comments. The t-SNE diagram was generated from the sc-RNA data of TPCs. TPCs were isolated from the primary tumors of two non-metastatic and two liver-metastatic colorectal cancer patients though microdissection combined with pericyte medium-based approach (MPMA) according to our previous study[3] and applied for sc-RNA analysis. TPCs were divided into 13 clusters (cluster 0-12), among which, cluster 3 was significantly enriched in liver-metastatic patients. To better present the distribution of cluster 3 in liver-metastatic patients, the t-SNE of the 4 individual samples were shown **(Figure R5a, b)**. The number of TPCs in each sample was labeled in the images **(Please see Supplementary Fig. 2 in the revised Supplementary Information)**.

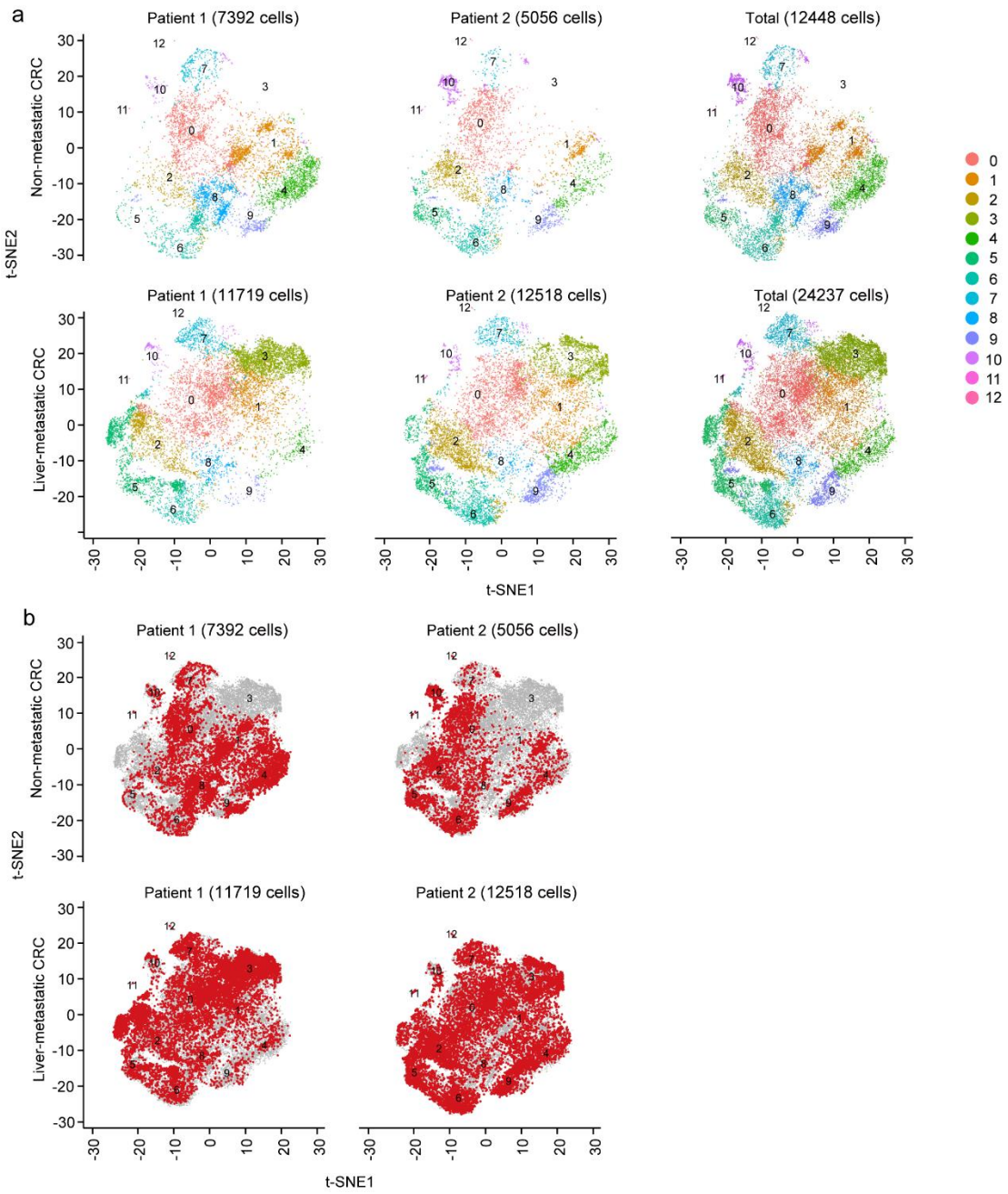

Figure R5. t-SNE of TPC subsets. a t-SNE visualization of TPC subsets derived from primary tumor tissues of CRC patients with (n = 2) or without (n = 2) liver metastasis. **b** t-SNE plot of TPCs derived from individual CRC patients with (n = 2) or without (n = 2) liver metastasis. Red plots indicate the individual TPC data, while the gray plots indicate the whole dataset; n denotes the number of samples each group. CRC, colorectal cancer; t-SNE, t-distributed stochastic neighbor embedding.

The authors state: “Concerning the colorectal cancer patients with liver metastasis or

locally advanced stage (T4), although preoperative neoadjuvant radiotherapy or chemotherapy is an important treatment option, a large number of cases with complications require palliative surgical resection or fistula treatment, which is also in line with the Chinese Society of Clinical Oncology (CSCO) guidelines for colorectal cancer version 202458. Therefore, to rule out the effects of preoperative neoadjuvant therapy on the metastasis, colorectal cancer patients without radiotherapy or chemotherapy prior to surgery were included in this study as a source of clinical specimens."

- If the authors collected specimens from emergency/palliative operations of advanced tumors, I am afraid this adds another confounder to the data in Figure 1 because T1/2 tumors were operated electively, while T4 tumors, for which the authors showed increased blood flow, were operated due to, e.g., ileus or fistula. This would invariably lead to inflammation and increased blood flow, questioning the results presented in Figure 1.

Response: Thanks for your constructive comments. We are sorry that we didn't describe it clearly before. According to NCCN and CSCO guidelines [4], for specimens derived from patients with liver metastasis, not all of these patients were from emergency/palliative operations. A subset of patients with liver metastases can undergo direct resection without radiotherapy or chemotherapy, based on the following criteria: those with only liver metastases and the number of metastatic foci is ≤ 5, with a carcinoembryonic antigen response score (CRS) of 0-2. The surgical requirements include sufficient residual liver volume and achieving R0 resection margins. The recommended treatment for these patients is synchronous or staged colorectal cancer resection followed by adjuvant chemotherapy.

To minimize confounding by surgery-related inflammation, we replaced patients with preoperative infections (according to patient white blood cell count, C-reactive protein and Neutrophil-to-Lymphocyte Ratio) and re-analyzed the data **(Figure R6 and R7) (Please see page 22, line 477-478; Fig. 1 and Fig. 2g-j in the revised manuscript)**.

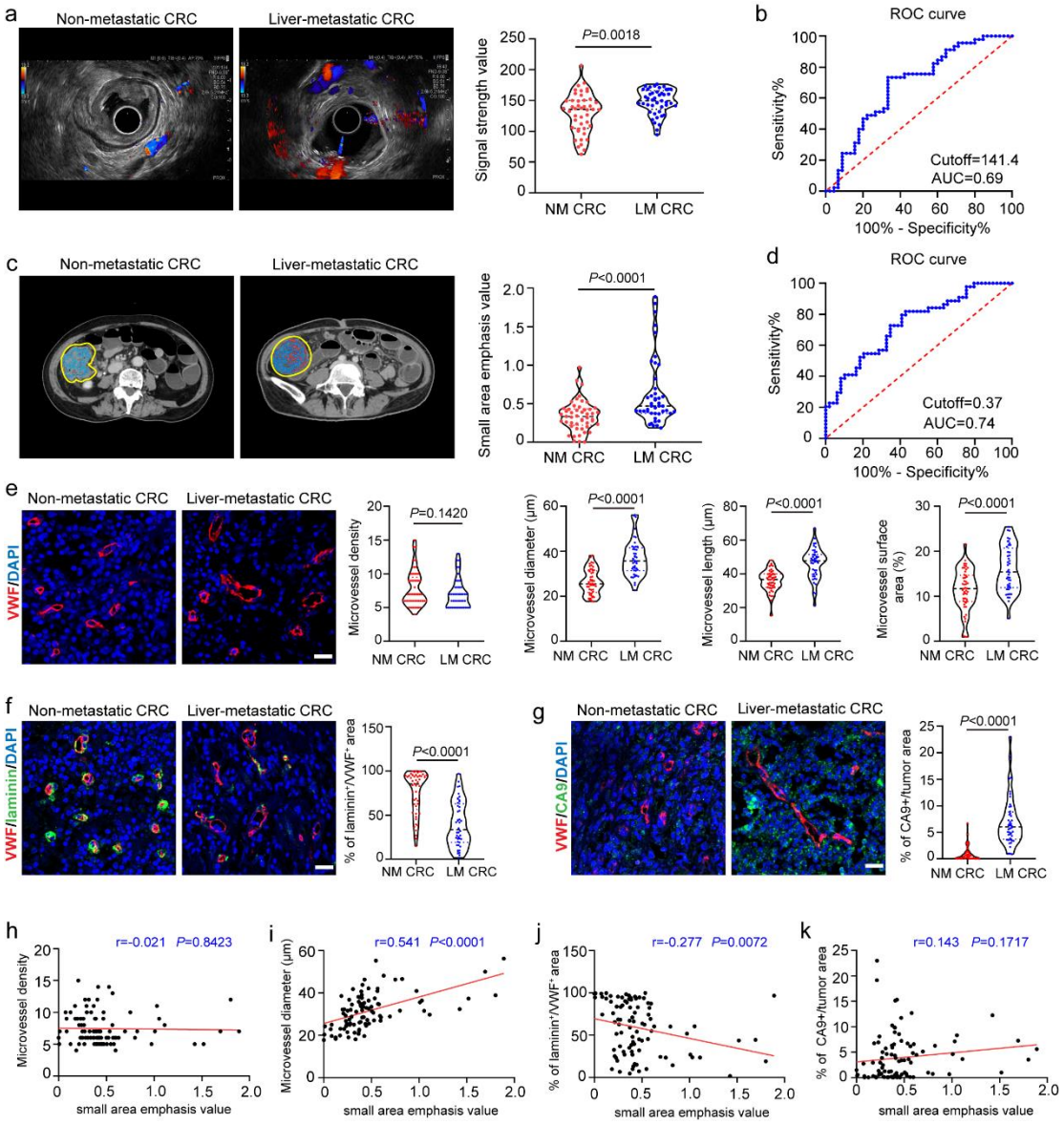

Figure R6. Hemodynamic changes in primary tumor are associated with colorectal cancer liver metastasis. a Doppler ultrasound images of blood flow signal derived from the primary tumor tissues of NM CRC (n = 45) and LM CRC patients (n = 45). The quantification of blood flow signal is shown (right). **b** ROC curve analysis of the blood flow signal in CRC patients (n = 90)**. c** Representative CT images and quantification for blood flow signal in NM CRC (n = 49) and LM CRC patients (n = 44). **d** ROC curve analysis of the blood flow signal (small area emphasis value) in CRC patients (n = 93). Yellow circles indicate primary tumor region. **e** Immunofluorescence analysis of microvessel density, diameter, length and surface area in the primary tumor of NM CRC (n = 49) and LM CRC patients (n = 44). Scale bar, 20 μm. **f**

Immunofluorescence analysis of laminin$^+$/VWF$^+$ area per field in the primary tumor of NM CRC (n = 49) and LM CRC patients (n = 44). Scale bar, 20 μm. **g** Immunofluorescence analysis of CA9$^+$/tumor area in the primary tumor regions derived from NM CRC (n = 49) and LM CRC patients (n = 44). Scale bar, 20 μm. **h-k** Pearson correlation analysis of microvessel density (**h**), microvessel diameter (**i**), % of laminin$^+$/VWF$^+$ area (**j**), and % of CA9$^+$/tumor area (**k**) with the signal of blood flow (small area emphasis value) in **c** (n = 93). Each sample in the violin plots represents data from an individual patient. *P* values were determined by two-tailed unpaired *t*-test, n denotes the number of patients. AUC, area under curve; CRC, colorectal cancer; CT, computed tomography; LM CRC, liver-metastatic colorectal cancer; NM CRC, non-metastatic colorectal cancer; ROC, receiver operating characteristic.

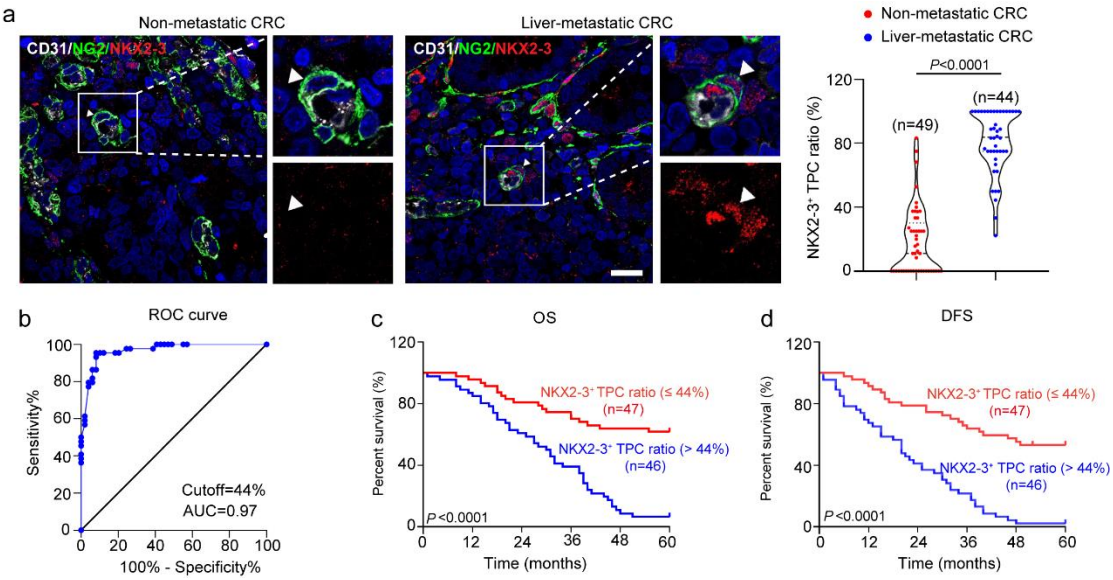

Figure R7. NKX2-3 is highly expressed in TPCs derived from CRC patients with liver metastasis. a Immunofluorescence staining and quantification of the NKX2-3$^+$ TPC ratio in tumor sections from CRC patients (n = 93). The white arrows indicate NKX2-3 staining in TPCs. Scale bar, 20 μm. Each sample in the violin plots represents data from an individual patient. **b** ROC curve analysis of the NKX2-3$^+$ TPC ratio in CRC patients (n = 93). **c, d** Kaplan-Meier analysis of OS **(c)** and DFS (**d**) in CRC patients with a high or low NKX2-3$^+$ TPC ratio (optimal cutoff value of 44%, n = 93). *P* values were determined by two-tailed unpaired *t*-test **(a),** log-rank (Mantel-Cox) test

(c, d), n denotes the number of patients. AUC, area under curve; CRC, colorectal cancer; OS, overall survival; DFS, disease-free survival; ROC, receiver operating characteristic; TPC, tumor pericyte.

In their rebuttal, the authors state:

"Anti-angiogenic therapies including bevacizumab and DC101 are frequently used to treat tumor in clinic, however, which often result in local invasion and distant metastasis while blunting tumor growth". This is incorrect, at least for the clinical setting. While there are mouse data to suggest increased metastases on monotherapies with antiangiogenic drugs, this is not commonly observed in the clinical setting, as stated here by the authors. While the combination with chemotherapy might partly explain this phenomenon, Ramucirumab, e.g., is approved as a single therapy (REGARD trial, Lancet 2014).

Response: Thanks for your valuable comments. We agreed with the reviewer's opinion, the conclusions that "Anti-angiogenic therapies often result in local invasion and distant metastasis while blunting tumor growth" are primarily based on the preclinical cancer models including mouse breast cancer, pancreatic neuroendocrine carcinoma, glioblastoma and colorectal cancer[5-8]. These studies indicate that anti-angiogenic therapies lead to hypoxia in the tumor microenvironment and triggers metastasis in preclinical xenograft models.

Minor points:

On page 10, the authors state "the downregulated genes in $TPC_{LM}^{gNKX2-3}$(637) were defined by Venn diagram (https://bioinfogp.cnb.csic.es/tools/venny/)."

- Venn diagrams are used to visualize overlapping data; the authors have simply identified overlapping genes in two lists.

Response: Thanks for your comments. Venn diagram was used to present the overlapping data in two or more data lists according to previous study[9-11]. Here, the overlapping genes between NKX2-3 peak genes-associated with calcium signaling pathway (110) and the down-regulated genes in $TPC_{LM}^{gNKX2-3}$ (637) were defined by

Venn diagram. NKX2-3 peak genes associated with calcium signaling pathway (110) were derived from Chromatin immunoprecipitation (ChIP)-seq analysis, and the down-regulated genes in $TPC_{LM}^{gNKX2-3}$ were examined by RNA-seq analysis, 5 overlapping genes were found between these two lists. To make it clear, we have improved the picture in Figure 3c (**Figure R8**) **(Please see page 10, line 204; Fig. 3c in the revised manuscript)**.

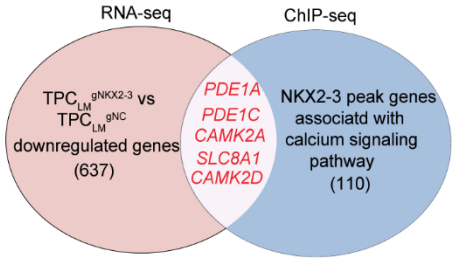

Figure R8 Venn diagram for overlapping genes in RNA-seq and ChIP-seq. Venn diagram showing the number of overlapping genes derived from NKX2-3-regulated genes and NKX2-3 peak genes associated with calcium signaling pathway. RNA-seq was performed on $TPC_{LM}^{gNKX2-3}$ (n = 3) vs TPC_{LM}^{gNC} (n = 3), n denotes the number of samples.

The authors added data on lymph node metastases in a mouse model (Suppl Figure 14) and state "Mouse metastasis was detected by in vivo imaging system and H&E staining." In vivo imaging (IVIS) cannot reasonably distinguish caecal tumor growth (where tumor cells were injected to) to lymphnode metastases as it lacks anatomical resolution for this, rather, it measures overall tumor growth. On the histological images shown, it is hard to see any tumor cells due to the limited resolution, but I cannot discern a clear primary tumor in the caecum.

Response: Thanks for your constructive comments. Mouse lymphnode metastasis was detected by *in vivo* imaging system (IVIS) and H&E staining. To distinguish caecal tumor growth and lymphnode metastasis, the whole intestinal tissues were acquired and examined by IVIS at the end of experiments, which helped improve the readability of results. IVIS revealed that specific deletion of *Nkx2-3* in TPCs had negligible effects on lymph node metastasis of CRC **(Figure R9a, b)**. For H&E staining, it was hard to

embed the primary tumor and lymphatic metastasis lesion together due to the limited size of slice embedding box, therefore, the lymphnode metastases were examined by H&E staining separately, furthermore, the large views of these pictures were provided, the results indicated that specific deletion of *Nkx2-3* had negligible effects on lymphnode metastasis (**Figure R9c**) **(Please see Supplementary Fig. 16 in the revised Supplementary Information)**.

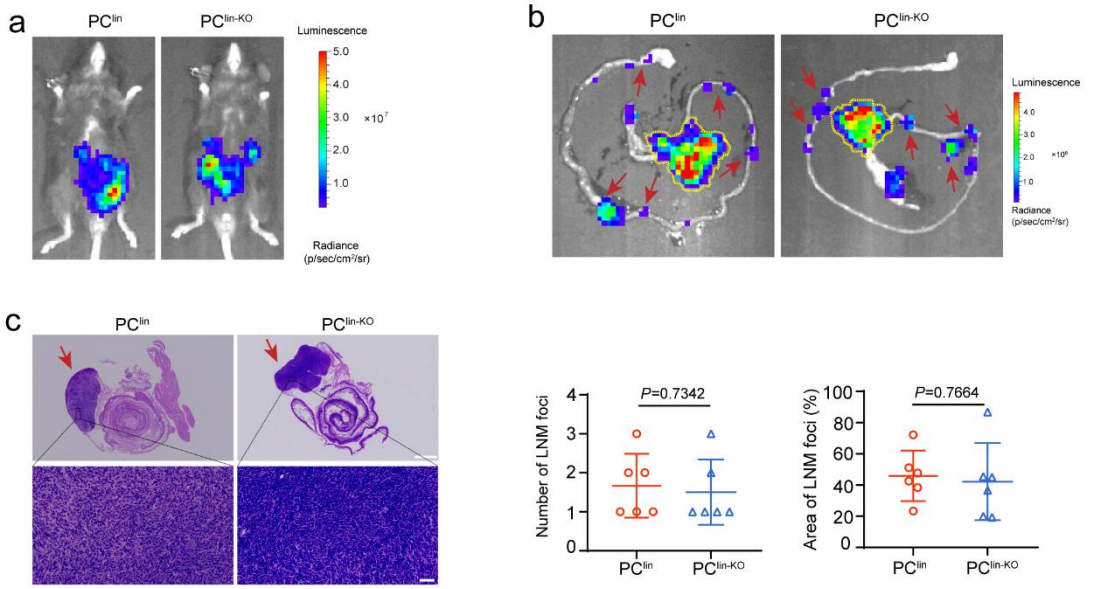

Figure R9 Pericyte specific deletion of *Nkx2-3* has negligible effects on lymph node metastasis. a Representative images of bioluminescence signals in mice orthotopically injected with MC-38-luc-LNM cells. **b** Bioluminescence images of caecal tumor and lymphnode metastatic foci. Red arrows indicate lymphnode metastases, yellow dotted lines indicate primary tumor region. **c** H&E staining and quantification for lymphnode metastases in tumor-bearing PC^{lin} and $PC^{lin\text{-}KO}$ mice. Scale bar, 3.25 mm (upper), 80 μm (down). Red arrows indicate lymphnode metastases. Data are presented as mean ± SEM (n = 6, n denotes the number of samples each group). *P* values were determined by two-tailed unpaired *t*-test. LNM, lymph node metastasis; PC, pericyte.

Reviewer 10 (Replacement Reviewer for Reviewer #3)

Comments to the Author:

The majority of Reviewer#3's concerns were satisfactorily addressed. The following

minor clarifications are required.

1. For experiments involving PClin mice and PClin-KO mice there seem not to be enough information/evidence on a) whether the efficiency of tamoxifen-mediated PC lineage labelling is comparable between PClin and PClin-KO mice and b) to what extent and when the tamoxifen-mediated depletion of NKX2-3 expression in the PClin-KO mice is achieved and maintained throughout the length of the experiment. It will be helpful to provide some quantitation as e.g. Supplementary Fig. 11 b-d fall short to inform this, hence, to characterize the model.

Response: Thank you for your kind review and comments. The efficiency of tamoxifen-mediated PC lineage labeling was calculated as tdTomato expression on NG2 positive TPCs (%), and the results showed that the efficiency of PC lineage labeling was similar between PC^{lin} mice and $PC^{lin\text{-}KO}$ mice (**Figure R10a**). To examine the efficiency of *Nkx2-3* depletion in tumor pericytes, the expression of NKX2-3 in the $tdtomato^{+}$ TPCs derived from PC^{lin} and $PC^{lin\text{-}KO}$ mice were examined at Day10, Day20 and Day30 after tamoxifen injection (**Figure R10b**), the results revealed that *NKX2-3* was knockout in TPCs of $PC^{lin\text{-}KO}$ mice after 10 days-injection of tamoxifen and continued until the end of experiments (**Figure R10c**) **(Please see page 12, line 252-253 in the revised manuscript; Supplementary Fig. 13a-c in the revised Supplementary Information).**

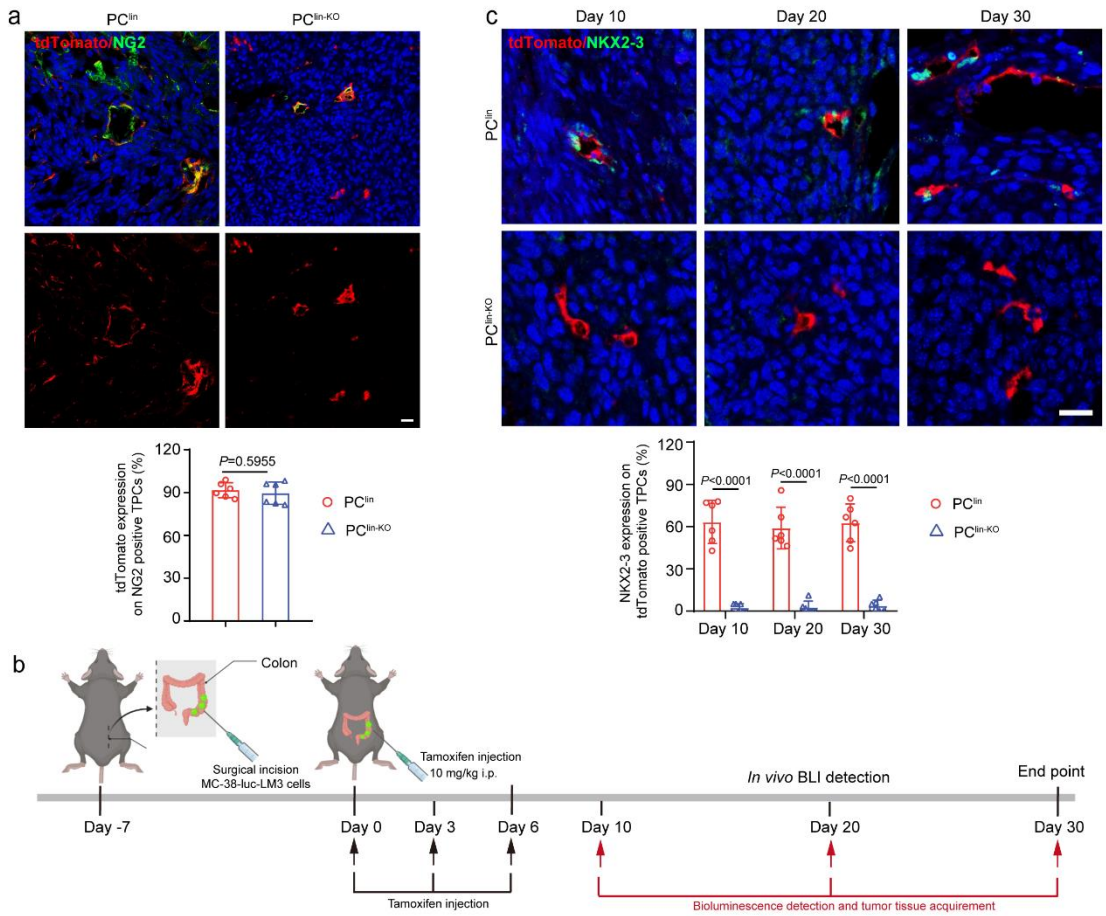

Figure R10. Characterization of PC^{lin} and PC$^{lin\text{-}KO}$ mice. a Immunofluorescence assay for tdTomato expression on NG2 positive TPCs (%). Scale bar, 20 μm. **b** Schematic diagram describing the experimental design of *in vivo* experiments. PC^{lin} mice and PC$^{lin\text{-}KO}$ mice were orthotopically injected with MC-38-luc-LM3 cells. 7 days later, mice were treated with tamoxifen (10 mg/kg) through intraperitoneal (i.p.) administration every three days for three times, and mouse tumor growth and liver metastasis were detected by in vivo tracking. Black arrows indicate tamoxifen administration; red arrows indicate bioluminescence detection and tumor tissue acquirement. **c** Representative images and quantification for NKX2-3 expression on tdTomato positive TPCs (%). Scale bar, 20 μm. Data are presented as mean ± SEM (n = 6, n denotes the number of samples each group). *P* values were determined by two-tailed unpaired *t*-test. BLI, bioluminescence imaging; TPC, tumor pericyte.

2. For western blot analysis, particularly those shown in Fig. 2e, the authors must clarify

in the Fig. legend how the membrane was processed e.g. are the blots presented belong to the same membrane, which was cut, and each part probed the desired target? Or are the blots presented belong to the same membrane, which was probed first for one target, stripped, and subsequently re-probed for another target? Or are the blots presented belong to different membranes performed with the same samples/protein lysates? This is relevant as for analysis (quantitation) and data interpretation purposes. This comment applies to all the western blots presented in this manuscript.

Response: We appreciate your valuable comments. Western blot bands were derived from different membranes performed with the same samples/protein lysates, and each Western blot assay had three biological repetitions. The uncropped bands and quantitative analysis were presented in the source data. As the reviewer suggested, we have added the description in the figure legends (**Please see page 37, line 792-793; page 38, line 818-819; page 42, line 897-898 in the revised manuscript; figure legends the revised Supplementary Information**).

3. For contractility studies, particularly those shown Fig. 3l, the representative images shown by the authors for TPCNMNKX2-3 + siPDE1C in the presence or absence of Verapamil do not align with what they have shown in the associated quantitation plot. It will be good for the authors to check if those 2 images are mislabelled/misplaced?

Response: Thank you for pointing out this problem. We checked the results and replaced representative image of $TPC_{NM}^{NKX2\text{-}3 + siPDE1C}$+ Verapamil group (**Figure R11**) (**Please see Fig. 3l in the revised manuscript**).

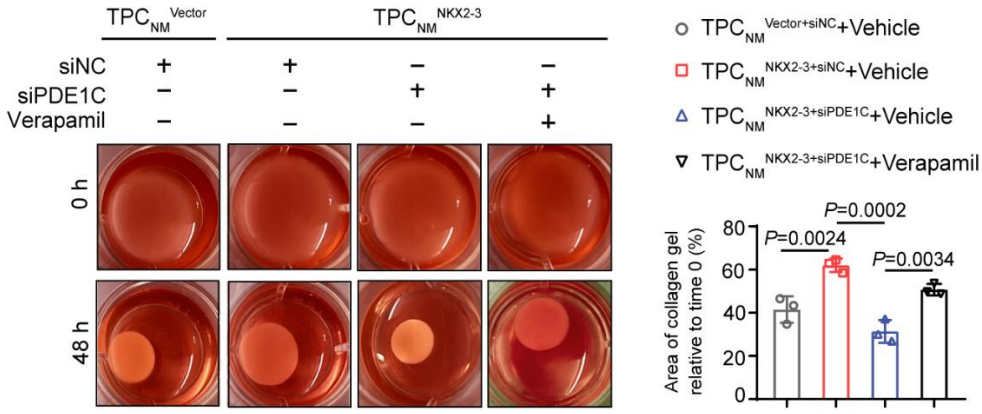

Figure R11. NKX2-3 in TPCs inhibits cell contraction through suppressing the Ca^{2+} axis. Representative images and quantification of collagen contraction induced by the indicated TPC_{NM}^{Vector} and $TPC_{NM}^{NKX2\text{-}3}$. TPCs with indicated transfection were pre-treated with verapamil (5 μM). Data are presented as mean ± SEM (n = 3, n denotes the number of samples each group). *P* values were determined by one-way ANOVA followed by Tukey's post hoc. TPC, tumor pericyte.

4. For microvascular density in primary tumours, particularly that shown in Supplementary Fig. 15, the representative image shown for PClin appears to have more CD31 positive vessels than that shown for PClin-KO. This is relevant as the authors claim that microvascular density is not different between genotypes, further I understand the % of BV with different diameters is calculated considering the total number of BV, hence microvascular density. Please clarify and replace image as needed.

Response: Thanks for your comments. Vascular density was comparable between PC^{lin} and $PC^{lin\text{-}KO}$ mice. We have improved the quality of images in Fig. S15A (**Figure R12**) (**Please see Supplementary Fig. 17a in the revised Supplementary Information**).

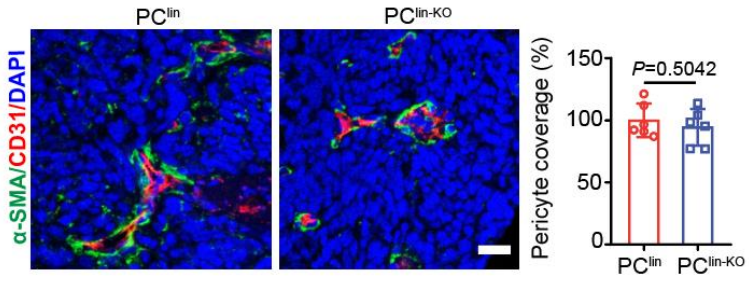

Figure R12. Pericyte-specific deletion of *Nkx2-3* has negligible effects on pericyte coverage. Immunofluorescence analysis of pericyte coverage in orthotopic tumor tissues. Scale bar, 20 μm. Data are presented as mean ± SEM (n = 6, n denotes the number of samples each group). *P* values were determined by two-tailed unpaired *t*-test. PC, pericyte.

5. For the EVs analysis, particularly that shown in Supplementary Fig. 21, as currently shown Z-GP-NB2 seems to upregulate NKX2-3 expression. It will be good for the

authors to crosscheck if the blot image is mislabeled (?) as TPCs should have been incubated with DLD-1NEAT1 EVs and further treated (akas + in the legend) with Z-GP-NB2. Please clarify.

Response: Thank you for pointing out this mistake. We have corrected the labeling in Supplementary Fig. 21 (**Figure R13**) (**Please see Supplementary Fig. 23j in the revised Supplementary Information**).

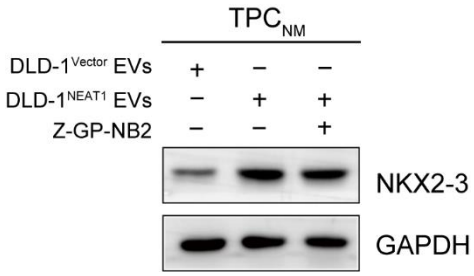

Figure R13. Z-GP-NB2 has negligible effects on NKX2-3 expression. Western blot assay for NKX2-3 expression in TPCs treated with DLD-1 cells-derived EVs and Z-GP-NB2. EVs, extracellular vesicles. Western blot bands were derived from different membranes performed with the same protein lysates; each had three biological repetitions.

6. In general, throughout the whole manuscript, the n numbers in the figure legends and/or in the methods text seems poorly described. For examples, n=3 in Supplementary Fig. 21 is it for number of TPC samples treated or for number of WB performed with same samples? A more precise description is needed.

Response: n = 3 in Supplementary Fig. 21 refers to three independent biological replicates. TPC samples were collected from three separate experiments, followed by protein extraction and Western blot analysis, with the presented image being a representative result. The detailed information of n values was added in the figure legends (**Please see figure legends the revised manuscript and Supplementary Information).**

References

1. Sharma M., et al. General principles of image optimization in EUS. *Endosc*

Ultrasound **10**, 168-184 (2021).

2. Brandt A. H. Evaluation of new ultrasound techniques for clinical imaging in selected liver and vascular applications. *Dan. Med. J.* **65**, B5455 (2018).
3. Li X., et al. TCAF2 in Pericytes Promotes Colorectal Cancer Liver Metastasis via Inhibiting Cold-Sensing TRPM8 Channel. *Adv. Sci.* **10**, e2302717 (2023).
4. Wang, F. et al. The Chinese Society of Clinical Oncology (CSCO): Clinical guidelines for the diagnosis and treatment of colorectal cancer, 2024 update. *Cancer Commun (Lond).* **45**, 332-379 (2025).
5. Ebos J. M., et al. Accelerated metastasis after short-term treatment with a potent inhibitor of tumor angiogenesis. *Cancer Cell* **15**, 232-239 (2009).
6. Pàez-Ribes M., et al. Antiangiogenic therapy elicits malignant progression of tumors to increased local invasion and distant metastasis. *Cancer Cell* **15**, 220-231 (2009).
7. Yang Y., et al. Discontinuation of anti-VEGF cancer therapy promotes metastasis through a liver revascularization mechanism. *Nat. Commun.* **7**, 12680 (2016).
8. Frentzas S., et al. Vessel co-option mediates resistance to anti-angiogenic therapy in liver metastases. *Nat. Med.* **22**, 1294-1302 (2016).
9. Swisa A., et al. PAX6 maintains β cell identity by repressing genes of alternative islet cell types. *J. Clin. Invest.* **127**, 230-243 (2017).
10. Suryatenggara J., Yong K. J., Tenen D. E., Tenen D. G., Bassal M. A. ChIP-AP: an integrated analysis pipeline for unbiased ChIP-seq analysis. *Briefings Bioinf.* **23**, 537 (2022).
11. Yan F., et al. BEL1-LIKE HOMEODOMAIN4 regulates chlorophyll accumulation, chloroplast development, and cell wall metabolism in tomato fruit. *J. Exp. Bot.* **71**, 5549-5561 (2020).

Point-by-point response letter

Point-by-point responses to the reviewers' comments

The authors thank all the reviewers for their constructive comments and suggestions. Here, we provide the response to Reviewer 2.

Reviewer 2 (expert in vasculature (hemodynamics, calcium signaling), intravital imaging)

Comments to the Author:

The authors have done tremendous amount of work to comply with the requested changes and have addressed all concerns. I would like to still point to the fact that vessels diameters (at baseline) are very distinct between experimental groups). It might pay to highlight this and state it clearly.

Response: We thank this reviewer for the kind consideration and professional review work. Actually, the different initial vascular diameter was due to the effect of NKX2-3 in tumor pericytes (TPCs). Specific deletion of *Nkx2-3* in pericytes led to vasoconstriction and the vascular diameters (at baseline) were decreased compared to control group. Similarly, co-injection of NKX2-3-overexprssing TPCs (TPC_{NM}^{NKX2-3}) with tumor cells resulted in vasodilation and the initial vascular diameters were increased compared with TPC_{NM}^{Vector} co-injection group.